MONITORING AND MODELLING FOREST AND WOODLAND DECLINES UNDER A DRYING CLIMATE, FROM INDIVIDUAL TREE CANOPIES TO LANDSCAPES, ACROSS THE SOUTHWEST OF WESTERN AUSTRALIA

by

Bradley John Evans

A thesis submitted in fulfillment of the
requirements for the degree of Doctor of Philosophy
in the School of Veterinary and Life Sciences
Murdoch University

I declare that this thesis is my own account of my research, unless otherwise stated. It contains as its main content work which has not previously been submitted for a degree at any tertiary institution.

Bradley John Evans

Dedication

I dedicate this thesis to my loving wife Sabina Serneels and my daughters Zoe Olivia Evans and Mae Anneleen Evans who suffered the loss of their partner and father for the four years I slaved over this body of work.

Abstract

Severe reduction in precipitation over the last three decades has resulted in forest and woodland decline and mortality across the southwest of Western Australia (SWWA). This precipitation-reduction driven drought is shown to have come with significant increases in diurnal thermal variability. These bioclimatic changes are shown to correspond to declining forest and woodland condition and in the case of the Northern Jarrah Forest, the mortality of the endemic keystone species *Eucalyptus marginata* (jarrah) and *Corymbia calophylla* (marri). Quantifying the bioclimatic link between these localized events is a key to understanding the dynamic drivers of change and to the development of ongoing adaptive strategies to reduce the impact and severity of forest and woodland declines. A novel measure of crown health, named the total crown health index (TCHI), is proposed and validated by combining the use of remotely sensed airborne digital multispectral imagery (DMSI) and in-situ assessments of crown condition. The approach provides a means to quantify changes in individual tree crown condition through space and time. Landscape scale remote sensing and climatologies are used to develop a methodology for mapping forest mortality and quantifying the bioclimatic envelopes of seven eucalypt dominated forest and woodland zones across the SWWA. Reported decline events across SWWA are investigated and together, this cross-scale range of methodologies, constituting a framework, can be applied at a range of scales from an individual tree up to landscapes. The extent of forest and woodland declines are spatially aggregated using remotely sensed imagery at 0.5m, 10m, 250m, 500m and climatologies of around 5000m. A set of bioclimatic thresholds are determined for each of the seven forest and woodland zones across SWWA. These thresholds could have been used to predict the declines across SWWA up to 12 months in advance. I conclude with a set of recommendations suitable for land managers and policy makers that suggests how to apply these methods and tools for the ongoing monitoring and modelling of forested and woodland areas.

Acknowledgements

This thesis wouldn't have seen the light of day if Dr. Christine Stone, Prof. Colin Prentice and Prof. Sandy Harrison hadn't stood in my corner and believed in me- I am eternally in your debt! This thesis would not have been started without the support of a number of contributors including Prof. Tom Lyons, Prof. Giles Hardy, Dr. Paul Barber, Prof. Jorg Hacker, Prof. Nicholas Coops and of course my understanding and supportive family to which it is dedicated.

My work was generously supported by Murdoch University through the provision of a 3 year PhD scholarship. I also wish to thank SpecTerra Services Ltd. for their substantial support of the Centre of Excellence for Climate Change Woodland and Forest Health who provided additional scholarship funding. I especially thank Dr. Frank Honey, Andrew Malcolm and Dustin Bridges for their feedback at various stages.

This work was also supported by iVEC (http://www.ivec.org) through the use of advanced computing resources provided by the Australian Resources Research Centre Facility located at Technology Park, Perth. The Australian Research Network for Earth Systems Science (ARCNESS) provided travel and accommodation funding for attending the ARCNESS Winter School held at the University of New South Wales in September 2009.

Thanks to Peter Biggs and Dr Michael Raupach from CSIRO Marine and Atmospheric Research for making the AWAP runs 26g and 26h datasets publicly available, for several discussions on recent version changes and review of my work with these data.

TABLE OF CONTENTS

LIST OF TABLES

LIST OF FIGURES

CHAPTER 1
INTRODUCTION

1.1 Forest and woodland declines in southwest, Western Australia

Declines in the health and condition of forest and woodland ecosystems are now a global concern. The past 30 years have seen significant shifts in the climate of these biomes and it could fundamentally alter their structure and composition (Allen et al., 2010). Ecosystems that cannot relocate to suitable climatic conditions face a reduction of range, fragmentation, mortality and in extreme cases extinction (Hughes, 2010). One of the most vulnerable biome types, the Mediterranean, is scattered across five continents including the Mediterranean Basin, the western United States (California) and Mexico (northwest Baja), central Chile, the cape region of South Africa, and south and southwestern Australia (Klausmeyer and Shaw, 2009). These regions represent just 2% of the earth's surface yet support 20% of the earth's known vascular plant diversity (Cowling et al., 1996). The southwest of Western Australia (SWWA) is part of the world's second largest Mediterranean region (Figure 1.1) with approximately 25% of the global biome area. As with Mediterranean climes across the globe, SWWA faces a spatial contraction of native forests and woodlands in the order of 77% to 49% over the next century (Klausmeyer and Shaw, 2009) as the climate in the region becomes warmer and drier, caused by shifts in global circulation that result in a reduction of cold fronts that bring winter rains to the region (Bates et al., 2008).

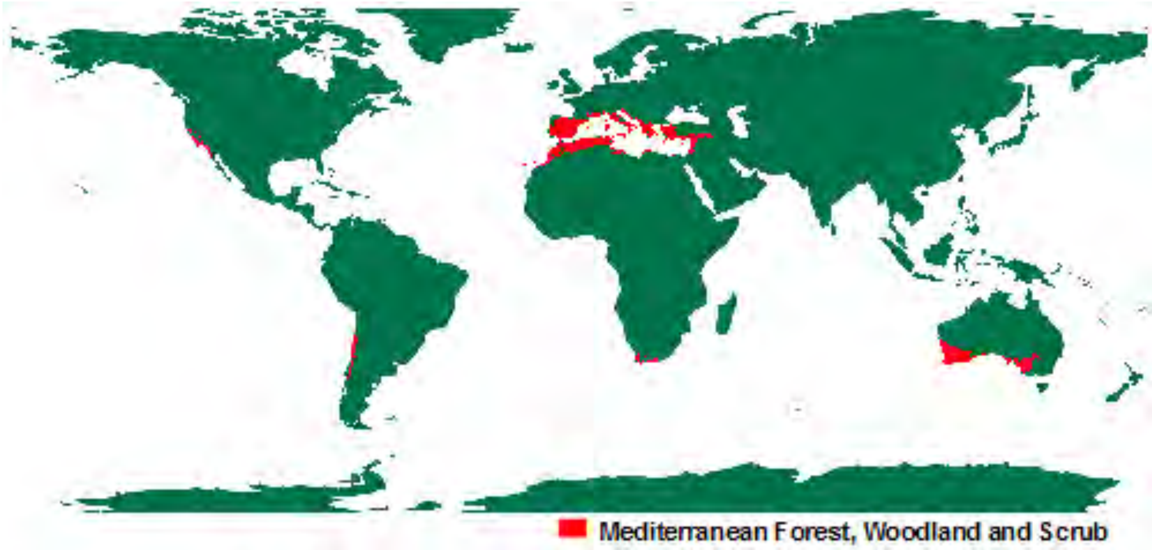

Figure 1.1: World Wide Fund for Nature biome data featuring their classification of Mediterranean Forest, Woodland and Scrub (WWF, 2013)

Such dramatic landscape transformations are not likely to occur rapidly; rather they are expected to evolve as a response to abiotic and biotic changes (Kinal et al., 2011). The signs of changes to forest and woodland structure and condition are already beginning to emerge (Klausmeyer and Shaw, 2011; Allen et al., 2010). In eucalypts, dieback is a symptom of declining vegetation condition and manifests as a reduction in the abundance, distribution and greenness of foliage within the tree's crown, a propagation of branch defoliation (i.e. a loss of leaf cover or area), which in turn leads to an overall reduction of vigor (productivity) and therefore condition (Close et al., 2009; Edwards et al., 2009; Hooper and Sivasithamparam, 2005; Jurskis, 2005).

The primary decline symptom in native eucalypt trees, dieback, can ultimately lead to mortality despite eucalypts being well adapted to extreme climate variability (Harper et al., 2009; Peel et al., 2005; Pepper et al., 2008). A eucalypt in decline is said to be dying-back, the term 'dieback' is used to describe this. Eucalypts have a dynamic ability to recover from dieback, yet mortality remains a possibility if symptoms persist. Eucalypts often respond vigorously to dieback, sprouting epicormic shoots from surface tissues.

Declines of this kind are not new to the SWWA. A range of iconic eucalypt species of SWWA have been suffering severe dieback now for decades. A number of these declines have been recorded in the literature (Table 1.1). Over the last decade, severe drought has impacted on the climate of southern (Mitchell et al., 2012) and SWWA adding further pressure to vegetation stress, that is also having an impact on plantation forestry (Harper et al., 2009). However, the most famous ongoing decline event is affecting the jarrah, *E. marginata*, and rather than climate, this event was attributed to a root pathogen, *Phytophthora cinnamomi.* The pathogen has been claimed to be responsible for causing the decline and destruction of thousands of hectares of Jarrah forest since the early 1900's (Shea et al., 1984; Shearer and Smith, 2000).

Table 1.1. Forest and woodland zones across the SWWA with reported dieback

Description	Species under threat	Reference
Swan Coastal Plain	*E. gomphocephala* (tuart) *E. rudis* (flooded gum)	Archibald et al., 2004; Edwards 2004
Northern Jarrah Forest	*E. marginata (*jarrah*)* *C. calophylla* (marri)	Chapters 4,5; Matusick et al., 2012, 2013; Brouwers et al., 2012a, 2012b
Yalgorup (Yalgorum National Park)	*E. gomphocephala* (tuart)	Chapters 1, 2; Cai et al., 2011
Southern Jarrah Forest	*E. marginata (*jarrah*)* *C. calophylla* (marri)	Shearer and Smith, 2000
Wandoo Area North (Wandoo National Park)	*E. wandoo* (wandoo) *E. marginata (jarrah)* *C. calophylla* (marri)	Hooper and Sivasithamparam (2005)
Dryandra (Wandoo)	*E. wandoo* (wandoo)	Hooper and Sivasithamparam (2005)

The declines are not limited to jarrah, other iconic eucalypts including *E. rudis* (flooded gum), *E. wandoo* (wandoo), *C. calophylla* (marri) and *E. gomphocephala* (tuart) have suffered a rapid decline in health across forests and woodlands in SWWA (Figure 1.2). In a recent study investigating causes of wandoo declines, Hooper and Sivasithamparam (2005) suggested the interaction between unidentified borer insects and decay-causing fungi as the cause of wandoo decline yet also suggested the increase in drought severity over the past decade could be an inciting factor, such that trees under stressed condition were more susceptible to insect attack.

The decline of the marri, which is found co-occuring in several communities across SWWA and recognized as an important habitat and resource species, has been attributed to a severe canker causing fungus. Similar to the wandoo declines, the recent increase in susceptibility begs the question as to what environmental factors may be predisposing or contributing to the impact of this disease *Quambalaria coyrecup* (Paap et al., 2008). Kimber (1981) attributed the decline of marri across the south-west to a combination of the rapid decline in rainfall in the 1970's preceded by a longer term decline in rainfall since the 1920's. Since the 1970's the southwest has received 15-20% less than average rainfall (Petrone et al., 2010) and a 0.4°C degree increase in temperature (Bates et al., 2008) that are also attributed to a marked depletion of stream flow through the forested region surrounding Perth (Kinal and Stoneman, 2011; Petrone et al., 2010) where jarrah, marri, flooded gum and wandoo occur.

At the same time, considerable effort has been made into determining the causes of the decline of the tuart along the Swan Coastal Plain (SCP) of Western Australia (Cai et al., 2011; Chapters 1, 2; Matusick et al., 2012, 2013). Tuart is a magnificent woodland tree dominating the coastal dune system in the south-west of Australia, which is approximately 400km in length and frequently only 1km wide (Boland et al., 2006). Unfortunately, less than one-third of the once extensive tuart woodland remains (Government of Western Australia, 2002) due to clearing for urbanisation, agriculture and industry.

The natural range of tuart is in Perth's most sought after costal development land, as such, extensive areas of these woodlands continue to be removed for housing development. There is also increasing concern over the health of the remaining fragments as a severe decline of unknown cause(s) is having a major impact upon them (Archibald et al., 2004; Edwards, 2004), resulting in declines of the Tuart forest on the Swan Coastal Plain (south of Perth refer Figure 1.2) in the late 1990s and 2000s (Cai et al., 2011). In response to these decline events, The Tuart Health Group was formed and together with the Western Australian Government Department of Environment and Conservation set about a series of *in-situ* ground assessments and remote sensing studies.

The Australian Forestry Standard requires forest managers to identify, assess and prioritize agents that may impact forest health and vitality (Barry et al., 2008). This yields data critical to our understanding of the impacts of climate variability on forest health across landscape and biome boundaries and is work that must be undertaken across a range of spatial and temporal scales. Such mandated monitoring, in both space and time, requires methods that are both repeatable and economically viable. The only tool for achieving near real time, contiguous landscape and continental scale monitoring is remote sensing. Used in combination with gridded and modeled climatologies both can provide greater insight into the temporal and spatial dynamics of decline events. Today, a range of data can be obtained to enable this work; Figure 1.3 illustrates the spatial and temporal domains of each source.

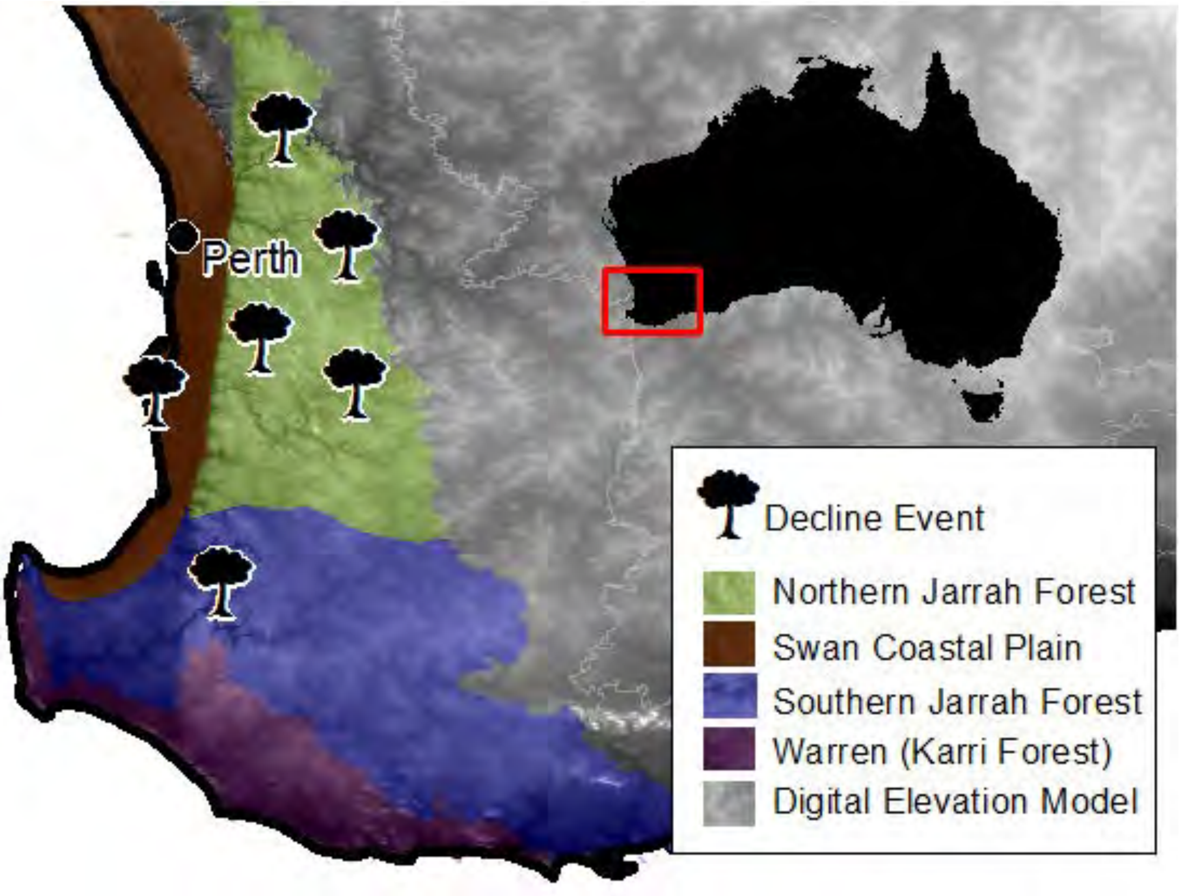

Figure 1.2. Southwest, Western Australia featuring the Interim Biogeographic regionalisation of Australia classification of the Swan Coastal Plain and Northern Jarrah Forest overlaid on a 10m Digital Elevation Model from the Western Australian Government Department of Environment and Conservation. Regions with known decline events are marked.

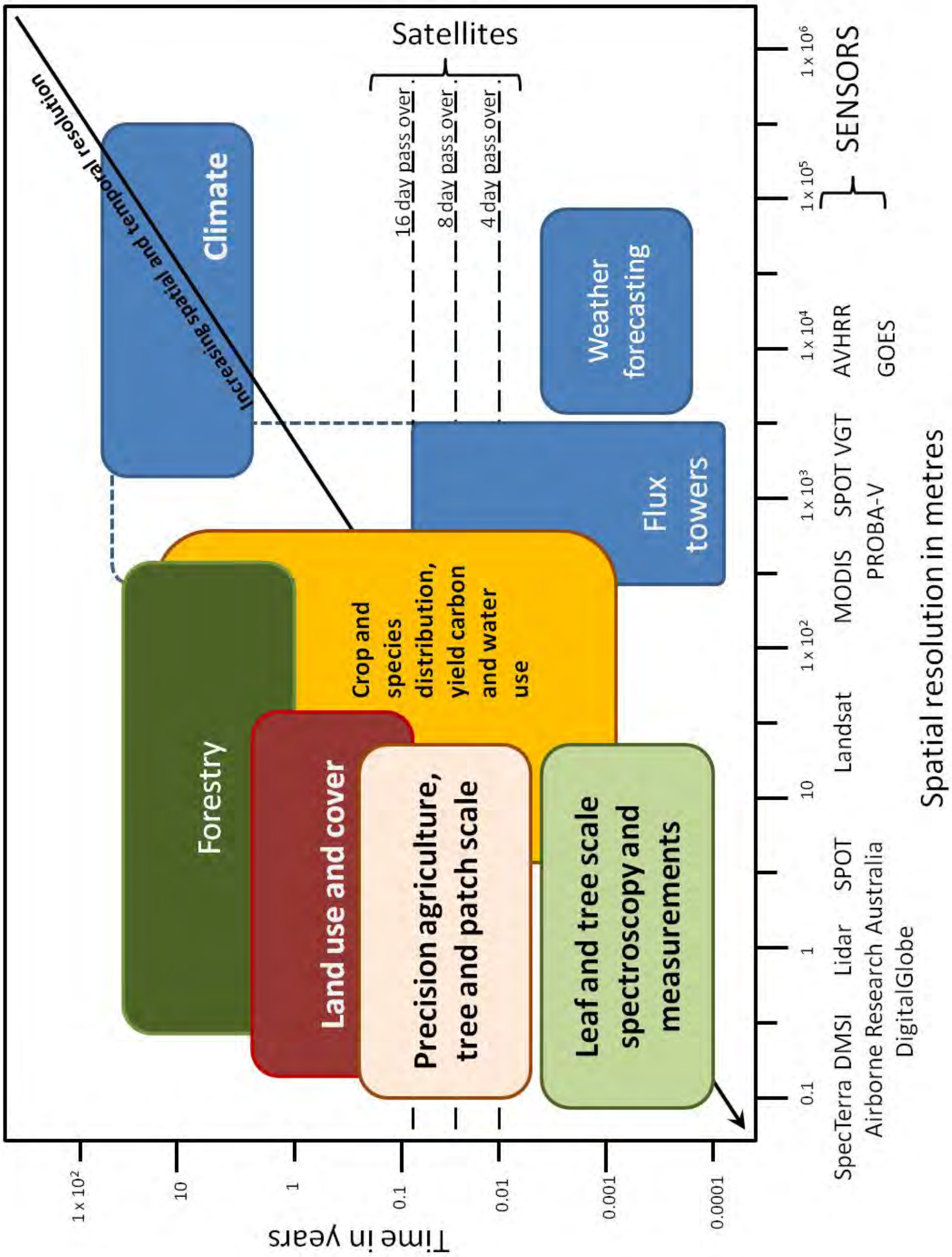

Figure 1.3. Spatial and temporal domains in the remote sensing and observation of vegetation. Some examples sensors are listed on the *x* axis.

1.2 Applications of remote sensing and climatologies for monitoring forest and woodland declines

Airborne and satellite remote sensing has long been considered an effective tool for monitoring large spatial extents (Kerr and Ostrovsky, 2003; Goodwin et al., 2008; Wulder et al., 2008; Gillanders et al., 2008). However, until recently the limited spatial resolution of satellite remote sensing platforms has limited their application at the individual tree scale, which has remained the domain of airborne remote sensing (Coops et al., 2004; Verbesselt et al., 2010a). The choice of when to use aerial or satellite data is a function of scale, cost and time. Accordingly, to monitor and model vegetation condition across scale, a combination of remote sensing tools is often used, generally following the spatio-temporal domain spaces illustrated in Figure 1.3. Before such work can begin, one must have a deeper understanding of the nature of the problem- most often this is obtained through a deeper understanding of the regional ecosystem dynamics.

Remote sensing is a non-invasive means of acquiring image data over large areas useful for monitoring vegetation. In broad terms, the science of remote sensing of vegetation includes aerial and satellite borne sensor observations of the earth's surface. Modern vegetation sensor systems have been designed to maximize their sensitivity to photosynthetically active materials, targeting specific wavelengths of the electromagnetic spectrum known to be sensitive to both absorbed photosynthetically active radiation (400-700 nm) and scattered electromagnetic energy (700-1300 nm). Applying this knowledge, in the form of image interpretation has provided insight into the distribution, phenology and physiology of vegetation (Weiss et al., 2004; Jackson and Jenson, 2005).

Vegetation indices (VI) are a numerical simplification of the reflectance characteristics of a pixel at different wavelengths of the electromagnetic spectrum.

Typically, VI exploit the numerical variance between the primary absorption bands for chlorophyll in green leaves (430-450 nm and 650-670 nm) and scattering caused by the spongy mesophyll (700-1300 nm). Much work has been done to improve VI through the investigation of multiplicative or additive moderators to limit unwanted noise (Huete, 2002). Figure 1.4 shows this using spectroradiometric scans of a green healthy leaf showing the distinct `hockey-stick' curve exploited in the development of VI.

The most common of all VI is the Normalized Difference Vegetation Index (NDVI) developed by Rouse et al. (1974) and because it is widely used, provides a useful demonstration of the overall concept. By normalizing the dynamic range (-1 to +1) of the ratio of scattered near-infrared (usually larger in magnitude) electromagnetic energy, reflected back to the sensor, to red. NDVI is larger (closer to one) for green, chlorophyll rich pixels and smaller for chlorophyll poor pixels.

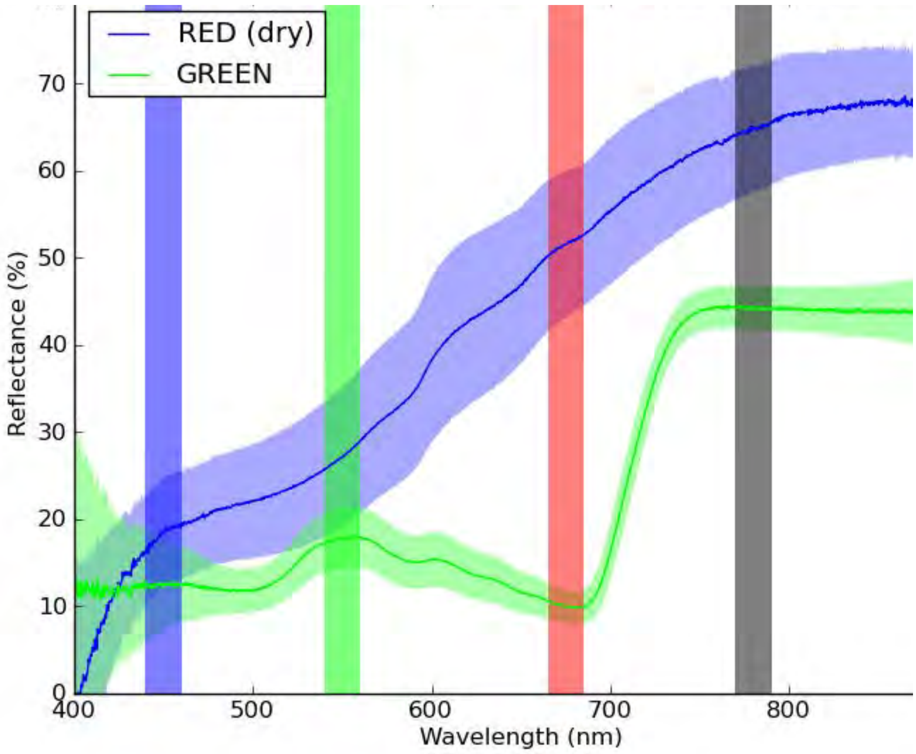

Figure 1.4.Spectral reflectance of dry and green *E. marginata* leaves from the southwest of Australia. The red-green absorption and near infrared reflectance difference between the two illustrate the variance inherent in changes in chlorophyll content. The blue, green, red and grey stripes indicate the spectral bands of the SpecTerra Services Digital Multispectral Imagery product.

It is because NDVI summarizes the absorption and reflection of electromagnetic energy interacting with green vegetation that it is considered as a robust indicator of photosynthetic activity, or more plainly, greenness. Huete et al. (2002), in a study covering a range of crops and forests, identified that NDVI was useful for the detection of seasonal and inter-annual changes in vegetation growth and activity and that the normalization, as compared to a simple ratio, reduces many forms of multiplicative noise effects (sun illumination, cloud shadows, atmospheric attenuation and topographic valuations). Huete et al. (2002) showed that NDVI is non-linear and can be influenced by additive effects such as atmospheric path radiance and that it is sensitive to canopy background variations.

It is important to note that every sensor has its own electronic, physical and spectral characteristics and whilst it is possible to calculate an NDVI from any RED and NIR band, it is not necessarily comparable to that of another sensor. For example, when Huete et al. (2002) investigated MODIS NDVI they found that, whilst it was sensitive to chlorophyll, it was less responsive to biophysical changes (e.g. leaf area), thus implying a need to account for canopy background effects such as soil and understory. Huete et al. (2002) proposed a new index, the Enhanced Vegetation Index (EVI), derived from MODIS bands to improve greenness estimations under variable canopy structural variations, particularly dense vegetation conditions. This demonstrates the need to test the specific sensitivities of sensors.

Most passive remote sensing systems in operation today capture a number of bands (i.e. multispectral) in the visible wavelengths (400-700 nm), the near-infrared (700-1300 nm) and shortwave infrared (1300-2500 nm). A list of some of the sensors known to be used in the southwest of Western Australia can be found in Table 1.2.

Table 1.2: Common remote sensing systems used for remote sensing of vegetation in southwest Australia including SpecTerra Services Digital Multispectral Imaging (DMSI), Landsat Thematic Mapper (TM), Systeme Pour l'Observation de la Terre (SPOT) high resolution geometrical (HRG) and high resolution visual infra-red (HRVIR), SPOT VEGETATION (VGT) and the The Moderate Resolution Imaging Spectroradiometer (MODIS)

Systems	Bands	Spatial (m)	Temporal (days)
DMSI	B1: 465-485 nm B2: 540-560 nm B3: 665-685 nm B4: 770-790 nm	0.25-5 m	On demand
SPOT 5 HRVIR and HGR -multispectral -panchromatic	B1: 500-590 nm B2: 610-680 nm B3: 790-890 nm B4: 1580-1750 nm PAN: 480-710 nm	2.5 m, 10 m	Programmable
Landsat TM 4,5	B1: 450-520 nm B2: 520-600 nm B3: 630-690 nm B4: 760-900 nm B5:1550-1750 nm B6: 10400-12500 nm B7: 2080-2350 nm	30 m, 120 m	16
MODIS	36 Bands: 405-14,385 nm	250 m, 500 m, 1000 m	1-2
SPOT VGT	B1: 430-470 nm B2: 610-680 nm B3: 780-890 nm B4: 1580-1750 nm	1150 m	1

All of the sensors listed in Table 1.2 collect digital data, as opposed to analog data (for example hard-copy photography). Digital data are in an array (raster) of brightness values (digital numbers) obtained using either a scanner or frame camera. Differences in the bands between each system (or even within systems missions e.g. Landsat) are common and exist for a variety of reasons including, first principles (i.e. the science of spectroscopy), legacy and technical constraints. For example, the SPOT HRVIR mission does not have a blue band (350-400 nm) resulting in the inability to make a true colour composite using the raw bands, a common feature of most remote sensing platforms. Nonetheless, it remains possible to use these sensors and available spectral bands to monitor and map changes in vegetation condition across a range of spatial and temporal scales.

Vegetation condition is continually changing; it is dynamic in both space and time exhibiting both slow and subtle growth and successional changes, but also through abrupt and sudden natural (climate, fire, drought, earthquakes, floods) and externally driven disturbances such as land use change and pollution (Oliver and Larson, 1990). Land cover change is known to impact both floristic and faunal biodiversity (Hansen and Dale, 2001) and regional climate (Lyons, 2002; Kala et al., 2011).

The term vegetation condition is becoming more widely used in land management policy for describing aspects of aesthetics, production and the biodiversity of ecosystems (Keith and Gorrod, 2006; Stone and Haywood, 2006). Vegetation condition is a reference to the relative naturalness and biodiversity of an ecosystem in context of its biophysical structures i.e. trees, shrubs and grasses (Parkes et al., 2003; Stone and Haywood, 2006). Moderate resolution satellite remote sensing systems, such as MODIS, which cannot resolve individual tree crowns, must rely on 'mixed pixels'. MODIS pixels combine information from the overstory (i.e. trees), understory (i.e. grasses and snow) and soils. As such, lower resolution satellite systems are a useful `first pass' filter (Barry et al., 2008), indicating areas of potential change in vegetation condition (Fraser et al., 2005; de Beurs et al., 2005; Eklundh et al., 2009; Verbesselt et al., 2010a) that can be used to deploy higher resolution (and cost) airborne systems (Wulder et al., 2008).

Furthermore, seasonal and inter-annual fluxes of greenness (i.e. ecosystem phenological cycles) add noise and complexity to the process of extracting true changes in condition. In the southwest of Western Australia these cycles are somewhat simplified by the growth cycle following the winter rains and senescence following the onset of the dry summer heat (i.e. the Mediterranean climate). This is particularly useful for monitoring the overstory given winter grasses burn off quickly following the growth season, thereby allowing for the use of late summer as a good indicator of overstory growth or decline (Caccetta et al., 2002). Exploiting this phenomena, the Landsat TM based LandMonitor programme (Caccetta et al., 2002) has successfully demonstrated the use of a single annual image for monitoring overstory vegetation (i.e. eucalypts) in southwest Western Australia. However, the spatial resolution of Landsat™ (30 m) is insufficient to monitor individual trees.

High resolution remote sensing with pixels in the order of 1m or less enables the exploitation of another useful biophysical trait of eucalypts, crown dieback. It follows that using remote sensing systems with pixels less than 1m enables the identification of the dieback of individual branches. However, the logistics (cost and quantity of data) associated with collecting high resolution data across the southwest of Western Australia prohibits its capture at a higher frequency than LandMonitor.

High temporal frequency monitoring remains the domain of the moderate and low resolution remote sensing systems such as MODIS and SPOT VEGETATION (1km scale). MODIS is the most commonly used satellite system for seasonal, phenological and inter-annual studies. In Australia, MODIS data have been applied to mapping fractional cover, specifically the fractions photosynthetic vegetation (f_{pv}), non-photosynthetic vegetation (f_{npv}) and bare soil (f_{bs}) at 500m resolution. This national dataset has been developed by Guerschman et al. (2009) for national monitoring of ground cover (Stewart et al., 2011) and is currently the only estimate of fractional cover validated for the Australian continent.

1.3 Knowledge gaps

Whilst *in-situ* crown assessments have already been applied to eucalypt species (Stone and Haywood, 2006), including *E. gomphocephala* (tuart) (Horton et al., 2011), no previous study has attempted to link measures of *in-situ* condition of individual *E. gomphocephala* species to high resolution digital multispectral imagery (DMSI). Addressing this gap, Chapter 2 proposes a novel total crown health index (TCHI) based on *in-situ* tree crown assessments and validates its use with DMSI. This provides a clear link between vegetation greenness and crown condition. In doing so, it establishes the link between remotely sensed vegetation condition and the actual health condition of individual trees. Tuart was selected for the development of the TCHI because declines were observed in the late 1990's and again in the early 2000's (Horton et al., 2011) and a suitable time series of DMSI was available with a corresponding set of *in-situ* crown assessments.

Recently, a range of *in-situ* techniques has been developed to understand the declines of the tuart forest including the functional diversity of soil bacterial communities (Cai et al., 2010) and a range of fire and climate drivers (Archibald, 2004, 2006), yet none of these previous studies on tuart have used remote sensing or DMSI. More specifically, none have used a combination of textural, spectral and geometric variance derived from DMSI together with a machine learning algorithm to model the changes they observe through space and time. Addressing this gap, Chapter

3 extends the analysis of DMSI to include textural variance and spectral variances calculated from all bands of the DMSI imagery, together with geometric statistics of the Yalgorup tuart dataset. Chapter 3 is an enhancement of the work presented in Chapter 2 because it uses a more complex statistical methodology to yield a similar yet incrementally improved result. Both chapters demonstrate applications of remote sensing to monitoring forest condition and declines at the individual tree level.

Two studies have investigated the severe decline events which lead to the patches of mortality across the NJF following the summer of 2010-2011 (Brouwers et al., 2012a; Matusick et al., 2013). Yet, neither of these studies used satellite remote sensing to investigate the spatial distribution or temporal genesis of the event prior to its occurrence. Whilst Brouwers et al. (2012a) and Matusick et al. (2013) did investigate aspects of meteorological conditions surrounding the events, neither investigated the long-term (30 year) bioclimatic envelope of the forest, and neither attempted to relate this to satellite observations of changes in land cover. Providing assistance to address this gap, Planet Action granted resources to investigate the potential to model and map the event across the forest using SPOT 5 imagery and ENVI EX software. Chapter 4 proposes and validates a novel feature extraction model, utilizing both of these, that was developed using a subset of sites presented by Matusick et al. (2013) and validated with additional *in-situ* assessment of the event (Batini, personal comms.). In addition to mapping the event, which became a first step in the chapter, a novel approach to combining the use of both MODIS fractional cover (Guerschman et al., 2009) and Australian Water Availability Project (AWAP, Raupach et al., 2009) data is presented and used to quantify the decadal changes in cover (i.e. as a surrogate for condition) across the forest.

Whilst the remote sensing and climatology datasets used in Chapters 4 and 5 were designed with monitoring applications in mind, neither Guerschman et al. (2009) and Raupach et al. (2009) have used their data for investigations of forest declines in

SWWA. Similarly, Geoscience Australia's Dynamic Land Cover Dataset (Lymburner et al, 2010) has not been combined with Interim Biogeographic Regionialisation of Australia (IBRA) in the way presented in Chapter 5 for the mapping of persistent forest cover zones for the investigation of forest declines. Additionally, studies focused on changes in hydrology (e.g. Kinal and Stoneman, 2011) of the NJF ignore changes in forest cover and quantification of forest declines over the same period. It follows that analysis of bioclimatic envelopes preceding forest mortality events in the southwest of Western Australia is not reported in the literature.

Whilst a number of studies have looked at the climate over the last three decades (Chapter 4, Brouwers et al, 2012a) and its role icn the declines, none have focused specifically on the use of low resolution data over the last decade using the most recently available datasets. In addressing this gap, the most recently released versions (Guerschman et al., 2009) of the AWAP (Raupach et al., 2009) data (i.e. run 26h) and temporally and spatially aggregated MODIS time series satellite data (2000-2012) are used. In using these new data, Chapter 5 both consolidates and extends the quantification of bioclimatic thresholds identified in Chapter 4 and finds similar effects across SWWA- particularly those following the summer of 2010-2011. The methodologies developed in Chapter 4 and enhanced in Chapter 5 address a significant gap in previous works on the declines of SWWA (Cai et al., 2010, Brouwers et al., 2012a, 2012b; Matusick et al., 2012, 2013). None one of these previous studies investigated the variability of the mean diurnal range of temperature and apparent lack of usable water (i.e. not just rainfall, but also sub-surface water supplies i.e. soil moisture). This gap is addressed in both Chapters 4 and 5 through the use of an aridity index based on actual and potential evapotranspiration (Prentice et al., 1994) which is calculated from the AWAP dataset (Raupach et al, 2009).

1.4 Specific aims of the thesis

This thesis applies and validates state-of-the-art remote sensing and climatology data and methodologies for quantifying vegetation condition and change through space and time. The four major experimental chapters focused on known eucalypt decline and mortality events. Each is interdisciplinary and novel yet designed to combine in scale from an individual tree through to the patch and forest scale and finally to the landscape/ regional scale (SWWA). The specific aims of this thesis were to;

1. Develop and apply a method for combining *in-situ* assessment of individual crown condition with high resolution multi-spectral imagery.
2. Enhance and extend this methodology to use complex textural, spectral and geometric variance to improve the relationship established empirically in (1).
3. Develop a methodology to map and quantify the drivers behind the most significant decline event in recent history, the mortality event across the NJF following the extreme summer of 2010-2011. This includes scale progression from the individual tree scale from objectives (1) and (2) to develop and apply a patch-to-landscape scale range of assessment such that this method is relevant to the spatial extent of a forest. Additionally, combine both remote sensing and climatologies to quantify the bioclimatic drivers preceding the event and test the significance of spatial resolution on the results.
4. Extend (3) to investigate all of the recorded declines across SWWA in the last decade at low resolution (5000m). Further develop the methods used in (3) and determine if the observations and conclusions made over NJF are applicable to all of the SWWA. In

doing so, determine a set of comparable bioclimatic thresholds for areas of known decline and therefore provide means for predictions of forest declines that could be incorporated into regional management and climate change adaptation strategies.

CHAPTER 2
DIEBACK CLASSIFICATION MODELLING USING HIGH-RESOLUTION DIGITAL MULTISPECTRAL IMAGERY AND *IN-SITU* ASSESSMENTS OF CROWN CONDITION

2.1 Overview of author contributions

This Chapter addresses the first aim of developing and applying a novel method for combining *in-situ* assessment of individual tree crown condition with high resolution digital multi-spectral imagery (DMSI). This Chapter was published as Evans, B. J., Lyons, T. J., Barber, P. A., Stone, C., and Hardy, G. (2012). "Dieback Classification Modelling using High Resolution Digital Multi Spectral Imagery and *in-situ* Assessments of Crown Condition." Remote Sens. Lett., 3: 541-550.

Four expert made measures of individual *E. gomphocephala* (tuart) crown condition are combined to become a Total Crown Health Index (TCHI). An empirical relationship between TCHI and vegetation indices extracted from the DMSI is then established in 2012. A classification scheme is applied to the results, covering a range of possible crown conditions from unhealthy through to healthy. The resulting model is then applied to a second DMSI scene acquired in 2010 and the change of crown condition of each tree is analyzed through time.

Evans wrote all sections of this chapter, performed all of the data and image analysis and prepared the manuscript for publication. Barber, a forestry expert, carried out the assessments of the *E. gomphocephala* across the study area in 2008, Yalgorup (south of Perth). The work of Barber was funded from the Australian Research Council (LP0668195) with additional support from Department of Conservation and Environment, Alcoa of Australia, Mandurah City Council and Bemax Cable Sands.

Stone, Coops and Honey provided guidance on the development of the methodology and reviewed previous drafts of the manuscript. SpecTerra Services Pty Ltd, Perth provided the DMSI imagery and the work was supported by iVEC (http://www.ivec.org) through the use of super-computing facilities. Primary supervisor, Lyons provided support throughout the development and writing phases. Co-author Hardy contributed continuous review of the work.

2.1.1 Background on SpecTerra Services Digital Multispectral Imagery and its calibration

The digital multispectral imagery (DMSI) used in this and subsequent chapters was supplied by SpecTerra Services Pty Limited, Perth, Western Australia (SpecTerra) under agreement with the Centre of Excellence for Climate Change, Woodland and Forest Health. The data was supplied as SpecTerra proprietary pre-processed, mosaicked, spectro-radiometrically, and bidirectional distribution function (BRDF) calibrated scenes to Evans for use in this thesis and subsequent publications. The SpecTerra sensor used is called the High Resolution Airborne Multispectral Sensor System (HiRAMS).

SpecTerra define their HiRAMS sensor as a four-camera system fitted with interchangeable narrow-band spectral filters. The full width half maximum centroids (FWHM) of these bands are 450nm (blue), 550nm (green), 670nm (red) and 780nm (near infra-red). The bandwidth of each band is 20nm. Each camera captures continuous digital images as the aircraft traverses the flight line. Using data from the aircrafts GPS, synchronized with the camera, these frames are geospatially overlaid each other by SpecTerra's image processing team and mosaicked into a contiguous scenes. Once mosaicked, the image is corrected for bi-directional differences (i.e. BRDF correction for each pixel used in the final mosaic) and the scene is brightness balanced. SpecTerra do not provide further information on their methodology and have not published their source code in the public domain and require only the solar angle (provided in this thesis and publications) to solve their proprietary BRDF equations.

Multiple years of DMSI data are used in this thesis. To ensure that change between scenes was ‘real’, and not an artifact of spectro-radiometric variance, the Furby and Campbell (2001) method was adapted from its originally designed purpose (i.e. Landsat ‘like to like’ or ‘scene to scene’ calibration) and applied to the DMSI, hereafter called a “variant of the Furby and Campbell (2001) method”. This was possible because the SpecTerra HiRAMS bands are very similar to Landsat. The Furby and Campbell (2001) method requires the operator to select a number of ‘invariant’ targets common to each scene and the selection of a ‘baseline’ scene, the scene against which each is calibrated. Selection of these targets and the baseline scene can be manual, as the case in this thesis. The dark and light targets were identified across all of the scenes and 2008 was chosen as the baseline. A number of pixels were selected for this purpose and averaged to produce a mean value for each invariant target. The invariant target data was extracted from each band and scene and the values were recorded.

The invariant target data from each band was plotted independently and a linear regression (i.e. y=mx+b) was performed to derive a set of coefficients (i.e. m and b) which are then used to scale the radiances of each of the bands. The digital images (i.e. scenes) were reconstructed by the scaling each of the bands. Evaluation was conducted through the generation and comparison of priori and posterior histograms of each band and scene. Accordingly, the calibration was deemed satisfactory. The calibrated sets of bands and scenes were saved and subsequently used in the publications and this thesis.

2.2 Abstract

Quantifying dieback in forests is useful for land managers and decision makers seeking to explain spatial disturbances and understand the cyclic nature of forest health. Crown condition is assessed as reference to dieback in terms of the density, transparency, extent and in-crown distribution of foliage. At 20 sites in the Yalgorup National Park, Western Australia, a total of 80 *E. gomphocephala* crowns were assessed both *in-situ* (2008) and using two acquisitions (2008 and 2010) of airborne imagery. Each tree was assessed using four crown-condition indices: Crown Density, Foliage Transparency, the Crown Dieback Ratio and Epicormic Index combined into a single index called the Total Crown Health Index (TCHI). The airborne imagery is like value calibrated then classified and modeled using *in-situ* canopy condition assessments resulting in a quantification of crowncondition change over time. Comparison of Normalized Difference Vegetation Index (NDVI), Soil-Adjusted Vegetation Index (SAVI) and a novel Red-Edge Extrema Index (REEI) suggests that the latter is more suited to classification applications of this type.

2.3 Introduction

Eucalyptus have an elastic ability to decline and recover relative to a number of biotic factors including pests and pathogens, drought and heat stress and variable rainfall. In southwest Western Australia, eucalyptus decline has increased over recent decades (Close et al., 2009, Horton et al., 2011) at the same time that the region has experienced prolonged drought and a reduction in rainfall.

E. gomphocephala (tuart) once dominated swathes of the coastal dune systems near Perth, Western Australia (Boland et al., 2006). Since the early 1990s, there has been concern for the spread of decline of tuart throughout parts of this region

(Edwards, 2002; Close et al., 2009; Archibald et al., 2010; Horton et al., 2011). This community concern has promoted research into innovative ways to monitor large areas in decline in order to aid the restoration of equilibrium, a task inevitably implemented by the regional land managers, research groups, private land holders and volunteers.

The visible symptom of decline is defoliation that often manifests in upper branches and evolves into a reduction in the overall density and distribution of foliage throughout a crown. Eucalyptus often respond vigorously to dieback, sprouting epicormic shoots from surface tissues. Despite this dynamic ability to recover, mortality can occur suddenly or as a result of persistent decline. With high-resolution (0.5 m) digital multispectral imagery (DMSI), it is possible to observe the extent of dieback in large eucalypts like the tuart because crown diameters often exceed several pixels in diameter. Such insights can be useful to land managers seeking to understand the spatial extent of declines.

High spatial resolution radiance data in the red and near infrared regions have been widely used for studying variability in photosynthetic activity. The region between 690 and 740 nm, known as the 'red edge' (Curran et al., 1990), is useful for characterizing chlorophyll content (Pinar and Curran, 1996; Jago et al., 1999), density of chlorophyll in plant cells and crown density (Datt, 1998; Stone et al., 2001, 2003; Coops et al., 2002, 2003, 2004; Pietrzykowski et al., 2006; Barry et al., 2008) and numerous studies have exploited the location, gradient and position of this region (Demetriades-Shah et al., 1990; Dawson and Curran, 1998).

The objectives of this study were to assess the potential of using only high resolution DMSI derived Vegetation Indices (VI) for classifying the condition of tuart crowns and then use this to predict the change-of-condition over time. DMSI crown condition classifications were validated against ground-based assessments using data available from 2008. Accordingly, the DMSI-based classification was applied to multi-year (2008, 2010) time series to produce a change-over-time condition trajectory for individual trees.

2.4 Methods

2.4.1 *In-situ* crown assessments

The Yalgorup region (see figure 2.1) lies between 32° 38' 0" S and 32° 44' 0" S and 115° 36' 0" E and 115° 40' 0" E. Between 2005 and 2007, 20 sites were established to cover a range of vegetation cover change trend classes from the 15-year (1990–2005) Land Monitor 25 m × 25 m multispectral imagery method described in Caccetta et al. (2000). In July 2008, four tuart crowns were randomly selected at each site and extents delineated using a differential GPS (dGPS) with an accuracy of less than 1 m. Physical attributes of each crown were recorded including (i) Crown Density (C), (ii) Foliage Transparency (F) adapted from USDAFS (2005) and Schomaker et al. (2007), (iii) Crown Dieback Ratio (D) and (iv) Epicormic Index (E) after Kile et al. (1981). The tree crowns were assessed for each measure on a scale of 0–100 in 5-point increments (USDAFS, 2005; Schomaker et al., 2007). For example, a *C* score of 100 represents a completely defoliated tree crown. Similarly, an *E* score of 0 means that the tree has no flush growth (epicormic shoots sprouting from its branches).

2.4.2 DMSI acquisition

DMSI imagery was acquired and preprocessed by SpecTerra Services Pty Ltd (Perth, Western Australia) with an airborne sensor developed specifically to map and monitor vegetation status at higher spatial yet finer spectral and radiometric sensitivities than the LandsatTM bands. The DMSI was acquired at 0.5 m resolution in June 2008 and 2010 at similar solar angles and under clear atmospheric conditions.

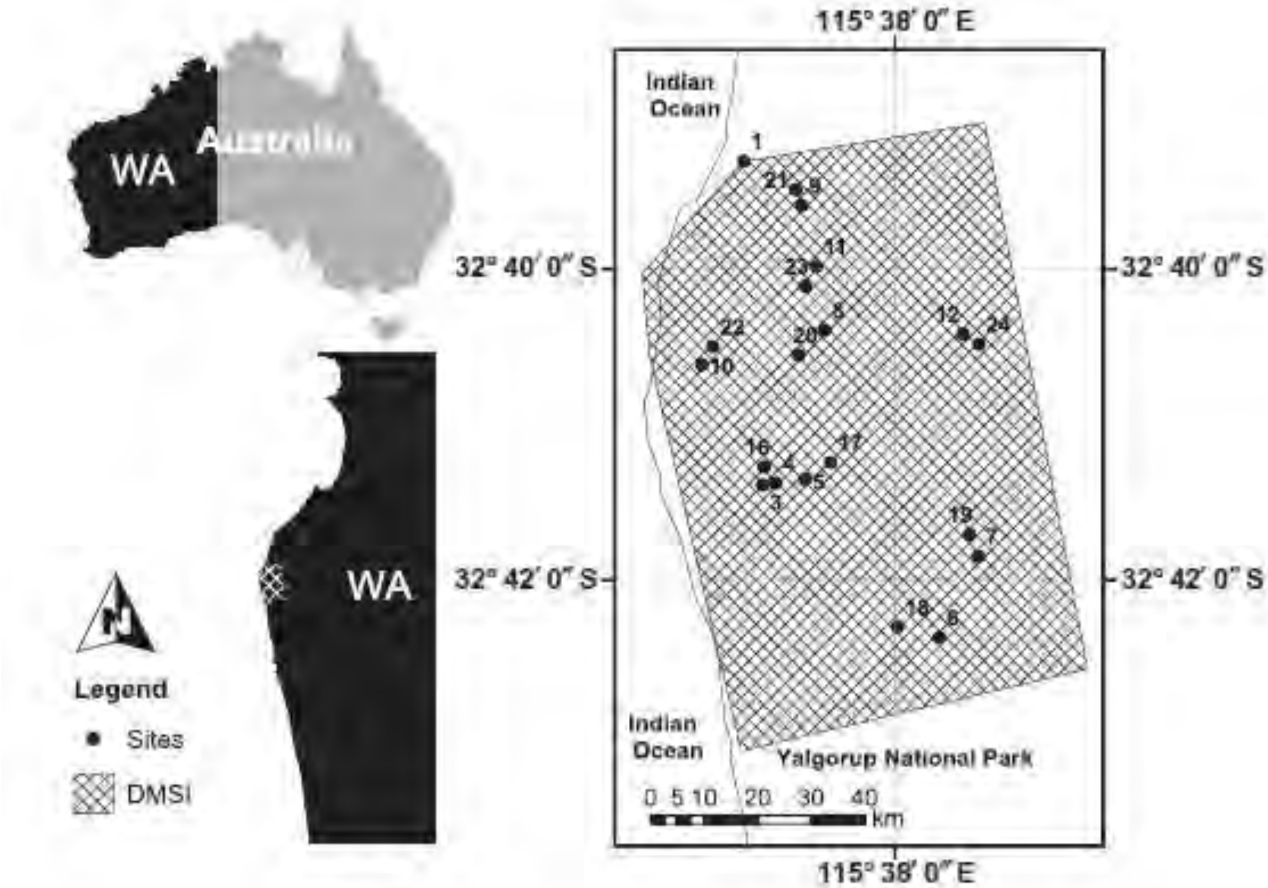

Figure 2.1. Map of the study area in Western Australia (WA) showing the DMSI grid over the sites (irregularly numbered).

The sensor acquires 12-bit unitless digital numbers simultaneously in four 20 nm wide spectral channels in the visible and near-infrared regions of the electromagnetic spectrum using narrow bandpass filters centred at Blue (450 nm), Green (550 nm), Red (675 nm) and NIR (780 nm). Post flight processing of the data included precise band to band registration and spectro-radiometric correction for bidirectional reflectance distribution function (BRDF) variations. A 'like-value' calibration of the 2008 and 2010 DMSI data was conducted using a variant of the method described in Furby and Campbell (2001).

2.4.3 Vegetation indices

The three vegetation indices chosen for this study (refer to figure 2.1) are (1) the Normalized Difference Vegetation Index (NDVI), (2) the Soil-Adjusted Vegetation Index (SAVI) and (3) the Red-Edge Extrema Index (REEI). Each is calculated with the SpecTerra bandwidths and their equations can be found in table 2.1. SpecTerra DMSI bands are significantly narrower than the broader bands used on satellite systems. Spectral distortion caused by water vapour and aerosols in the atmosphere was not an issue because the DMSI was acquired from a low-flying aircraft under cloud-free and clear sky conditions.

Table 2.1. Vegetation indices used in this study

Vegetation Index
NDVI=(NIR-RED)/(NIR+RED)
after Rouse et al. (1974), Deering and Rouse (1975) and Huete (2002)
REEI= NIR/RED
after Sims and Gamon (2002), Gitelson and Merzlyak (1996)
SAVI =(1+L)(NIR-RED)/(NIR+RED)+L
where L is a canopy background factor accounting for 780 nm and 675 nm extinction through the canopy and L = 0.5 after Huete et al. (1994).

2.4.4 Crown-condition classification

Crown-condition metrics were assessed in 5-unit increments by trained forestry professionals. The metrics are combined into a single continuous variable, the Total Crown Health Index (TCHI), which quantifies condition as a function of the density, distribution and gappiness of foliage in the horizontal and vertical. This crown-condition classification scheme is intentionally simplistic and the quintile classes mask inherent observational error in the *in-situ* assessments. TCHI is defined as

$$TCHI = \frac{C + F + D + E}{4} \tag{1}$$

Table 2.2. Classification thresholds used to model the vegetation indices NDVI, REEI, SAVI and *in-situ* TCHI assessments to the tree condition classes (1–5).

Class	NDVI	SAVI	REEI	TCHI
5	0.308−0.409	0.467−0.620	2.222−2.572	81–100
4	0.206−0.307	0.313−0.466	1.871−2.221	61–80
3	0.104−0.205	0.159−0.312	1.520−1.870	41−60
2	0.002−0.103	0.005−0.158	1.169−1.519	21−40
1	−0.100−0.001	−0.149−0.004	0.818−1.168	1−20

Condition assessment scores were binned into quintiles decreasing from healthy (5) through to declining (1). Each TCHI quintile covers a 20-unit range, for example, 5 represents a crown of approximately 80–100% of its ideal (assumed to be a 100% foliated, healthy specimen). The model is described in table 2.2 and can be calculated by applying thresholds to each of the vegetation indices using their standard deviations (see table 2.3).

2.4.5 Statistical analysis

A least squares linear regression was conducted using the 2008 TCHI and mean crown VI to establish the relationship between them and assess whether the uncertainties in the data would best suit regression or classification. The normality and distribution of each mean crown VI was examined in order to quantitatively assess these relationships. Summary descriptive statistics of minimum, maximum, mean, lower control limit (LCL) mean, upper control limit (UCL) mean, variance, standard deviation, skewness and kurtosis were derived for each set of mean crown values for both years.

Table 2.3. Descriptive statistical summary of the vegetation indices calculated from the 2008 and 2010 DMSI.

	2008			2010		
Statistic Name	**NDVI**	**REEI**	**SAVI**	**NDVI**	**REEI**	**SAVI**
Minimum	−0.079	0.854	0.117	−0.036	0.930	−0.054
Maximum	0.394	2.301	0.589	0.450	2.635	0.673
Mean	0.243	1.680	0.364	0.274	1.809	0.409
LCL mean	0.223	1.613	0.331	0.250	1.723	0.373
UCL mean	0.264	1.748	0.395	0.298	1.896	0.445
Variance	0.009	0.092	0.020	0.012	0.150	0.026
Standard deviation	0.094	0.303	0.140	0.108	0.387	0.162
Skewness	−1.227	−0.459	−1.223	−0.914	−0.220	−0.911
Kurtosis	2.087	0.190	2.075	0.580	−0.320	0.574

Note: Each statistic is a mean of all pixels across all crowns.

2.5 Results

2.5.1 DMSI vegetation indices

A mean NDVI, SAVI and REEI intensity value of all in-crown pixels was calculated for the 80 tuart crowns, for 2008 and 2010 (table 2.3), and the density function generated (refer to figure 2.3(a)–2.3(c)). REEI features the most normalized distribution whilst NDVI and SAVI are closely correlated. REEI is the least skewed (table 2.3) and has the lowest kurtosis. The skewness and kurtosis of both NDVI and SAVI are similar despite significant difference in the UCL and LCL means (table 2.3). Both NDVI and SAVI, as normalized indices have some negative values. As is to be expected from a simple ratio, REEI has the highest range of all three across both years. Analysis of the mean, median and maximum peak of NDVI and SAVI (table 2.3) shows the classic saturation of VI near their upper limit. This feature is less evident in REEI, consistent with its more normalized distribution, skewness and kurtosis.

2.5.2 Regression and classification

In order to determine the goodness of fit of the continuous variable, TCHI to each of the VI, a least squares linear regression was conducted on the entire sample (n = 80). This produced coefficients of determination (R^2), p values (p) and residual standard errors (RSEs) of $R^2 = 0.54$ ($p < 0.0001$, RSE = 0.07) for NDVI, $R^2 = 0.54$ ($p < 0.0001$, RSE=0.11) for SAVI and R^2=0.53 (p<0.0001, RSE=0.24) for REEI. Outliers were removed (based on residual distance) and $R^2 = 0.72$ ($n = 62$, $p < 0.0001$, RSE = 9.60) were derived for all three VI. Regression analysis was not pursued further and the data were further explored for classification.

The probability density function plots (figure 2.2(a)–2.2(c)) compare the VI to TCHI and can be used to visually understand the statistical differences (tables 2.2 and 2.3) in the distribution of each VI. Figure 2.2(a) NDVI and 2.2(b) SAVI feature sharp density peaks (saturation) in the upper limits and is a direct result of their higher skewness and kurtosis compared with REEI. It follows that the more normalized REEI (figure 2.2(c)) is more bell shaped and evenly distributed across its full range.

Compared directly against TCHI, NDVI and SAVI (see figure 2.3(a) and 2.3(b)) predict the healthy classes better than REEI (see figure 2.3(c)) because of their saturation in this region. Generally, NDVI and SAVI performed similarly, with insignificant differences between their distributions. Both NDVI and SAVI predicted classes 1, 2 and 5 poorly (i.e. the tails of the distribution), whilst REEI did not predict the mid range classes (see figure 2.3(c) classes 3, 4) as accurately as NDVI and SAVI, the tails of REEI's distribution were predicted more accurately and the net result is a more robust prediction of the range. REEI was selected as the preferred VI for subsequent analysis.

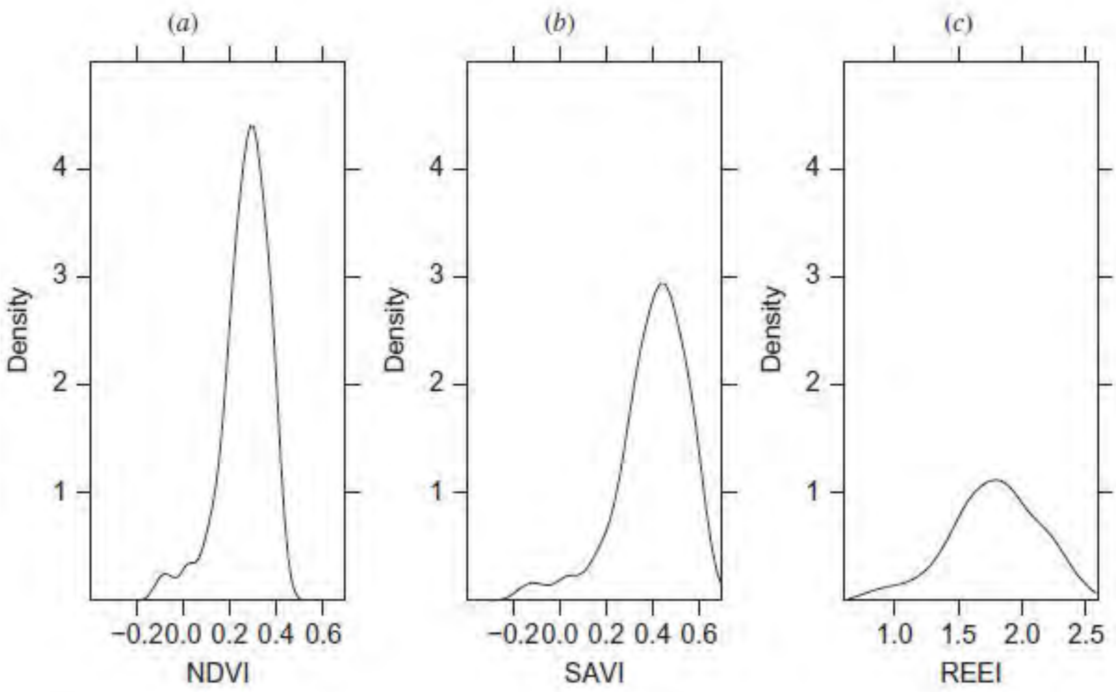

Figure 2.2. Sub-plots (a) NDVI, (b) REEI and (c) SAVI are density functions derived from the mean in-crown DMSI VI pixel intensity values from all 80 tuart crowns.

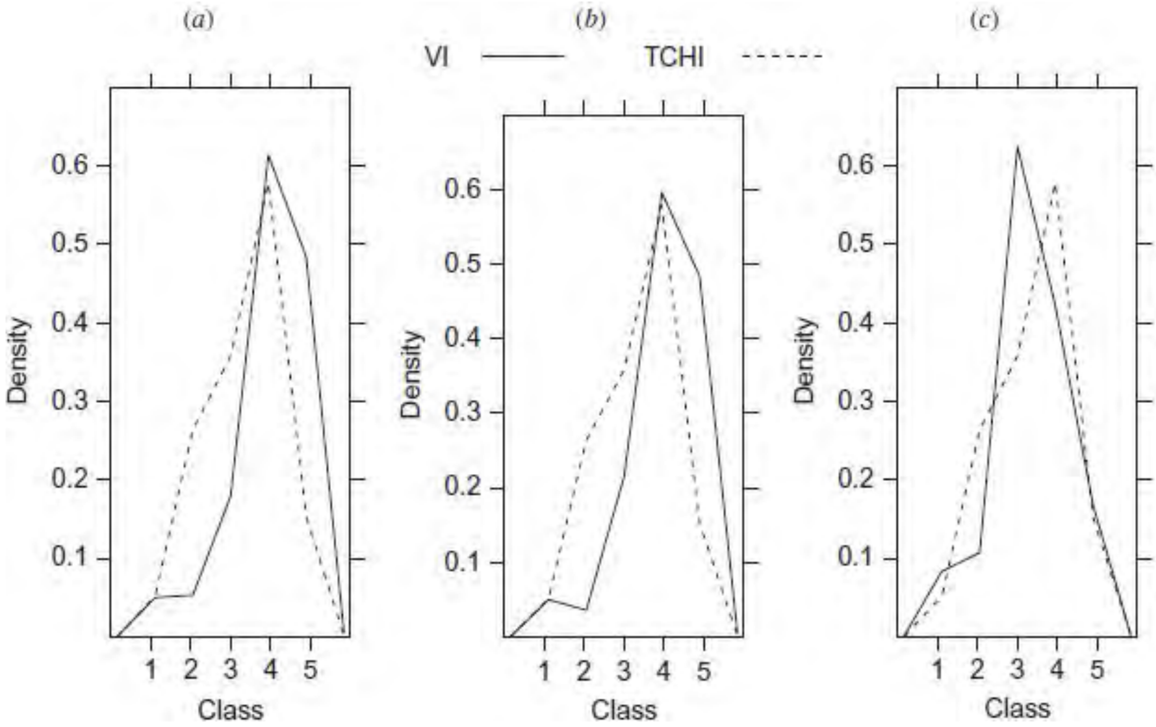

Figure 2.3. Density functions indicating the difference between the TCHI derived from the mean in-crown pixel values of 80 tuart crowns (dashed lines) from each vegetation index (solid black lines): NDVI (a), SAVI (b) and REEI (c).

2.5.3 Condition change between 2008 and 2010

Figure 2.4 shows the change in modelled condition class between the two scenes and is calculated from the mean in-crown pixel values of 80 tuart crowns using only REEI. There was a net reduction in mid range healthy crowns (from class 3 to class 2) and stability in all other classes.

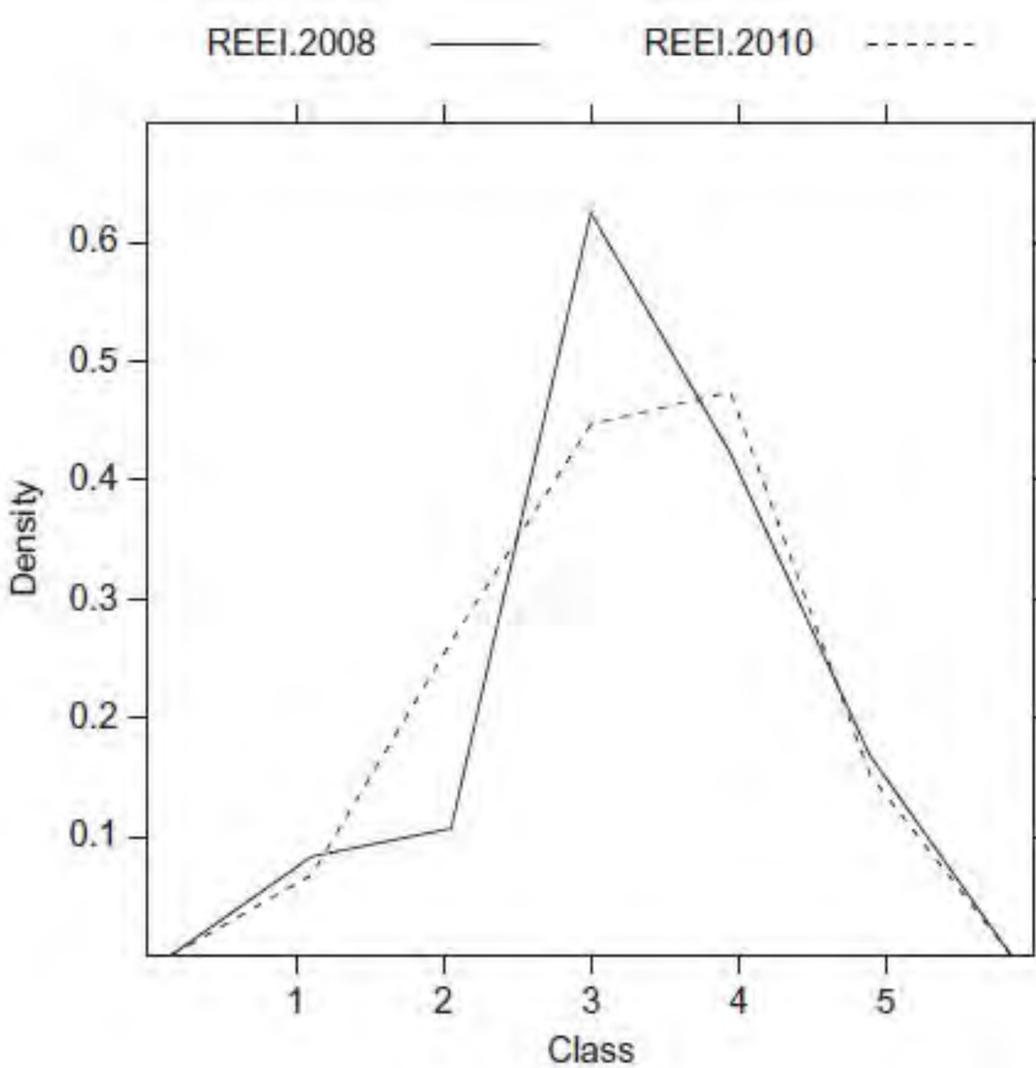

Figure 2.4. Probability density functions indicating the difference between classes predicted from the mean in-crown pixel values of 80 tuart crowns using REEI between 2008 (dashed line) and 2010 (solid line).

2.6 Discussion

These results suggest that it is practical to classify semi-quantitative tree health assessments to high-resolution DMSI. The uncertainties inherent in expert-based assessments present challenges in deriving linear models yet are suitable for classification applications with less precision than a continuous variable (i.e. THCI).

Similarly, potential changes between assessment and image acquisition, and registration errors could also contribute to this uncertainty. No significant differences were found between the three VI assessed in this study (NDVI, SAVI and REEI) suggesting that the underlying spectral information (i.e. RED and NIR bands) was more critical than the difference between the ratio-based (REEI) and normalized indices (NDVI and SAVI).

In addition to reducing pixel variance effects, the object-based approach, which makes the crown objects the carriers of the underlying spectral information, enhances statistical processing performance. Whilst this is advantageous in the laboratory, the fieldwork required to manually delineate crowns is both time-consuming and expensive. Recent studies using Object-Based Image Analysis (OBIA) software, such as eCognition and ENVI EX, have been demonstrated to be a viable alternative for delineating crowns and the process is becoming commonly known as feature extraction or segmentation (Yu et al., 2006; Johansen et al., 2010; Ke et al., 2010).

The *in-situ* assessments chosen for this study are not novel; there are numerous methodologies for assessing canopy density, density of foliage across the crowns canopy and foliage distribution, and much work has already been done on validating these for eucalypts (Stone and Haywood, 2006). Recent work of Horton et al. (2011) found that crown denisty (C) and the epicormic index (E) were the best-performing indicators of crown condition. Horton et al. (2011) also studied only 80 tuart in Yalgorup, from another patch of tuart in the vicinity of these sites. The strong positive correlation results suggest that the TCHI is a good indicator of condition for comparsion with high-resolution DMSI using REEI and is a simple, computationally efficient approach.

2.7 Conclusion

It is concluded that high-resolution DMSI is suited to tree health applications of crown-condition classification. It was found that REEI has the largest range of all three indices, and this provided greater flexibility for quantile classification against tree health classes. The VI and ground-based assessment techniques presented provide a means of assessing changes to individual tuart crowns over time, making annual to seasonal change detection of tree decline possible at the individual tree scale providing a species-and classification-specific training data set is used and that the sample size is sufficient.

CHAPTER 3
ENHANCING A EUCALYPT CROWN CONDITION INDICATOR DRIVEN BY HIGH SPATIAL AND SPECTRAL RESOLUTION REMOTE SENSING IMAGERY

3.1 Overview of author contributions

This Chapter builds on the first aim, thereby addressing the second aim of enhancing the complexity of the methodology and extending the image analysis to the use of textural, spectral and geometric variance to improve the relationship between the Total Crown Health Index (TCHI) and high resolution digital multi-spectral imagery (DMSI). Accordingly, compared to the first chapter, greater detail into the methodology behind the *in-situ* assessments, image acquisition and data analysis is provided. This Chapter was published as Evans, B., Lyons, T., Barber, P., Stone, C., and Hardy, G. (2012b). "Enhancing a eucalypt crown condition indicator driven by high spatial and spectral resolution remote sensing imagery." J. Appl. Remote Sens., 6.

Treating each *E. gomphocephala* crown as an object, this enhanced approach summarizes the pixel data into mean crown indices assigned to crown objects which became the carrier of information. Random Forest, a machine learning algorithm, was used to determine which combination of the textural, spectral and geometric indices best described the variances in the condition and health of the *E. gomphocephala* tree crowns. In addition to the use of the same DMSI scenes used in Chapter 2, a third year (2007) of DMSI was used to assess changes in TCHI back through time. The results are indicative of declining and recovering trends in eucalypts. A condition reduction (i.e. decline) in the healthiest class was found between 2008 and 2010 and the results are compared to the previous chapter.

Evans wrote all sections of this chapter, performed all of the statistical modeling, data processing and image analysis. Evans prepared the manuscript for publication. It utilizes the same dataset, made by Barber, as was used in Chapter 2. The work of Barber was funded from the Australian Research Council (LP0668195) with additional support from Department of Conservation and Environment, Alcoa of Australia, Mandurah City Council and Bemax Cable Sands. Honey, Stone and Coops provided guidance on the development of the methodology and reviewed previous drafts of the chapter. SpecTerra Services Pty Ltd, Perth provided the DMSI imagery and the work was supported by iVEC (http://www.ivec.org) through the use of super-computing facilities. Primary supervisor, Lyons provided support throughout the development and draft stages. Co-author Hardy contributed continuous review of the work.

3.2 Abstract

The condition of *E. gomphocephala* tree crowns was assessed on the ground and using two condition classification models to understand changes in forest health, tree by tree, through space and time. Using high resolution (0.5 m) digital multispectral imagery, predictor variables were derived from textural, spectral and geometric variance characteristics of all pixels inside the crown area. The results estimate crown condition as a surrogate for tree health against the total crown health index, derived from combining ground based crown condition assessment techniques that assess the density and transparency of the crown as well as the dieback and regrowth of foliage. This object based approach summarizes the pixel data into mean crown indices assigned to crown objects which became the carrier of information. Models performed above expectations, with substantial and significant weighted Cohen's kappa ($\varkappa > 0.60$ and $p < 0.001$) using 70% of available data and accuracy increased accordingly. Using all available 2008 *in-situ* data for model development, crown condition was predicted forwards (2010) and backwards (2007) in time. The results are indicative of declining and recovering trends and a condition reduction in the healthiest class between 2008 and 2010.

3.3 Introduction

Quantitative indicators of tree crown condition across large areas are a management imperative and critical for the assessment of ecosystem biodiversity, health and function (Coops et al., 2008; Bastin et al., 2002). Australia's eucalypt forests and woodlands cover a diverse range of ecosystem structure and biodiversity. Declines in these ecosystems have been linked to insects and fungi (Hooper and Sivasithamparam, 2005), pathogens (Scott et al., 2011), fire frequency (Close et al., 2011) and fauna (Haywood and Stone, 2011). In southwestern Australia, some eucalypt species have shown evidence of decline, especially *E. gomphocephala* (tuart) which dominates the dune systems of the Swan coastal plain (Boland et al., 2006). Tuart declines have been linked to soil bacterial communities (Cai et al., 2010), pathogens (Scott et al., 2011), fire patterns and severity (Archibald, 2006; Archibald et al., 2010; Close et al., 2009) and a range of potential causes have been considered (Edwards, 2002). Symptoms of decline manifest as a reduction in the abundance, distribution and greenness of foliage (dieback) within the tree crown and an overall reduction of vigor and condition (Jurskis, 2005). This dieback can ultimately lead to mortality despite eucalypts being well adapted to extreme climate variability (Harper et al., 2005).

Ground-based, or *in-situ*, forest condition assessments are a common method for assessing changes in health over time (Stone et al., 2003; Souter et al., 2010). These techniques however are often subjective, semi-quantitative and given the size and remoteness of the forest resource, labor intensive and time consuming (Souter et al., 2010). As a result regular monitoring of forest condition over time is difficult yet is a management imperative under changing climatic and land use pressures.

Remote sensing methods and imagery from space borne or airborne platforms offer an alternative and cost-effective means of assessing forest condition over large areas in a way that is spatially explicit and repeatable through time (Kerr and Ostrovsky, 2003; Coops et al., 2004; Zarnoch et al., 2004). Across Australia, forests and woodlands are monitored annually using moderate spatial resolution sensors, such as Landsat, with images acquired in summer when the influence of the understory (grasses and herbs) is at its lowest (Caccetta et al., 2007; Wallace et al., 2004). The spatial resolution of the Landsat Thematic Mapper (TM) sensor limits the capacity to detect individual tree crowns and in-crown foliage variability whilst the broad spectral bands reduce its capacity to detect small changes in leaf pigments and structure.

Alternatively airborne high spatial resolution remote sensing imagery offers greater flexibility in image acquisition, the capacity to detect individual crowns and crown architecture and the ability to vary spectral wavelengths depending on the characteristics of the target. Conventionally, spectral information is used independently as a vegetation index (VI) to predict condition, such as the density of foliage. The most common VI is the normalized difference vegetation index (NDVI). VI's summarize spectral information from specific regions of the electromagnetic spectrum known to be sensitive to the interactions between light and leaf pigments (often mostly chlorophyll) (Pinar and Curran, 1996; Barry et al., 2008; Pietrzykowski et al., 2006). In high resolution data, where many pixels are captured across individual crowns, the spectral characteristics of neighboring pixels was highly variable and as a result, statistics produced in the spatial domain may yield more reliable estimates of crown condition than spectral indicators alone (Woodcock and Strahler, 1987). A number of techniques exist to measure the variation of spectral and spatial properties of remotely sensed images including texture and geometric measures.

Stone and Haywood (2006) demonstrated the use of a eucalypt crown condition index derived from remote sensing observations over areas of eucalypt dieback in New South Wales. The approach utilized high spatial resolution digital imagery linked to five key indicators of canopy decline. More recently (Evans et al., 2012a) demonstrated that a similar index could be used to predict crown dieback in Western Australia from remote sensing imagery. The results indicated the crown condition could be accurately modeled using the spectral properties of the imagery with significant coefficient of determination (R2) values developed from linear regression models ranging from 0.54 to 0.72.

The objectives of this study were threefold. Firstly, we evaluated the additional power of texture and geometric based indices to predict canopy condition across crowns exhibiting dieback in the Yalgorup National Park of Western Australia. Secondly we applied an innovative modeling approach, Random Forests (RF), a non-parametric, ensemble classifier, to assess the impact of varying the number of predicted canopy condition classes with the aim of developing accurate and robust indicators for forest managers. Lastly, with confidence in the developed models, we then applied them to images acquired before and after the *in-situ* assessments to better understand how the condition of these crowns has changed over time.

3.4 Methods

3.4.1 Region of Interest

The Yalgorup National Park, in southwest, Western Australia, is situated 80km south of the capital, Perth. The sites were located within the Yoongarillup, Karrakatta and Cottesloe vegetation complexes, based on their geological associations (Heddle et al., 1980). The majority of the sites were found on the Yoongarillup complex, comprised of *E. gomphocephala* (tuart), with a mid-storey of *Agonis flexuosa*, *Allocasuarina fraseriana*, *Banksia grandis*, *B. attenuata*, *B. littoralis* and an understorey of *Acacia saligna*, *A. pulchella*, *Jacksonia sternbergiana*, *Melaleuca acerosa* and *Hibbertia hypericoides* (Portlock et al., 1993). Tuart is listed by the

International Union for the Conservation of Nature as IUCN category II species and Yalgorup National Park is an area of high natural biodiversity value.

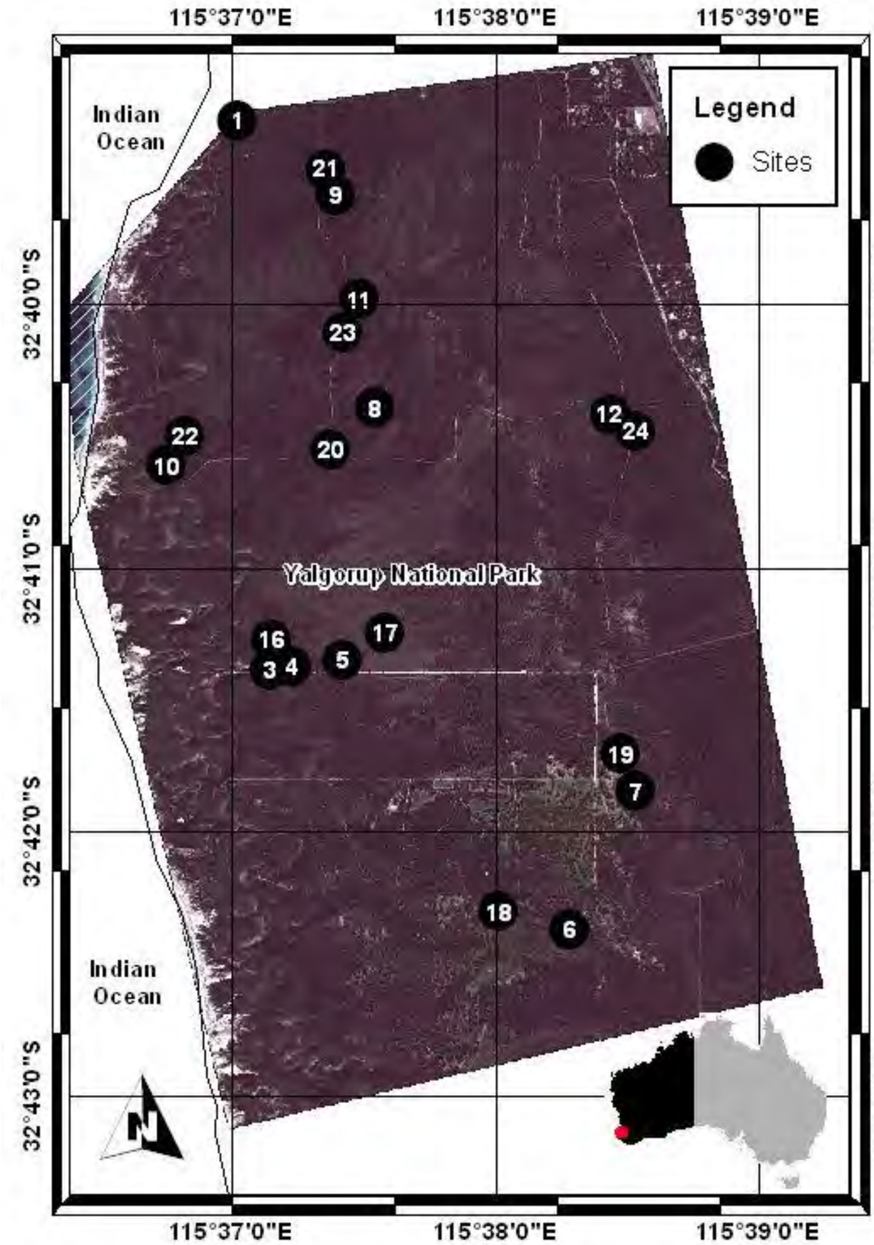

Figure 3.1. Map of the study area overlaid with a true colour version of the DMSI for 2008 and the study sites (irregularly numbered).

3.4.2 Crown Condition Assessment

The placement of crown condition plots within the national park was based on a stratification of vegetation trend classes derived from a 15-year (1990 – 2005) time series analysis of Landsat TM imagery based on the methodology of (Caccetta et al., 2007). A total of 20 sites were established in 2007 and in June 2008 the crown condition of four randomly selected tuart crowns within each of the 20 sites was individually assessed by two forest health professionals.

Each crown was assessed for four crown condition indices, based on previous research of (Barry et al., 2008) and recently discussed in (Cai et al., 2010; Evans et al., 2012a; Horton et al., 2011). The condition indices were measured in 5% classes across a 0 – 100% scale and included (i) Crown Density (CD), (ii) Foliage transparency (FT) (USDAFS, 2002; Schomaker et al., 2007) , (iii) Crown Dieback Ratio (CDR) and an (iv) Epicormic Index (EI) (Kile et al., 1981; Wardlaw, 1989) .

The two trained forest health professionals stood at right angles to each other, facing the tree at a distance from the main stem greater than its height. Two assessments were assumed to be more robust than a single observation and were averaged for an overall value. All four indices were then combined to produce the Evans et al. (2012a) Total Crown Health Index (TCHI). In addition to the assessment, the plot center, corners and the location of each individual crown was mapped using a differential GPS (dGPS).

3.4.3 Image Specification and Acquisition

High spatial resolution airborne Digital Multi Spectral Imagery (DMSI) was acquired by SpecTerra Services Pty. Ltd. (Perth, Western Australia) in May/June

2007, 2008 and 2010 under clear conditions (Table 3.1). During acquisition all DMSI was georeferenced based on GPS and subsequent post-flight processing of the data included band to band registration and spectro-radiometric correction for bi-directional reflectance distribution function (BRDF) variations. All imagery was acquired at 0.5 m resolution from an altitude of 2000 m. Once collected all the imagery was mosaicked, orthorectified and pixel matched to correct for the sun angle differences of each overpass (Table 3.1).

Table 3.1 Details of the multi-year acquisition flights made by SpecTerra Services.

Date	**Solar angle**
May 08, 2007	39.18° - 40.08°
June 06, 2008	34.01° - 34.60°
June 02, 2010	34.74° - 35.03°

The DMSI sensor acquires 12-bit digital number (DN) data simultaneously in four 20nm wide spectral channels in the visible and near-infrared regions of the electromagnetic spectrum using filters centered at 450, 550, 675, and 780nm covering blue, green, red and near infrared regions of the spectrum, respectively.

To ensure the relative radiometric consistency of the imagery over the three time periods a `like-value' calibration was undertaken using methods described by (Furby and Campbell, 2001). The method normalizes each scene to a 'base year' standard using a set of objects identifiable on all images and deemed to be invariant spectral targets (such as roads, deep water, exposed soil, and sand). Given the *in-situ* data were collected in 2008, this was chosen as the base year. For each invariant target a mean spectral value in all bands was extracted and matched using a simple regression approach which was then subsequently applied to the 2007 and 2010 images.

Visual inspection of the crown dGPS delineations on the imagery confirmed that the crowns were all well located. In a small number of cases crown locations were aligned to better fit the imagery. The *in-situ* crown condition assessment data were collated and spatially linked to the crowns in the imagery and crown perimeters formed a tree crown mask. Spectral values within each tree crown were then extracted for calculation of vegetation, pattern and geometric indices.

3.4.4 Index generation

3.4.4.1 Textural, spectral and spatial indices

A total of 125 indices were selected based on (a) the available spectra, (b) literary precedence and (c) open source availability of the algorithms. Indices fit into three broad categories of spectral (Table 3.2), textural (Table 3.3), and geometric (the area displaced by the crown by counting the number of pixels inside the delineated crown area).

The VI's used in this study (Table 3.2) fall into two broad categories (a) narrow-band versions of the Normalized Difference Vegetation Index (NDVI) and (b) simple ratios.

Table 3.2. Vegetation indices used in this study. NDVI= Normalized Difference Vegetation Index, mNDVI= modified Normalized Difference Vegetation Index, SR= Simple Ratio, REEI= Red Edge Extrema Index, mEVI= modified Enhanced Vegetation Index, SAVI= Soil Adjusted Vegetation Index, mARVI= modified Atmospherically Resistance Vegetation Index, RGRI= Red Green Ratio Index, mARI1= Anthocyanin Reflectance Index 1, mARI2=Anthocyanin Reflectance Index 2 and TVI= Transformed Vegetation Index.

Vegetation Indices
$NDVI = \frac{(NIR - RED)}{(NIR + RED)}$
$mNDVI = \frac{(NIR - RED)}{(NIR + RED) - (2 \times BLUE)}$
$SR = \frac{RED}{NIR}$
$REEI = \frac{NIR}{RED}$
$mEVI = G\frac{(NIR - RED)}{(NIR + C_1 \times RED) - C_2 \times BLUE + L}(1 + L)$
$where\ G = 2.5, C_1 = 6.0, C_2 = 7.5, L = 10$
$SAVI = \frac{(1 + L) \times (NIR - RED)}{(NIR + RED + L)}$
$where\ L = 0.5$
$mARVI = \frac{NIR - RB}{NIR + RB}$
$where\ RB = RED - \gamma(BLUE - RED), \gamma = 2.0, L = 0.5$
$RGRI = \frac{RED}{GREEN}$
$mARI1 = \frac{(GREEN - 1)}{(RED - 1)}$
$mARI2 = NIR\frac{(GREEN - 1)}{(RED - 1)}$
$TVI = 0.5(120(NIR - GREEN) - 200(RED - GREEN)$

Texture indices can be further divided into two sub groups, the Grey Level Covariance Matrix Textures (GLCM) and Grey Level Difference Vector Textural Indices (GLDV). Textural indices were calculated from the covariance between neighboring gray levels in an image. Rectilinear polygons were formed around each object with a one pixel buffer to extract the GLCM. Each GLCM was calculated for each object in the four cardinal directions. Each resulting GLCM was then cropped and all four directions averaged by band.

Once the individual indices were computed, a mean for each was calculated for the 80 tuart crowns and this dataset formed the basis of the modeling described below. The GRASS r.texture package was used to generate the textures (Haralick et al., 1973; Haralick, 1979).

Table 3.3. Textural indices used in this study. Pi,j represents the intensities of the pixel samples of i and j in the moving window (matrix), their spatial location depends on the cardinal direction of the grey level covariance matrix parameterization. Figure 3.2 provides an example of a true colour DMSI image with four tree crown delineations overlaid and an example of two texture measures for an individual crown. The figure shows the marked variation within each crown, as well as the variation through time.

Name	Equation
Homogeneity	$HOM = \sum_{i,j=0}^{N-1} \frac{P_{i,j}}{1+(i-j)^2}$
Contrast	$CON = \sum_{i,j=0}^{N-1} P_{i,j}(i-j)^2$
Entropy	$ENT = \sum_{i,j=0}^{N-1} P_{i,j}(-lnP_{i-j})$
Difference Entropy	$DEN = \sum_{k=0}^{N-1} P_k(-lnP_k)$
Variance	$VAR = \sigma_{i,j}^2 \sum_{i,j=0}^{N-1} P_{i,j}\left(i,j - \mu_{i-j}\right)$ $where\ \mu_{i-j} = \sum_{i,j=0}^{N-1} \frac{P_{i,j}}{N^2}$
Correlation	$COR = \sum_{i,j=0}^{N-1} \left[(i-\mu_i)(j-\mu_j)\sqrt{(\sigma_i^2)(\sigma_j^2)}\right]$

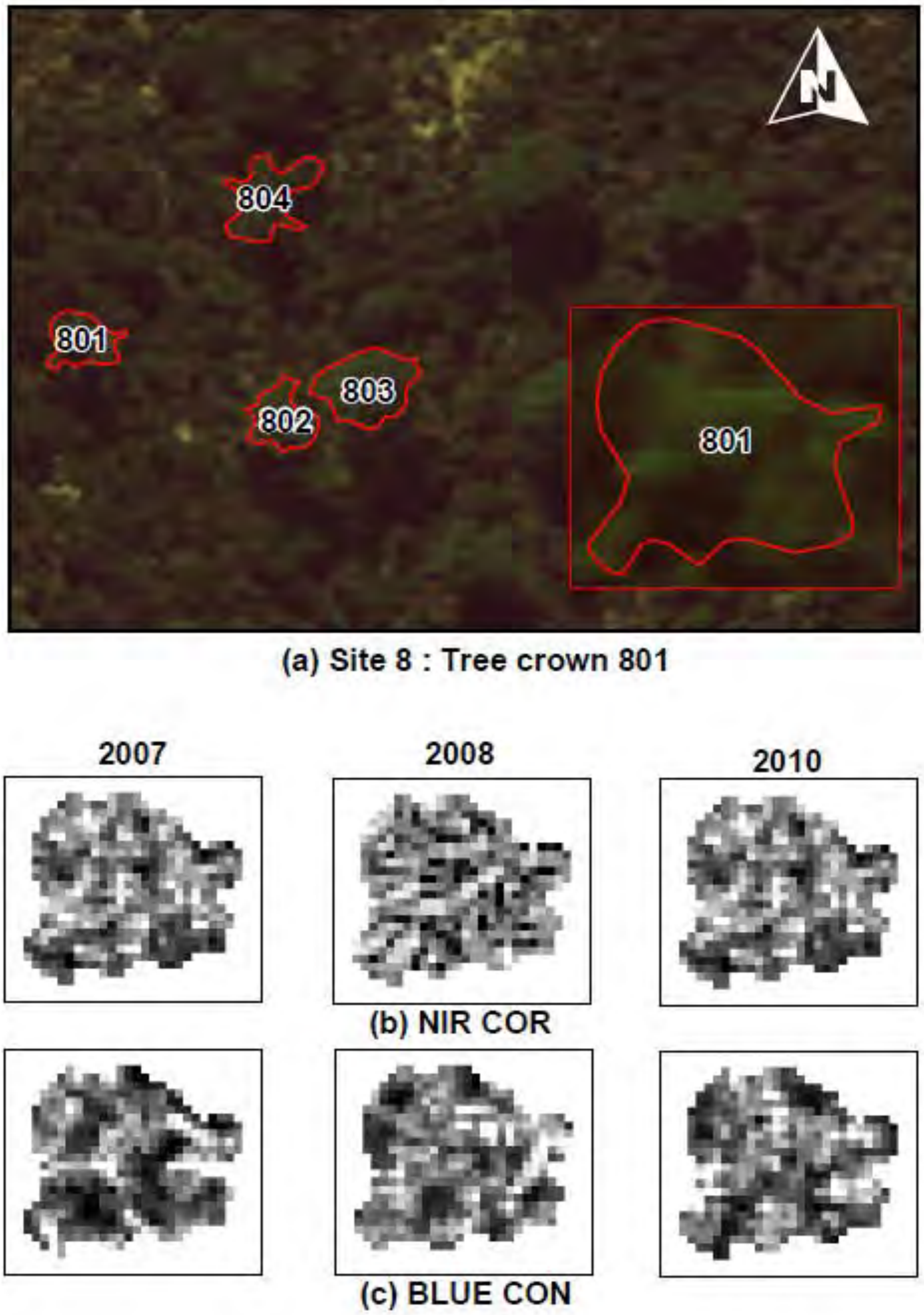

Figure 3.2. Map of site 8 featuring the delineated tree crowns (a) and two examples, (b) and (c) of textural crown matrices from which mean crown textural indices were derived. The example indices shown for crown 801 are (b) Correlation (COR) for the 780nm (NIR) band and (c) Contrast (CON) for the 450nm (BLUE) band and each group contains an image from 2007, 2008 and 2010.

3.4.5 Modeling Approach

The Random Forest (RF) algorithm (Breiman, 1996, 2001) is an ensemble classifier that fits decision trees (models) to sub-samples of training data, then combines predictions from the resulting trees. The algorithm bootstrap samples the training data and approximately 63% of the original observations are used at least once in model development. Data not included in the bootstrapped training sample are called out-of-bag observations. In addition to the randomness of the bootstrapping, the number of variables sampled at each decision tree node is randomly selected from a subset of predictors; by default the number tried (mtry) is the square root of all available predictors (Breiman, 2001). In this study, mtry is parameterized using the tuning function provided in the R implementation of RF by (Liaw and Wiener, 2002; Prasad et al., 2006) as is commonplace for RF applications with many predictor variables. The variable importance score is used to assess the contribution made by each of the spectral, texture and geometric remotely sensed variables made in the resultant RF classification models. Variable importance in RF is the normalized difference classification accuracy of each predictor, both when it is included as an observation and when it has been randomly permuted (Breiman, 1996, 2001).

RF was chosen because it has been shown to have superior predictive power in a number of classification studies (Bosch et al., 2007; Lawrence et al., 2006; Pal and Mather, 2003; Prasad et al., 2006; Cutler et al., 2007) and validated against a number of statistical modeling approaches for ecological (Cutler et al., 2007) and vegetation health modeling applications (Haywood and Stone, 2011).

The 2008 vegetation, texture and geometric indices were related to the *in-situ* crown assessments both individually, and for the combined TCHI score.

To assess the accuracy of the predictions and the robustness of the relationships two representations of the *in-situ* crown condition indices were used. The first reduced the THCI score to 10% increments, resulting in a 10 class variable. This level of aggregation is consistent with the measurement protocols discussed earlier. We recognize that as a practical management tool most forest condition assessment indices are applied across a five class scale, so a second analysis was undertaken which reduced the THCI score to 20% increments to give five classes.

To understand the robustness of the developed models, the relative size of the model development versus model testing datasets was varied from 10% to 100% with 10% indicative of a model which was developed using 10% of the data and tested on the remaining 90%, and a 100% model indicative of a model developed using all observations. Each RF was run 100 times for each split and the out of bag error (OOBE), and weighted Cohen's kappa coefficients (κ) were calculated (all were significant $p<0.01$), comparing the models predictions against the observations. κ is a statistical measure of inter-rater agreement between categorical data which accounts for a hypothetical probability of chance (Cohen, 1960; Cohen, 1968). Accordingly, $\kappa=+1$ represents complete agreement between observations and predictions and $\kappa=-1$ suggests there is no more agreement other than one would expect by chance. The Landis and Koch (1977) κ threshold scale (Table 3.4) provides a benchmark for interpreting the magnitude of κ in the context of the predictive strength.

Once the RF model was developed and assessed, the 100% data model was applied to the 2007 and 2010 imagery and changes in the crown condition index assessed.

Table 3.4 Weighted Cohen's kappa coefficient strength of agreement benchmarks after Landis and Koch (1977)

Weighted Cohen's kappa	Agreement
-1.00 - 0.00	Poor
0.00 - 0.20	Slight
0.21 - 0.40	Fair
0.41 - 0.60	Moderate
0.61 - 0.80	Substantial
0.81 - 1.00	Almost Perfect

3.5 Results

The κ scores were captured for the two models (Figure 3.3). A score is given for each of the 10 training and validation fractions (10%-100% in 10% increments) of the available data (n=80 tuart crowns across the 20 sites). As expected, κ increases as the fraction of data used for model development grows larger. Figure 3.4, a companion to Figure 3.5, shows the corresponding OOBE scores for the two models and expectedly, OOBE becomes smaller as the fraction of data used increases. In order to determine an ideal mtry parameterization, the (Liaw and Wiener, 2002) trainRF() method was used, and this resulted in mtry=6 for all models except the 10 class 30% and the 20 class 90% and 100% groups which were mtry=3.

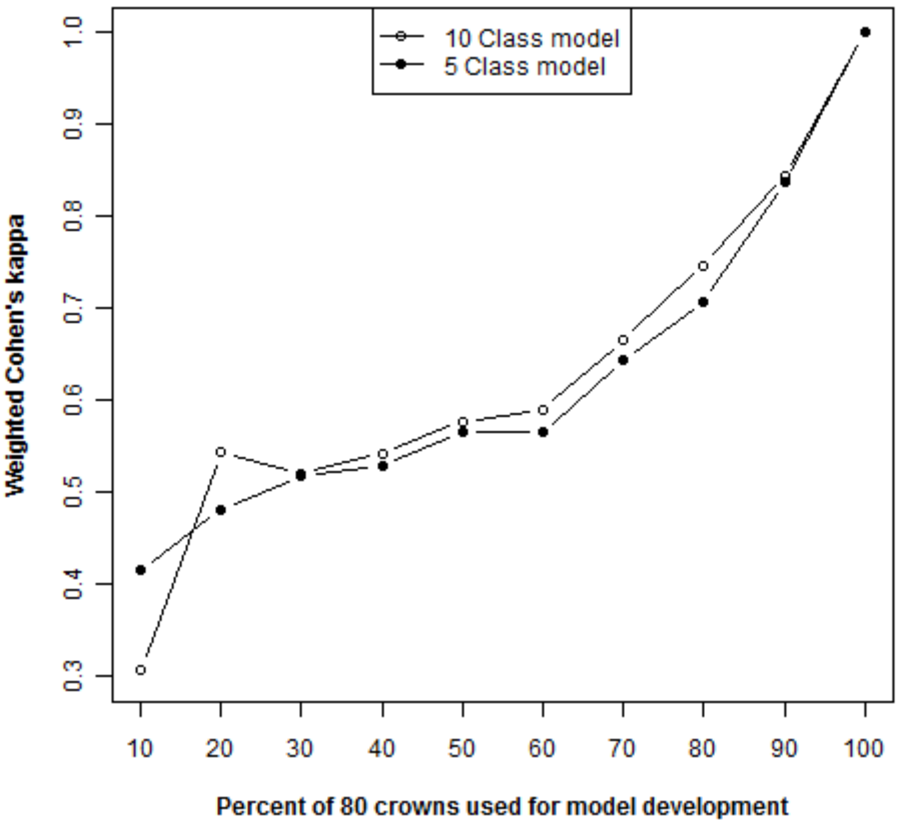

Figure 3.3 Comparison of the weighted Cohen's kappa for the 10 and 5 class models for each of the training and validation fractions used in the model development

Analysis of variable importance extracted from the 2008 100% training models (Figure 3.5) shows that the spectral and textural indices containing the 780 nm spectral band were most often selected in model development. The geometric index of the size of the crown was not a top 5 variable selected by any model. Generally, spectral indices containing the 675 nm and 780 nm bands were dominant. Although less frequently selected, the 450 nm and 550nm spectral bands were also important in both models.

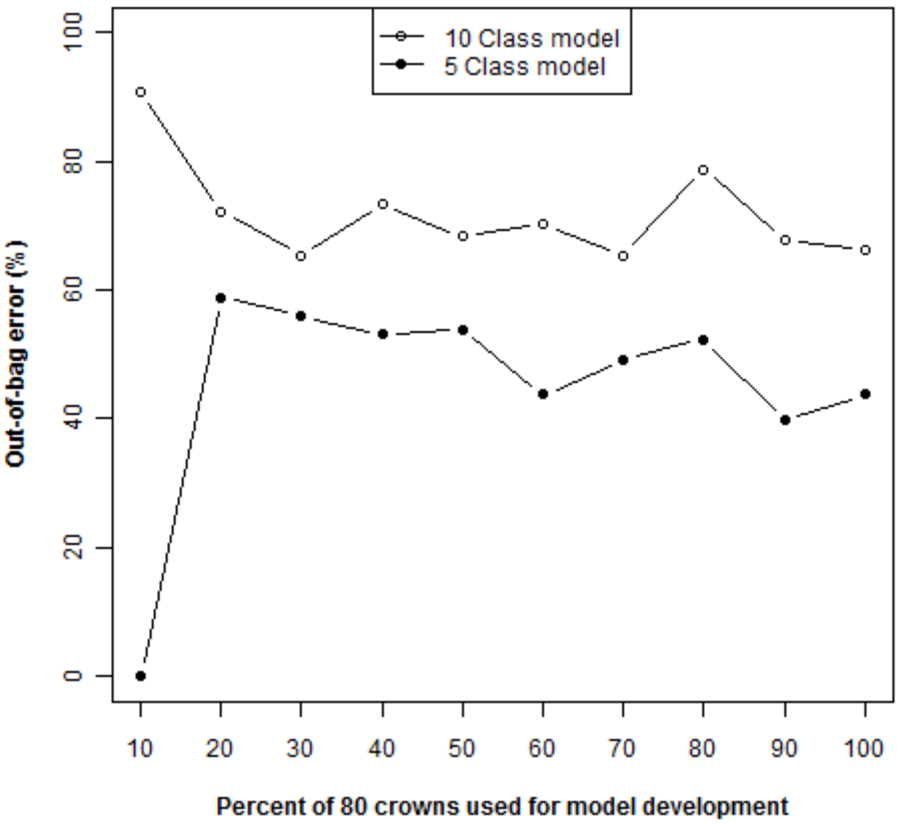

Figure 3.4 Comparison of the Random Forest out-of-bag error score for the 10 and 5 class models for each of the training and validation fractions used in the model development

Figure 3.6 and Figure 3.7 show the distribution of remote sensing derived THCI values of the 80 crowns for 2007, 2008 and 2010 using all the available 2008 data for model development. A shift of the distribution to lower classes (smaller number) is indicative of a decline in crown condition, whereas conversely a shift of the distribution to healthier classes (larger number) indicates of a recovery of condition. For example, Figure 3.6 shows some recovery between 2007 and 2008, with 10% of the crowns populating the healthiest class in 2008 that were not classified as class 5 in 2007.

Between 2008 and 2010 crowns contracted from both the least and most healthy classes to populate moderate health classes. The net result could be considered a recovery with the majority of crowns healthy, 60% were classified as class 4 (5 class model refer Figure 3.6) and class 7 (10 class model refer Figure 3.7) which represents a change of almost 20% from 2008 to 2010. Indeed, the least healthy classes 1 (Figure 3.6) and 1 and 2 (Figure 3.7) show continuous recovery between 2007-2008 but not complete recovery over this period. This suggests a recovery from disturbances (prior to 2007) can take a number of years to manifest. Conversely, the increased frequency of moderately healthy classes contributed by both additional healthy and declining crowns is indicative of the resilience of the species to dealing with, and recovering from dieback over many years.

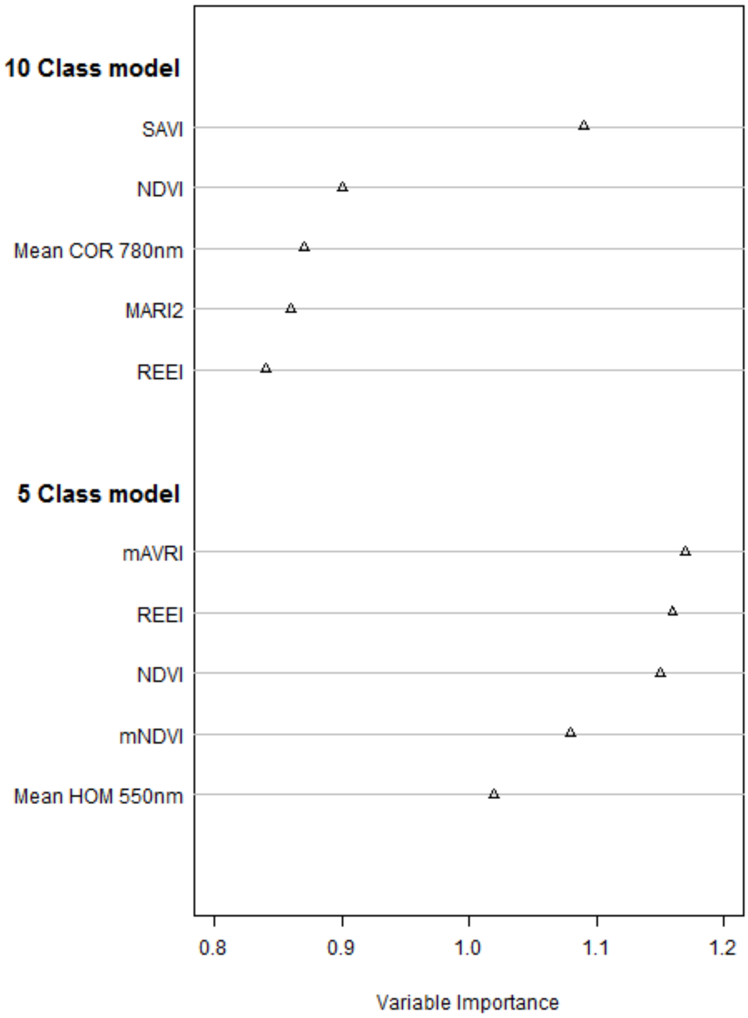

Figure 3.5 Top 5 variable importance from the models used to estimate the 2007 and 2010 TCHI scores using all available *in-situ* data (n=80) from 2008. SAVI= Soil Adjusted Vegetation Index, NDVI= Normalized Difference Vegetation Index, Mean COR 780nm is the mean Correlation of the 780nm (nir) spectral band, MARI2= Anthocyanin Reflectance Index 2, REEI= Red Edge Extrema Index, mAVRI= modified Atmospherically Resistant Vegation Index, mNDVI= modified Normalized Difference Vegetation Index and mean HOM 550nm is the mean Homogeneity of the 550nm (green) spectral band.

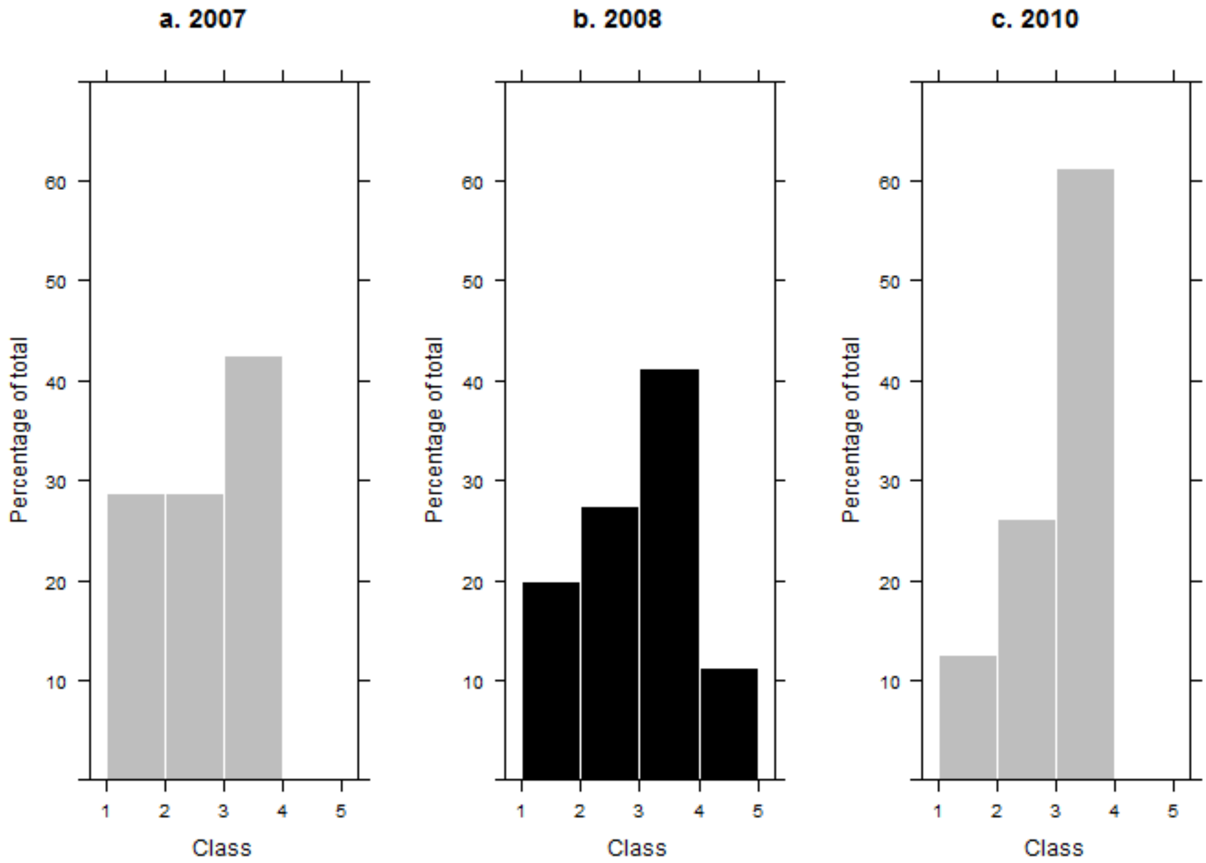

Figure 3.6 Histograms of the Total Crown Health Index (TCHI) classification using the 5 class model where 1=least healthy or declining (TCHI of 1-20%) and 5=most healthy (TCHI of 81-100%) predictions for 2007 (a) and 2010 (c) and the *in-situ* observations for 2008 (b). All percentages calculated using all available data (n=80).

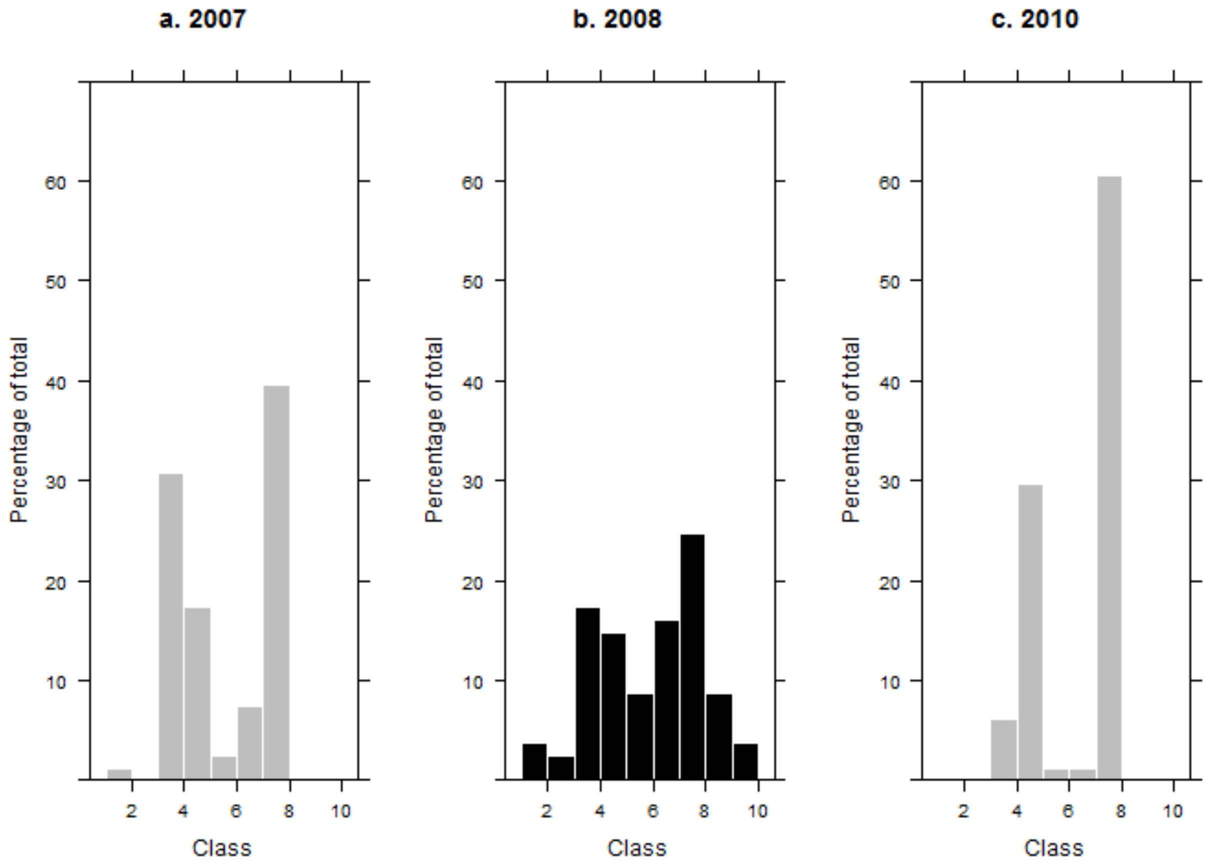

Figure 3.7 Histograms of the Total Crown Health Index (TCHI) classification using the 10 class model where 1=least healthy or declining (TCHI of 1-10%) and 10=most healthy (TCHI of 91-100%) predictions for 2007 (a) and 2010 (c) and the *in-situ* observations for 2008 (b). All percentages calculated using all available data (n=80).

3.6 Discussion

The remote sensing driven eucalypt crown condition indicator presented here provides insight into the extent and severity of tuart decline in Yalgorup National Park between 2007 and 2010. Crown condition shifts from the less healthy classes to healthier classes (2007-2008) and retracts back from the healthiest classes to moderately healthy classes (2008-2010). In the last year of observation, 2010, the majority of tuart (60%) are predicted to be of moderate health. These results are indicative of a combination of mild stressors impacting the condition of the tuart, a finding supported by recent evidence of pathogens (Scott et al., 2011) and soil bacterial communities (Cai et al., 2010), both slow acting agents, being linked to these declines. Eucalypt crown decline often occurs over a number of years rather than instantaneously, however, severe weather, in particular drought stress, pests and some diseases can cause rapid defoliation events from time to time. Generally, the condition of the dominant species is a surrogate for ecosystem condition health (Stone and Haywood, 2006) with crown condition becoming widely used as an indicator in land management policy for describing aspects of aesthetics, production and the biodiversity of ecosystems (Keith and Gorrod, 2006). Remote sensing driven techniques are increasingly useful in providing data to support the development of these critical indicators (Coops et al., 2008; Haywood and Stone, 2011a).

These results confirm an enhancement of the eucalypt crown condition indicator from (Evans et al., 2012a) and the RF variables importance results (Figure 3.6) indicate how this was done. Spectral and textural indices containing the 780 nm spectral band were most often selected. The evidence behind the use of the near infra-red, 780 nm spectral band for detecting and quantifying changes in foliage condition is well known (Coops et al., 2002, 2003; Stone et al., 2001). All of the VI's most commonly selected by the models utilized the 780 nm band in addition to 675 nm (red) which is a strong indicator of chlorophyll absorption. VI's containing 450 nm (blue) and 550 nm (green) were also important, and this suggests that variations in this part of the electromagnetic spectrum, for example green reflection and blue absorption, are being driven by changes in foliage condition. This strong relationship between the blue and green spectral bands is known to explain variance in crown chlorophyll content (Rabideau et al., 1946; Moss and Loomis, 1951; Lichtenthaler, 1987, 1996, 2001) and as a result of a shift in the location and position of the red edge from the red-nir to blue-green part of the electromagnetic spectrum as chlorophyll content decreases from leaf senescence or absence (Stone and Haywood, 2006; Pinar and Curran, 1996; Jago et al., 1999).

An interesting finding of this study is that as the number of increment classes changed from small (5 class) to large (10 class) the tendency of the RF to select texture based indices increased. This result implies that texture based measures allow finer levels of crown condition to be discriminated whereas spectral based indices allow for more broad scale canopy assessments.

The RF modeling approach used in this study allowed us to investigate two key aspects of the crown condition dataset. Firstly, as the RF modeling procedure is not computationally expensive, iterative modeling and the bootstrapping approach provides insight into the robustness of the developed models. The results indicate, as expected, that as a higher proportion of data is used in model development the overall accuracy of the model improves in both the 5 and 10 class datasets. Secondly, a typical jackknifing of the dataset into 70% for model development and 30% for independent model prediction in this study produces κ of 0.67 for the 10 class and 0.64 for the 5 class models, a substantial agreement on the Landis and Koch (1977) benchmark (Table 3.4), and similarly promising to reported accuracies of (Evans et al., 2012a) who applied standard linear regression of mean crown VI to classify condition. Both models achieve a κ of 0.84 when using 90% of the observations and κ=1 when all of the available data are used. It is important to note that given RF internally bootstraps, this means that when the models are developed using only 90% of the observations RF is actually using as little as 45 crowns.

Whilst RF is not a descriptive or inferential tool it is useful for identifying important ecological variables for interpretation (Cutler et al., 2007; Strobl et al., 2008). We have used RF variable importance to isolate useful spectral and textural indicators of crown health through classification and prediction of a categorical set of crown condition classes of the TCHI. RF is non-parametric, requires no distributional assumptions and can handle the ‘small n large p’ scenario demonstrated in this study, by the splitting the available data into incremental portions (Breiman, 2001; Liaw and Wiener, 2002). RF offers a robust, efficient and accurate alternative to parametric and semi-parametric methods for identifying ecological indicators.

As expected, when comparing the 10 to the 5 class datasets the results indicate the OOBE, a standard error indicator of RF’s internal predictive capacity, is higher for the 10 class when compared to the 5 class model confirming that a smaller number of crown condition classes produces a more accurate overall model (Breiman, 2001; Liaw and Wiener, 2002; Prasad et al., 2006; Svetnik et al., 2003; Díaz-Uriarte and de Andrés, 2006; Gislason et al., 2006; Evans and Cushman, 2009). The tradeoff between classification precision (number of classes) and model accuracy (OOBE and κ) is critical to its application as an indicator where it is likely a lower precision classification is sufficient for forest health management, given limitations to response options, and therefore greater accuracy would contribute to greater confidence in its application.

The development of remotely derived eucalypt crown condition indicators is imperative for the management of the large forested estates and to quantify changes in structure and health over time. High spatial and spectral remotely sensed data are a rich source of information for forest managers and as demonstrated in these results, can make accurate predictions of crown condition across a large number of plots and crowns. Critical to the success of this type of remote sensing data is the capacity to explicitly model changes in the biophysical properties of tree crowns, such as a reduction in chlorophyll and changes in crown structure such as defoliation.

In terms of the application of this technique to forest and woodland management the 5 class assessment could offer broad insights to overall canopy condition whereas the 10 class variable could offer potentially increased sensitivity to internal crown structure and condition. This additional sensitivity would be valuable, for example, when looking for evidence of the initial stages of eucalypt crown dieback and discerning the different agents involved in the declines.

As discussed, *in-situ* crown condition data collection is an expensive task and as a result remote sensing and modeling approaches could represent a potential cost saving through both limiting the number of site visits and reducing the sample size of crowns assessed in the field. We recognize that the assessment of 80 crowns across the national park for model development is relatively small and that, as this work continues, the collection of additional *in-situ* data is imperative, especially to test the predictions through time. Evans et al. (2012a) and Horton et al. (2011) however indicated that information on 80 tuart crowns was a suitable number for the assessment of canopy condition from the ground. In addition the capacity of the RF approach to allow investigation of both the number of classes, and the robustness of the relationships provides confidence in these results.

Finally, the collection of additional *in-situ* data and the use of remotely sensed mean crown statistics in the RF models required labour-intensive and expensive manual delineation of crowns both in the field and within the imagery. Future work will use Object Based Image Analysis (OBIA) software that has been demonstrated as an alternative to delineating crowns manually using processes such as feature extraction or segmentation. This process has been demonstrated on non-eucalypt biomes (Johansen et al., 2010; Yu et al., 2006; Ke et al., 2010) and eucalypt biomes (Haywood and Stone, 2011b), however, it has not been conducted at the crown scale on native eucalypts exhibiting advanced crown decline and will therefore present some challenges.

3.7 Conclusion

This study has demonstrated the application of RF models trained using remotely sensed spectral, textural and geometric indices to predict eucalypt crown condition and its change through time. The results indicate that two models, using 5 and 10 descriptor classes were accurate and robust and could represent a cost effective way of monitoring and quantifying crown condition of tuart over large areas within an operational environment. The results confirm that spectral and textural information in the 450, 550, 675 and 780nm spectral bands was critical in the model predictions and texture indices were more informative when increasing the sensitivity of the models to smaller variations in crown condition. Once validated, the models confirmed the overall condition of tree crowns within Yalgorup National Park declines from 2007 to 2010. This study has shown the potential exists for the use of this indicator of eucalypt crown condition indicator for monitoring changes in the crown condition of tuart and other eucalypt species in native and plantation forests.

CHAPTER 4
BIOCLIMATIC EXTREMES DRIVE FOREST MORTALITY IN SOUTHWEST, WESTERN AUSTRALIA

4.1 Overview of author contributions

This chapter was developed as a response to being witness to one of the most significant forest mortality events in recent history, namely the appearance of patches of mortality (POM) across the northern jarrah forest (NJF) following the extreme summer of 2010-2012. This chapter progresses in both spatial and temporal scales, from the inter-annual variance of individual tree crowns in Chapters 2 and 3 through to the monthly and inter-annual variability of the NJF. In doing so, this chapter is addressing the specific aim of applying data and methods relative to the spatial extent of the observed morality event, thereby enabling the use of climatology and remotely sensing high and moderate resolution imagery. This chapter has been published in the journal Climate.

This chapter combines state-of-the-art image analysis techniques (e.g. feature extraction) to detect and map the POM in high-resolution satellite data. Once the POM are spatially mapped, a range of bioclimatic indices are derived and investigated as potential drivers. This bioclimatic exposure analysis yielded a set of significant thresholds, the likely drivers of the mortality event. These bioclimatic thresholds are presented as a guide for future monitoring and modeling of the Northern Jarrah Forest ecosystem. Combined with chapters 1 and 2, this chapter presents a means of monitoring larger areas for identification of local areas suitable for the more expensive and intensive individual tree-scale methodologies.

Evans wrote all sections of this chapter, performed all of the data reformatting and analysis. Evans prepared the manuscript for publication. Hardy, Batini and Matusick conducted field observations of the mortality event and provided *in-situ* data for development and validation of the presented models. SpecTerra Services Pty Ltd, Perth provided the DMSI imagery. Primary supervisor and co-author, Lyons provided support throughout the development and draft stages. Planet Action and Astrium Services supplied the SPOT-5 Imagery. Excelis Visual Information services for provided student licenses of ENVI, ENVI EX and FLAASH for processing the imagery.

4.2 Abstract

Extreme and persistent reductions in annual precipitation and an increase in the mean diurnal temperature range have resulted in patch scale forest mortality following the summer of 2010–2011 within the Forest study area near Perth, Western Australia. The impacts of 20 bioclimatic indicators derived from temperature, precipitation and of actual and potential evapotranspiration are quantified. We found that spatially aggregated seasonal climatologies across the study area show 2011 with an annual mean of 17.7 °C (± 5.3 °C) was 1.1 °C warmer than the mean over recent decades (1981–2011,- 16.6 °C ± 4.6 °C) and the mean has been increasing over the last decade. Compared to the same period, 2010–2011 summer maximum temperatures were 1.4 °C (31.6 °C ± 2.0 °C) higher and the annual mean diurnal temperature range (Tmax−Tmin) was 1.6 °C higher (14.7 °C ± 0.5 °C). In 2009, the year before the forest mortality began, annual precipitation across the study area was 69% less (301 mm ± 38 mm) than the mean of 1981–2010 (907 mm ± 69 mm). Using Système Pour l'Observation de la Terre mission 5 (SPOT-5) satellite imagery captured after the summer of 2010–2011 we map a broad scale forest mortality event across the Forested study area. This satellite-climatology based methodology provides a means of monitoring and mapping similar forest mortality events- a critical contribution to our understanding the dynamical bioclimatic drivers of forest mortality events.

4.3 Introduction

Regional drought and heat stress over the past 30 years has resulted in climate-driven forest and woodland mortality events globally (Allen et al., 2010). Forests and woodlands that cannot relocate to suitable climatic conditions face a reduction of range, fragmentation, mortality and in extreme cases extinction (Hughes, 2010). The warming and drying of Mediterranean biomes increases their vulnerability (Prober et al., 2011; McDowell et al., 2008; Abbott and Le Maitre, 2009; Llorens et al., 2003) by reducing water availability and increasing vegetation stress and the frequency of mortality (Dunlop and Brown, 2008). Growing evidence suggests that as climates dry and warm the risks of biodiversity loss (West et al., 2012) and severe wildfires increase (Lane et al., 2010). Such dramatic landscape scale transformations are not likely to occur rapidly, rather evolve as a response to abiotic (Kinal and Stoneman, 2011) and biotic changes and the signs of change are already beginning to emerge (Klausmeyer and Shaw, 2009; Allen et al., 2010). As with other Mediterranean climates, the vegetation of southwest Western Australia (SWWA) is threatened by these changes.

Declines of this kind are not new to the SWWA, for example the declines of the tuart forest (Eucalyptus gomphocephala) on the Swan Coastal Plain (SCP) (refer to Figure 4.1) in the late 1990s and 2000s (Cai et al., 2010; Evans et al., 2012a, 2012b). Over the last decade, severe drought has impacted on the climate of southern (Mitchell et al., 2012) and southwest Australia resulting in marked declines in forest and woodland condition (Harper et al., 2009; Petrone et al., 2010). Since the 1970's the southwest has received 15–20% less than average rainfall (Petrone et al., 2010) and a 0.4 °C degree increase in temperature (Bates et al., 2008) leading to the marked depletion of stream flow through the forested region surrounding Perth (Kinal and Stoneman, 2011; Petrone et al., 2010) known as the Northern Jarrah (Eucalyptus marginata) Forest (NJF). For example, Petrone et al., (2010) shows that a reduction in the average streamflow in the NJF region (calculated as pre-1989 and post-2008 changes) range between −39% and −78% across the catchments monitoring sites. Petrone et al., (2010) also shows that, in the region surrounding the NJF, potential evaporation often exceeds precipitation and only a small portion (3–20%) of runoff is generated directly from rainfall and groundwater levels have been consistently falling (Ruprecht and Stoneman, 1993). Experimental results (Kinal and Stoneman, 2011) suggest that reductions in forest cover would result in increased streamflow and silvicultural forest canopy thinning has been used as a solution for increasing streamflow into drinking water catchments in the NJF.

In the context of forest distribution and health, bioclimatic limits (or thresholds) define how the forest is affected by its climate. A bioclimatic limit of the distribution of the Jarrah forest was first proposed by Gentilli (1948). At the time, the SCP received around 300 mm less annual rainfall (850 mm) than the Jarrah forest (1100 mm) which includes the NJF. Gentilli (1948) estimated that this restricted the Jarrah forests westward expansion towards the SCP on the basis of precipitation and evaporative demand: he defined the forest-sustaining bioclimatic threshold to be 800 mm of rain per annum and showed that a difference from the mean of 165 mm rainfall per annum would be significant to drive changes in the forests distribution across SWWA.

A severe inter-annual change in precipitation of the order of that described by Gentilli (1948) came to the region between 2009 and 2011. Specifically, nil rainfall was recorded for 122 days at Perth Airport between 21 November 2009 and 22 March 2010 (Tobin, 2010). Additionally, the state area average temperature for summer 2009–2010 was equal highest on record, 1.5 °C above average at 36.7 °C (Tobin, 2010). Autumn (March, April and May 2010) temperatures were the sixth warmest on record at 1.4 °C above the long term of state area average of 31.1 °C (Campbell, 2011). Furthermore, winter 2010 (June, July and August) was the driest and third coldest on record in the southwest (Imielska, 2012). The record winter cold and dry spell was followed by the fifth warmest average summer on record, spatially estimated to be +1.09 °C above the states long term average (Imielska, 2012).

Recently, the Bureau of Meteorology (2012) noted that the prolonged dry spell through summer 2010–2011 contributed to a series of out-of-control forest fires, in the presence of an abundance of dry-fuel, resulted in over 100 homes being destroyed or damaged. Extreme fire events such as these are not unprecedented yet are uncommon and formative in that they illustrate the threat posed by dry vegetation and hot conditions. It is critical to record and understand the spatial and temporal dynamics of these events (Gutschick and BassiriRad, 2003). It is expected that Mediterranean ecosystems will experience more frequent and prolonged climatic variability (Misson et al., 2011) and the need to understand the spatial extent and consequences of these impacts is central to the success of our adaptation strategies in the long term.

In regions where clear evidence of bioclimatic change is taking place, it is critical to develop suitable methodologies to record the extent and severity of forest and woodland mortality events and to quantify the bioclimatic-dynamics in order to understand the difference between natural variability and change. The only tool for achieving near real time, contiguous landscape and continental scale monitoring is remote sensing. Detection of eucalypt canopy dieback using high spatial resolution remote sensing imagery has been shown by a large number of authors and typically involves using spectral bands focused on chlorophyll pigments of the foliage, leaf structural attributes and defoliation (Barry et al., 2008; Coops et al., 2002, 2004; Datt, 1998; Haywood and Stone, 2011a; Pietrzykowski et al., 2006; Stone et al., 2001). Moderate resolution satellite remote sensing (e.g., 250 m–5 km) has been shown to be useful in detecting abrupt changes in greenness and cover (Guerschman et al., 2009; Verbesselt et al., 2010a, 2010b) by extracting a noiseless trend from the raw data once seasonal and high frequency changes are removed (Cleveland, 1990). Using remote sensing to map in combination with gridded and modeled climatologies (Greisbauer et al., 2011; West et al., 2012) can provide insight into the temporal and spatial dynamics of forested ecosystems.

The objectives of this study were, firstly to use remote sensing technology to map the extent of 'patches of mortality' (POM) resulting from the extreme weather of 2010-2011. Secondly, once spatially mapped, we analyze the bioclimatic conditions preceding the event and identify the underlying drivers of the forest mortality. We conclude with a number of potential future research directions on employing this methodology for understanding the responses of the forest stands to changing climatic conditions.

4.4 Methods

4.4.1 Overview

Following a severe mortality event (July 2011) the methodology for this manuscript was designed to map and investigate the drivers behind the declines. This involved establishing twenty field sites located across the forest, which a team of forest pathologists established and began monitoring immediately Matusick et al., (2012). Simultaneously, Système Pour l'Observation de la Terre mission 5 (SPOT-5)

Satellite imagery was acquired from PlanetAction.org and a feature extraction model, based on known biophysical relationships of remotely sensed imagery, was developed using the field sites with the aim of identifying POM across the imagery. An independent model evaluation dataset was used on the POM identified by the model. Bioclimatic space and time series analysis of Australian Water Availability Data (AWAP) (Raupach et al., 2009) and Moderate Resolution Imaging Spectroradiometer (MODIS) Fractional Cover were used to evaluate the environmental envelope of the study area. Spatially and temporally averaged statistics are evaluated over the period 1981–2011, hereafter the 30 year study period.

4.4.2 Study Area

The NJF directly east of Perth, Western Australia (Figure 4.1) has a Mediterranean climate, hot, dry summers and wet winters and has a history of tree declines (McDougal et al., 2007). The NJF is classified as a medium open forest of average height between 10-30m with canopy cover between 30-70% that lies atop the Darling Scarp on a substrate of archaen granite and metamorphic rocks with an average elevation of 300m above sea level (Heddle et al., 1980; Williams and Mitchell, 2002). Rainfall varies from around 1000mm on the western side of the scarp to 400mm to the northern and eastern extremes (Williams and Mitchell, 2002). The region serves as the main surface water supply for Perth as the Swan, Helena, Canning, Serpentine and Murray rivers flow off the Darling Plateau onto the SCP below Petrone et al. (2010).

The soils vary from lateric gravels to clay and the dominant plant species, *Eucalyptus marginata* (jarrah) are distributed in a mosaic across the western side and a mix of species dominate the eastern area with Jarrah co-occurring with *Corymbia calophylla*. The mid-storey consists of a mix of *Banksia grandis*, *Allocasuarina* *fraseriana*, *Persoonia longifolia*, *Xanthorrhoea preissii* and the shrub layer is comprised of a variety of perennial woody species. Across the region this topographical variability, granite substrate and gravel soils serve for rapid changes in floristic distribution from the winter water logged valley floors (drains) to the rocky granite outcrops (uplands).

The NJF is extensively mined for bauxite used in aluminum production, coal and other resources. Over the last three decades considerable emphasis has been placed on restoration of dormant mining sites throughout the forest. A post-mining re-vegetation prescription of 2500-10,000 stems/ ha is used and designed to produce 350 stems/ ha after 12 years of rehabilitation under the caveat that the sites are managed and thinned to this prescription (Koch and Samsa, 2007). Land use across the forest is thus a mosaic of mining, nature reserves, commercial forestry with areas set aside for Perth's water catchment.

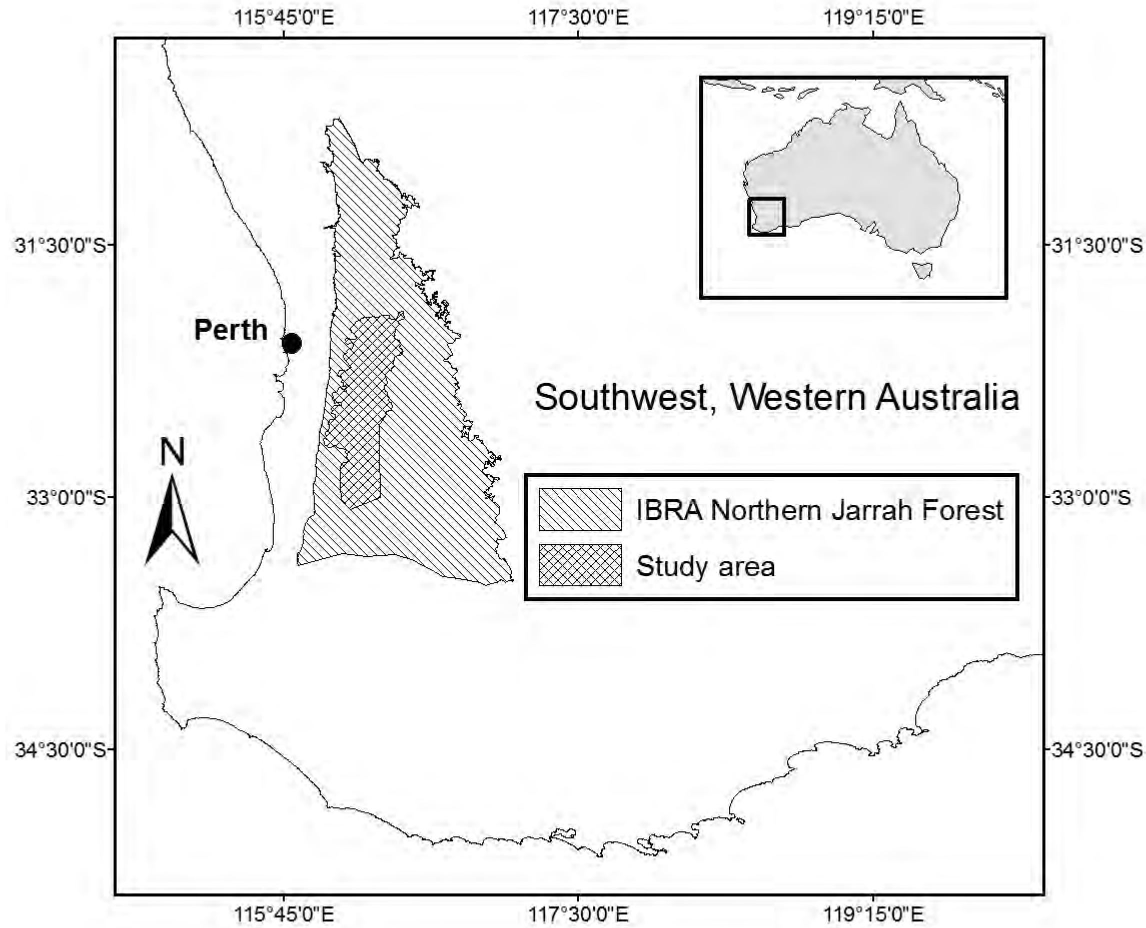

Figure 4.1. Study area featuring the study area and the Interim Biogeographical Region of Australia (IBRA) "Northern Jarrah Forest".

4.4.3 Field data for model development

In July 2011, patches containing mortality were located within the NJF by a team of forest pathologists on a number of field visits. The patches used in this study varied in size from 3,720 to 168,152 m2 and a complete inventory of the work can be found in Matusick et al. (2012). The objective of the field work was not to identify all patches in a region, rather identify a number of sites for detailed investigation of the causes (Matusick et al., 2012) and ultimately to use these for detecting and modeling the landscape scale of the POM in this study. Generally, the sites identified for use in this study were easily identifiable from high-ground and from the road whilst travelling through the forest. Twenty of these plots were located using differential Global Positioning System (dGPS) representing a range of dieback classes. Patches of healthy and dead trees were then delineated using dGPS by trained forest health professionals and a range of indices (not used in this study) were used to determine both the healthy and dead class.

4.4.4 Airborne imagery for validation of the model

To obtain additional information on the extent of the tree mortality across the forest Digital Multi-Spectral Imagery (DMSI) was acquired by SpecTerra Services (Perth, Western Australia) over small sections of the NJF as part of ongoing research into the hydrology of the forest (Batini personal comms., 2011) on the 18th of November 2010. This imagery provided a clear indication of foliage cover and a means to compare geographical features in the imagery to field made records of the presence and absence of decline since the imagery was taken when the forest did not contain any POM. A 1 km × 1 km grid (refer to Figure 4. 2(b).) was overlaid the imagery and a forest health assessment expert classified where POM were known to have occurred intersecting each grid point as either healthy or containing mortality following the summer of 2010–2011. ESRI (2011) was used for this exercise. This resulted in a validation area covering 135 km2 of the NJF. These pixels were then aggregated to produce a confusion matrix of pixels containing greater than 60% mortality and those containing less than 40% mortality, therefore considered healthy.

4.4.5 SPOT-5 satellite imagery

SPOT-5 satellite imagery was acquired across a large section of the forest in late June and early July 2011 before the first winter rains in order to determine the extent of vegetation declines across the region. The SPOT-5 imagery used was 10 m spatial resolution with four spectral bands green (GREEN: 500 to 590 nm), red (RED: 610 to 680 nm), near-infrared (NIR: 790 to 890 nm) and shortwave-infrared (SWIR: 1580 to 1750 nm). The four scenes used to cover the region came with radiometric correction of viewing angle and sensor related distortions in preprocessing level 1A (Spot Image, 2010). Imagery was orthorectified and converted to surface reflectance.

4.4.6 Feature extraction model development

Since, the 10m SPOT-5 imagery was insufficient to see individual crowns an object based 'feature extraction' approach was developed to identify POM across the study area located within NJF (EXELIS, 2011). Feature extraction was selected because the sites varied in size, structure and landscape position. Feature extraction involves first delineating areas of similar spectral and textural likeness by manipulating only spatial parameters, thus creating a mosaic of landscape features of similar spectral and textural likeness. The second step was to extract the features of interest (i.e. the POM) by classifying them based on their spatial, textural and radiometric properties, however, given the distinct differences between healthy, green forest and the POM, only radiometric and spatial properties were needed.

Three simple rules were identified by the object based image analysis systems to distinguish POM across the otherwise healthy forest; (1) the mean of the ratio of the near infra-red and red bands (i.e. mean patch greenness) of the imagery being less than 0.83 (unitless) was identified as a suitable threshold in a histogram analysis of agreement with the field data. (2) The POM size being between 5000 m^2, the FAO

(2000) definition of a minimum forest patch size and the upper size limit of 325000 m^2 being twice the size of the limited area field data and representative of POM identified across the entire study area. (3) The mean of the green band was zero, indicative of non-photosynthetic vegetation and the absence of greenness, thus complementing rule 1.

Using these three rules, the model was visually calibrated on the 20 healthy and 20 mortality field sites and resulted in the identification of a total of n=1853 POM when applied to the whole study area. The accuracy of the object based classification was then assessed by comparing a 135km^2 forest health assessment grid of 1km^2 cells with the classified objects in a standard confusion matrix allowing overall, user and producers' accuracy to be calculated.

4.4.7 MODIS fractional cover dataset

We used the MODIS-based vegetation fractional (MODFC) cover dataset developed by (Guerschman et al., 2009) to determine changes in fractional cover between 2000 and 2012 in order to establish the natural variability experienced by the forest against which we compare the impact of the 2010-2011 event. MODFC was selected because it has been used for national monitoring of ground cover (Stewart et al., 2011) and is currently the only estimate of photosynthetic vegetation (f_{pv}), non-photosyntheic vegetation (f_{npv}) and bare soil (f_{bs}) data validated for Australia. We address the issue of spatial and temporal disparity between remotely sensed greenness (SPOT-5 at 10m), cover observations (MODFC 500m) and climatologies by aggregating the fractional cover from its native resolution down to that of the climatologies used in our bioclimatic analyses and specifically for comparison across scale. In order to determine significant trends versus signal noise we use the STL package in the R-Project framework after Cleveland et al. (1990).

The STL method provides a loess smoothed trend by calculating and extracting a seasonal cycle and high frequency variability and subtracting these components from the raw f_{pv}, f_{npv} and f_{bs} signal. The resulting trend can then be used to reliably determine significant trends (i.e. positive or negative departures) from the time series mean (M) and standard deviation (SD). We define a significantly positive trend as being when the loess trend is greater than the sum of the time series M and SD, for example, a significant growth trend is said to occur when f_{pv} is greater than the sum of the M and SD (MSD) and a significant decline in cover when f_{pv} is less than MSD. Additionally, we calculate a rolling mean and standard deviation for the raw data using a moving window of 3 months. This provides an estimate of the local variance of the standard deviation of the raw data relative to the STL trend, useful for visually assessing the temporal variance in both the raw and trend signals simultaneously.

4.4.8 Gridded climatologies and bioclimate analysis

The AWAP dataset (Raupach et al., 2009) was used because it is recognized as an accurate resource of the state and trends of the terrestrial water balance of the Australian continent at a spatial resolution of 0.05 degrees (nominally 5 km) (van Dijk and Renzullo, 2011). Monthly climatologies of minimum and maximum temperature, precipitation, actual (total) evaporation and potential evaporation were spatially extracted from AWAP for the period 1970-2010. Spatially explicit climatologies of the study area and the NJF were then aggregated for the analysis across seasonal and inter-annual timescales necessary to understand the climatic envelope of the forested study area.

In the NJF, subsurface through-flows are coupled to soil moisture recharge (Kinal and Stoneman, 2011) and there is an annual moisture deficit (Petrone et al., 2010) consistent with other Mediterranean climes (Prentice et al., 1993). The net result is that wet season (winter) precipitation that is not intercepted or stored is lost to runoff and stream flow. In addressing this issue for similar climates, Prentice et al. (1993) proposed a scalar, α renamed to the Mean Annual Aridity Index (MAAI) for this study, designed to capture the seasonal variability of soil moisture independently of vegetation interception and considered it indicative of the growth-limiting drought stress on vegetation.

We calculate a MAAI as the ratio of actual (total) evaporation (E_a) to potential evaporation (E_p) derived from the AWAP climatologies (Raupach et al., 2009) which models evapotranspiration approximate to the methods of Priestley and Taylor (1972). We assume that E_a can never be greater than E_p and that E_a constrains both soil evaporation and transpiration from the vegetation. We calculate MAAI for each NJF pixel and compare mean annual precipitation and temperatures between the climate époque 1970-2009 and the annual average for 2010. We classify our MAAI in the same way as Middleton's (1997) aridity ratio of precipitation to potential evaporation for the purposes of comparison (Table 4.1).

Table 4.1. Aridity-humidity classification of the value of MAAI, the ratio of actual to potential evaporation (after Middleton, 1997).

Class	**Range**
Hyperarid	0 to 0.05
Arid	0.06 to 0.20
Semi-arid	0.21 to 0.50
Dry-subhumid	0.51 to 0.65
Humid and wet	>0.66

Detailed micrometeorological observations, greater than 5km resolution do not currently exist across the forest, and as such, the best available alternative to dynamic energy and water balance information are surrogate bioclimatic indices with known biological significance (Nix, 1986). Using the AWAP climatologies (Raupach et al., 2009) 19 bioclimatic indices (Table 4.2) were derived using the R-Project species distribution modeling package 'dismo' (Hijmans et al., 2012) to make a total of 20 indices. The bioclimatic indices summarize the total energy and water inputs across the NJF at seasonal and annual timescales. They characterize the climatic envelope and identify any thresholds driving the POM occurrences following the summer of 2010-2011.

Table 4.2 Nineteen bioclimatic indices calculated for the analysis (after Nix, 1986)

Index	Description
BIO01	Annual Mean Temperature
BIO02	Mean Diurnal Range (Mean of monthly (max temp - min temp)); T_{mdr}
BIO03	Isothermality (T_{mdr} / T_{ara}) (* 100)
BIO04	Temperature Seasonality (standard deviation *100)
BIO05	Max Temperature of Warmest Month; T_{wmo}
BIO06	Min Temperature of Coldest Month; T_{cmo}
BIO07	Temperature Annual Range (T_{wmo} - T_{cmo}); T_{ara}
BIO08	Mean Temperature of Wettest Quarter
BIO09	Mean Temperature of Driest Quarter
BIO10	Mean Temperature of Warmest Quarter
BIO11	Mean Temperature of Coldest Quarter
BIO12	Annual Precipitation
BIO13	Precipitation of Wettest Month
BIO14	Precipitation of Driest Month
BIO15	Precipitation Seasonality (Coefficient of Variation)
BIO16	Precipitation of Wettest Quarter
BIO17	Precipitation of Driest Quarter
BIO18	Precipitation of Warmest Quarter
BIO19	Precipitation of Coldest Quarter

The aggregate of monthly inputs into the seasonal variables enable the detection of inter-annual shifts in seasonality; BIO15 relates to shifts in seasonal precipitation occurrence, known to be directly related to vegetation drought stress (Neilson and Marks, 1994) and BIO14 focuses specifically to precipitation in the dry season, in the NJF this is in the summer months (December, January and February).

The mean summer diurnal temperature range, and annual precipitation, used in the climate space analysis, provides insight into the range and magnitude of the energy inputs of temperature and specifically on precipitation preceding the mortality event. The approach assisted in identifying the key variables in the bioclimatic space, preceding and thus contributing to the mortality event. This deterministic methodology is consistent with others which use the response of plant functional traits to model their distribution (Peel et al., 2005; Elith et al., 2006) and persistence under variable climate scenarios (Beaumont et al., 2005; Renton et al., 2012).

4.5 Results

4.5.1 Detection of POM and the accuracy assessment

The spatial extent of the study area was 6074.5 ha (60km^2). The expert assessment of the 135 km^2 grid resulted in greater accuracy in the detection of POM, 85% hit versus 74% missed, as compared to grid cells containing no death at all (Table 4.3). However, there were more than 2.5 times more cells containing POM than there were healthy ones. No POM were delineated inside the "validation" area (Figure 4.2(b)) and assessment of the presence and absence was conducted independently by forestry professionals (Batini personal communications, 2011).

Table 4.3. Confusion matrix of the object based classification of the presence and absence of healthy (n=38) and patches of mortality (POM) (n=97) across 135km^2 (n=135 cells) within the NJF

	Healthy	POM
Healthy	74% (n=28)	25% (n=10)
POM	15% (n=15)	85% (n=82)

Examples of the comparison of the POM identified *in-situ* and use for training the model (Figure 4.2a) reveal the complexity of the patch shapes and their stark visual differences between the surrounding, healthy vegetation. Figure 4.2 is a false-colour image in which red dominant colours indicate photosynthetically active cover (i.e., brighter red = more leaves), green-grey-black colours indicate non-photosynthetic cover and white colours are generally indicative of the high levels of reflection from bare soil and sands. Figure 4.3 shows the distribution of the POM across the study area including those areas excluded.

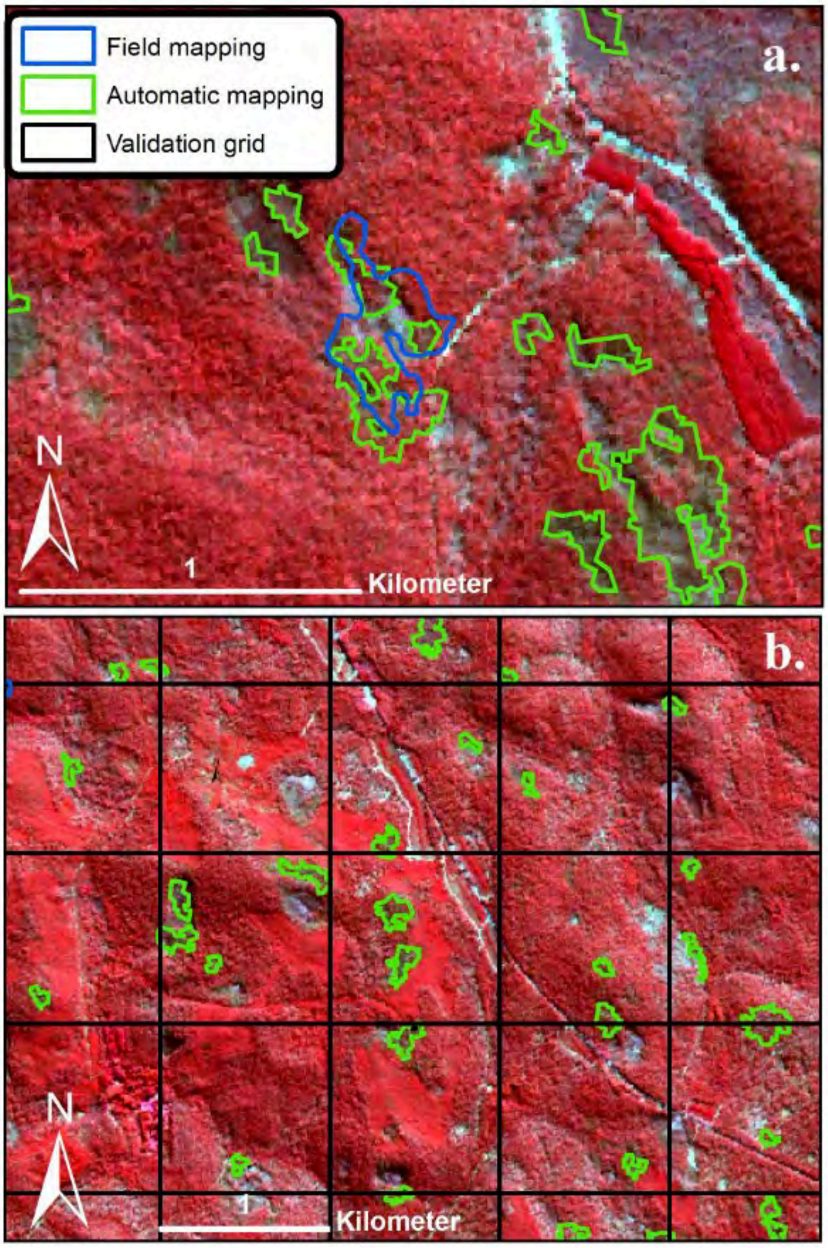

Figure 4.2. Système Pour l'Observation de la Terre mission 5 (SPOT-5) infrared imagery (10 m) overlaid with (**a**) field data and feature extraction modeled patches of mortality (POM) and (**b**) the model evaluation grid and POM contained within a number of cells.

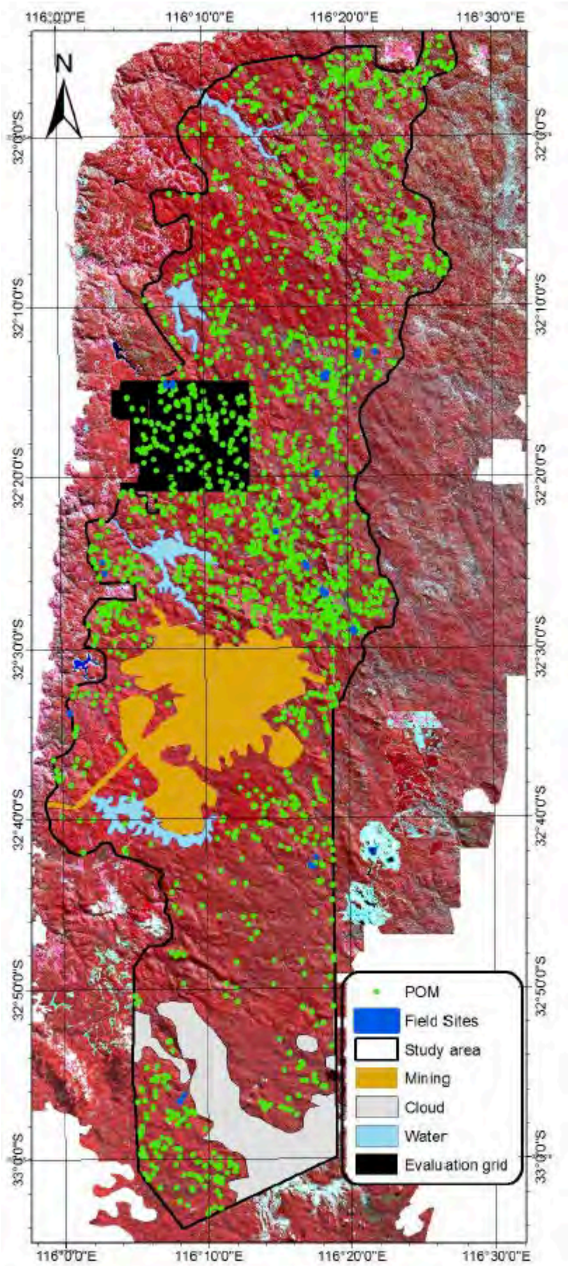

Figure 4.3 SPOT-5 Imagery overlaid with the mining, water and cloud masks used across the study area in the classification of the POM and the validation grid used.

4.5.2 Changes in fractional cover

The MODFC data were used to investigate if an event of comparable extent had occurred prior to the summer of 2010–2011 and quantify the decadal natural variability in fractional cover across the study area. At 0.5 km resolution the MODFC data potentially contains information on changes in fractional cover for none, one or many POM (i.e., those detected from 10 m resolution SPOT-5 data). When MODFC is aggregated to 5 km the climate data will contain information relevant to many MODFC pixels. Addressing this spatial disparity the MODFC data were aggregated to 5 km and both the study area and POM location trends are extracted for comparison. This provided spatial parity between the impact of the POM in MODFC and AWAP data at 5 km yet did not yield any significant differences in the occurrence of the MSD exceedance events (data not shown).

Considering all pixels across the study area, the MODFC time series (refer Figure 4.4) shows a simultaneous decrease in f_{pv} (Figure 4.4(a).) and increase in f_{npv} (Figure 4.4(b).) occurred following the summer of 2010–2011. Additionally, around 2001, there was a significant drop in f_{pv}, which did not coincide with an increase in f_{npv}. Comparing only pixels containing a modeled estimate POM, the average of all of these pixels (Figures 5) shows an equally clear and significant decline in f_{pv} corresponding with an increase in f_{npv} and importantly there was no significant change in f_{bs} over the summer 2010–2011 period. In contrast to the impacts across the study area (Figure 4.5) there was no significant decrease in f_{pv} during the summer of 2001–2002.

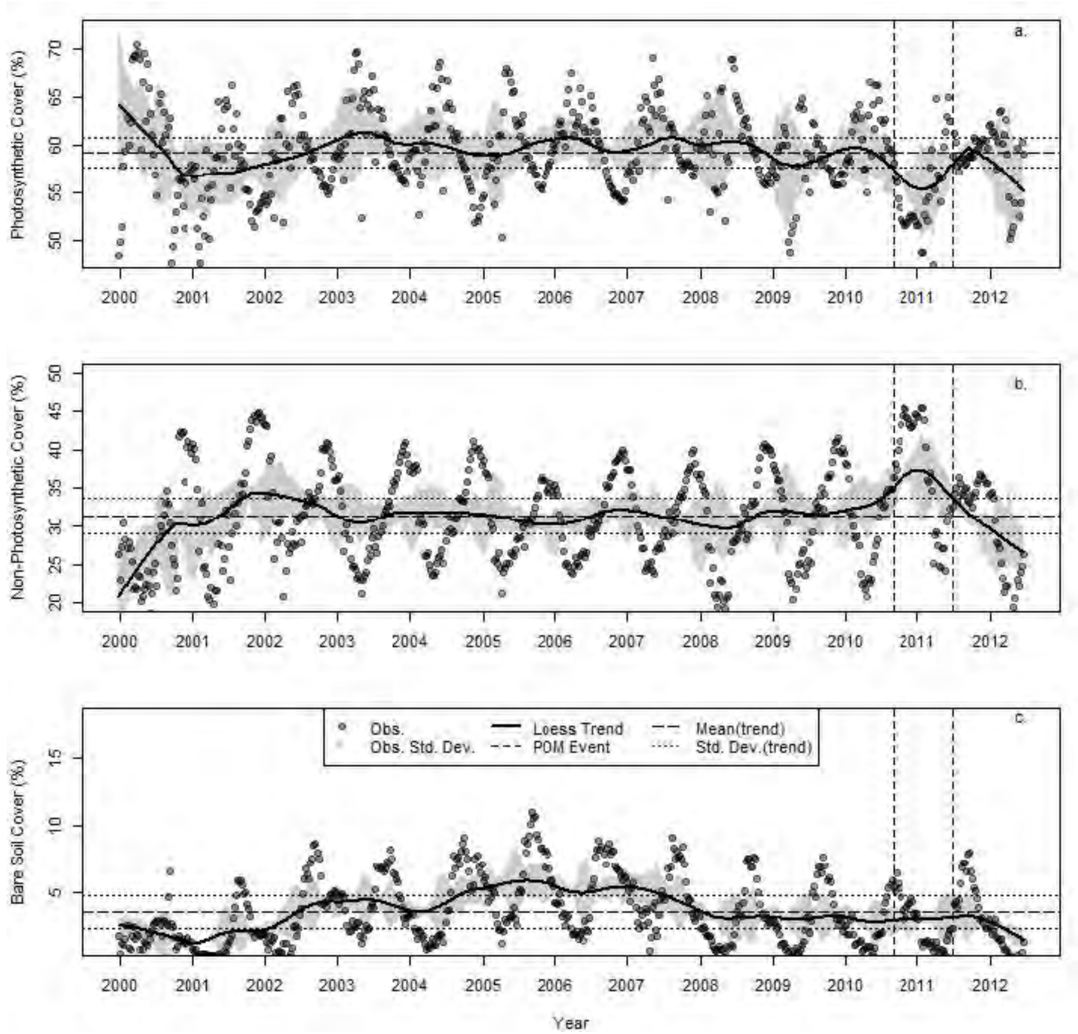

Figure 4.4. Spatially aggregated 0.5 km study area average Seasonal Trend Decomposition using Loess (STL) trend plots showing the 2000–2012 period with the summer of 2010–2011 marked for each component of MODFC Guerschman (2009). Subplot (a) is the fraction (%) of photosynthetic cover (f_{pv}); (b) the fraction (%) of non-photosynthetic cover (f_{npv}) and (c) the fraction (%) of bare soil (f_{bs}).

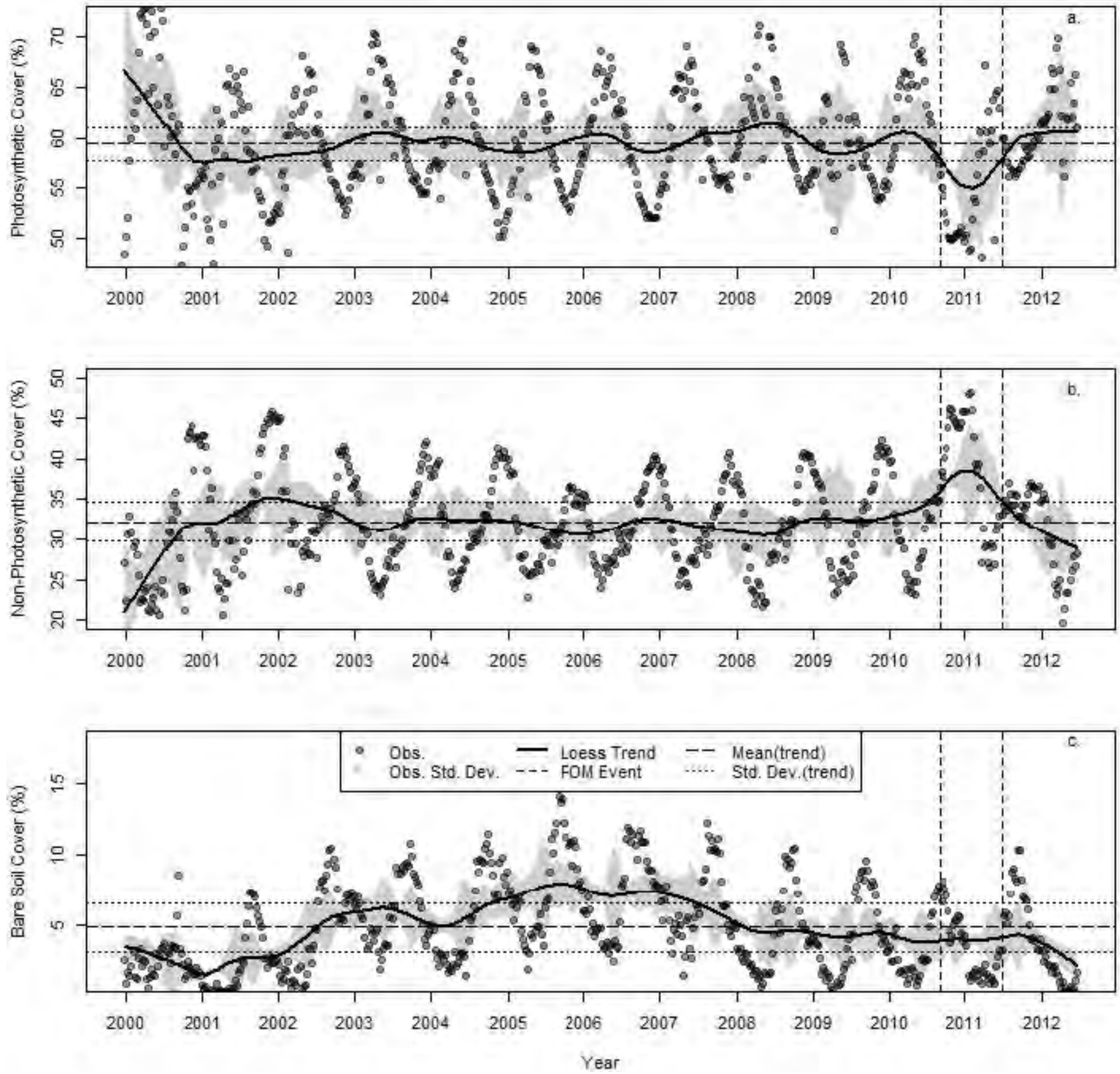

Figure 4.5. 0.5 km POM average STL trend plots showing the 2000–2012 period with the summer of 2010–2011 marked for each component of MODFC after Guerschman et al., (2009). Subplot (**a**) is the fraction (%) of photosynthetic cover (f_{pv}); (**b**) the fraction (%) ofnon-photosynthetic cover (f_{npv}) and (**c**) the fraction (%) of bare soil (f_{bs}).

4.5.3 The changing climatic space

Spatial analysis of the climate data revealed the NJF has been experiencing a sustained net average reduction in precipitation over the last three decades. Annual precipitation in 2009 was 69% less (301mm ± 38mm) than the mean of the 30 years prior (907mm ± 69mm). In 2010, was 47% less (477mm ± 38mm) over the same period (30 year mean, refer Figure 4.6). Over this two year period, the study area received 1038mm less precipitation than the long term mean which resulted in the ecosystem shifting to a more arid regime. Figure 4.7 shows pockets of sub-humid climate retracted to a more semi-arid climate.

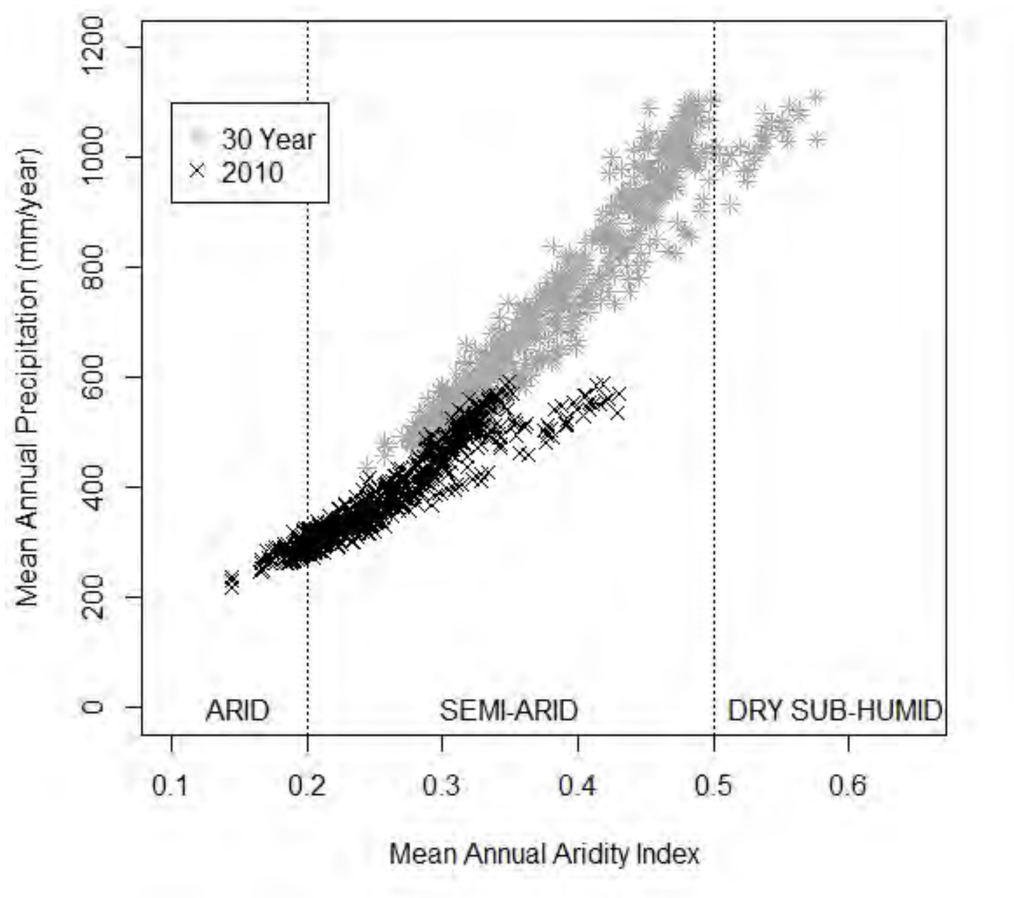

Figure 4.6. Spatially aggregated comparison of the NJF's Mean Annual Aridity Index versus Mean Annual Precipitation (mm/year). Averages over the period 1981–2009 are shown in grey and the 2010–2011 in black.

The study area has also been getting hotter over the study period. Summer 2010-2011 was 1.1°C (17.7°C ± 5.26°C) warmer than the average summer temperatures (16.6°C ±4.63°C) of the last three decades (1981-2011). This rate of warming has been increasing over the last decade. Whilst the annual mean minimum temperature across the study area was 0.21°C ± 4.68°C cooler (10.08°C ± 4.68°C) than the last three decades (10.29°C ± 3.59°C), the summer mean and maximum temperatures were higher. The mean 2010-2011 summer maximum temperature was 1.4°C (31.60°C ± 1.99°C) higher than the previous 30 years (30.17°C ± 2.01°C). The 2010 annual mean diurnal thermal variability (T_{max}-T_{min}) was 2.3°C higher (25.20°C ± 6.7°C) than the previous 30 years. As with precipitation, this illustrates a shift from a predominately semi-arid envelope towards an increasing arid one- completely departing its sub-humid zones (Figure 4.7).

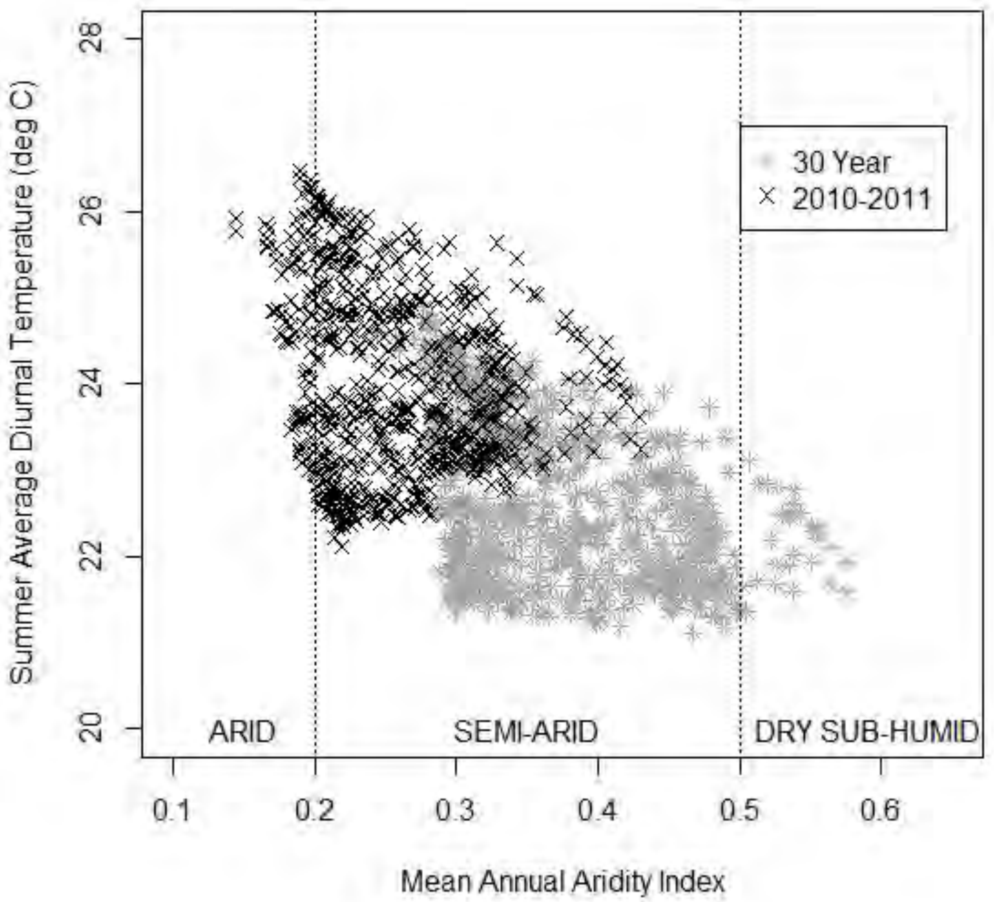

Figure 4.7. Spatially aggregated comparison of the NJF's Mean Annual Aridity Index versus Summer (December, January and February) Average Diurnal Temperature Range (deg C). Averages over the period 1981–2009 are shown in grey and the 2010–2011 in black.

4.5.4 Bioclimatic indices and the aggregated extremes

The spatially aggregated indices (Figure 4.8) show the biologically significant changes in climate across the NJF between 1971-2010. There is a gradually increasing trend (1971-2010) in mean annual temperature (BIO01 refer Figure 4.8) driven by both an increase in the frequency of mean temperature years (white) over the last decade and a reduction in the frequency of cooler years (blue) between the hotter, more extreme years (red). The temperature indices, BIO05 (maximum temperature of the warmest month) and BIO06 (minimum temperature of the coldest month), show that the warmest and coldest months have been less warm during 2000-2008 compared to 1981-1999. BIO06 shows three of the coldest months between 2006–2010 were colder. Simply put, the seasonal temperature extremes are expanding, the coolest months are getting colder and the warmest- hotter. In 2010, the annual range of temperature (BIO07) was the highest of the entire study period. Winter (i.e., June, July and August) in SWWA is usually the wettest part of the year and the mean temperature of the wettest quarter (BIO08) has been declining in intensity since 2005. Summer (i.e., December, January and February) usually falls in the driest and warmest quarter and the mean temperature of the driest quarter (BIO09) has been on a warming trend since 2005 as has the mean of the warmest quarter (BIO10). Although the coldest month (BIO06) is getting colder, the mean of the coldest quarter (BIO011) has been increasing.

The seasonal indices combining precipitation and temperature effects (BIO08-BIO11) present the same signal-of-change over the last decade and their intensities correlate with the wet winters of the period 2008-2010 which have been colder, drier and warmer. The precipitation indices, BIO12-BIO19 (Figure 4.8) show the observed reduction in rainfall progressively increasing over the last decade which decreases to an extreme minimum over the last three years with the most extreme deficit occurring in 2010. The annual precipitation (BIO12) clearly shows both a reduction in the magnitude of the wet years (1971-1990) and an increase in the magnitude of the dry years (1991-2010). The frequency of wet years shifts (BIO14 and BIO15) away from a cycle of a one-in-five marked wet years (1971-2000) to an eight year run of below-average precipitation (2001-2008) preceding the extremely dry period 2008-2010. This trend is also captured in the seasonal precipitation indicators (BIO16-BIO19), whilst the regularity of the trend is less strong; there are no extremely wet events since 1990.

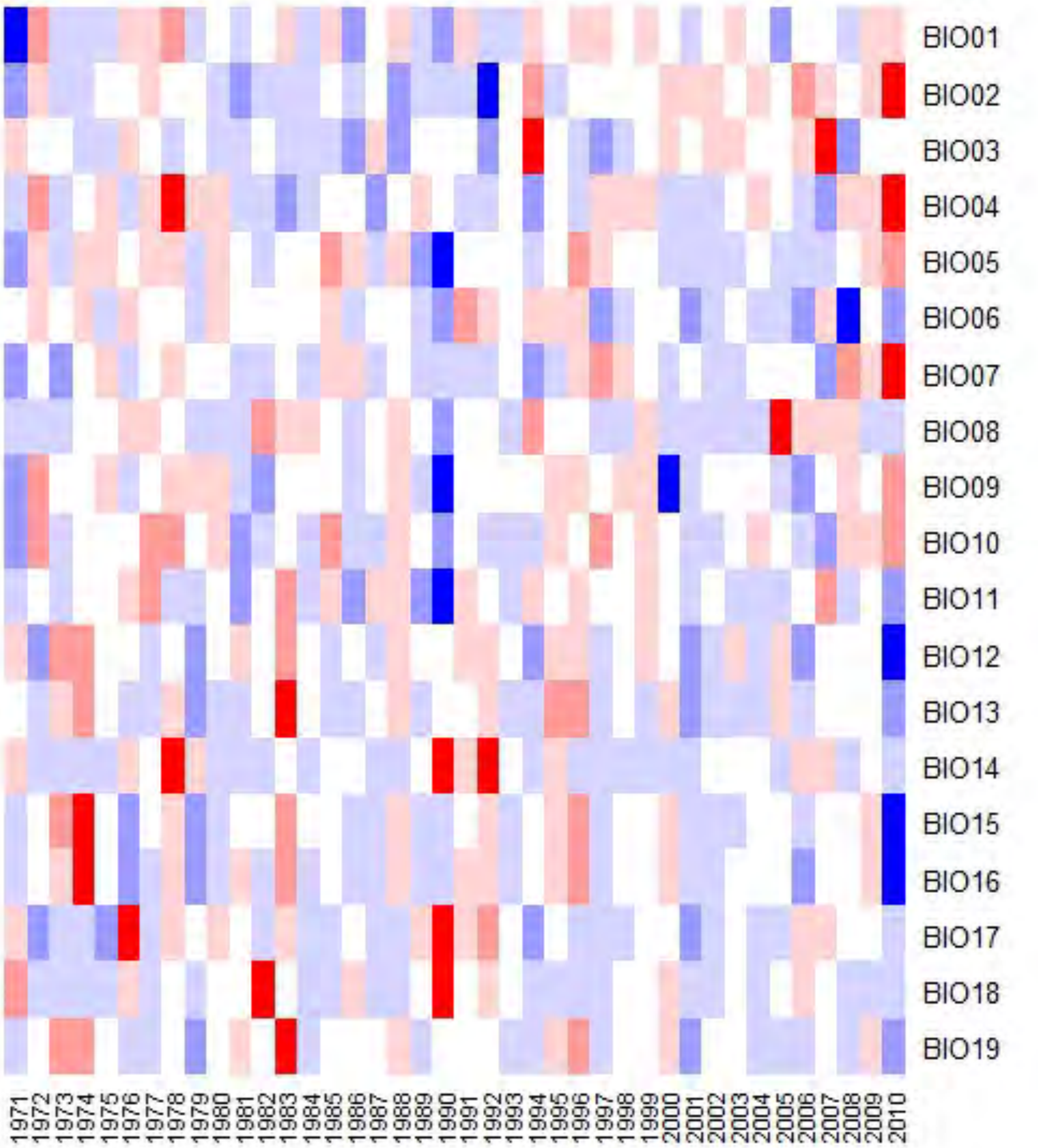

Figure 4.8. Relatively scaled (by index) hepta-class heatmap of NJF spatially aggregated bioclimatic variables (Nix, 1986) for the period 1971-2010. Derived from the AWAP (Raupach et al., 2009) using (Hijmans et al., 2012). Red colours represent quantities greater than the mean (white) and blue less than the mean, intensity represents magnitude.

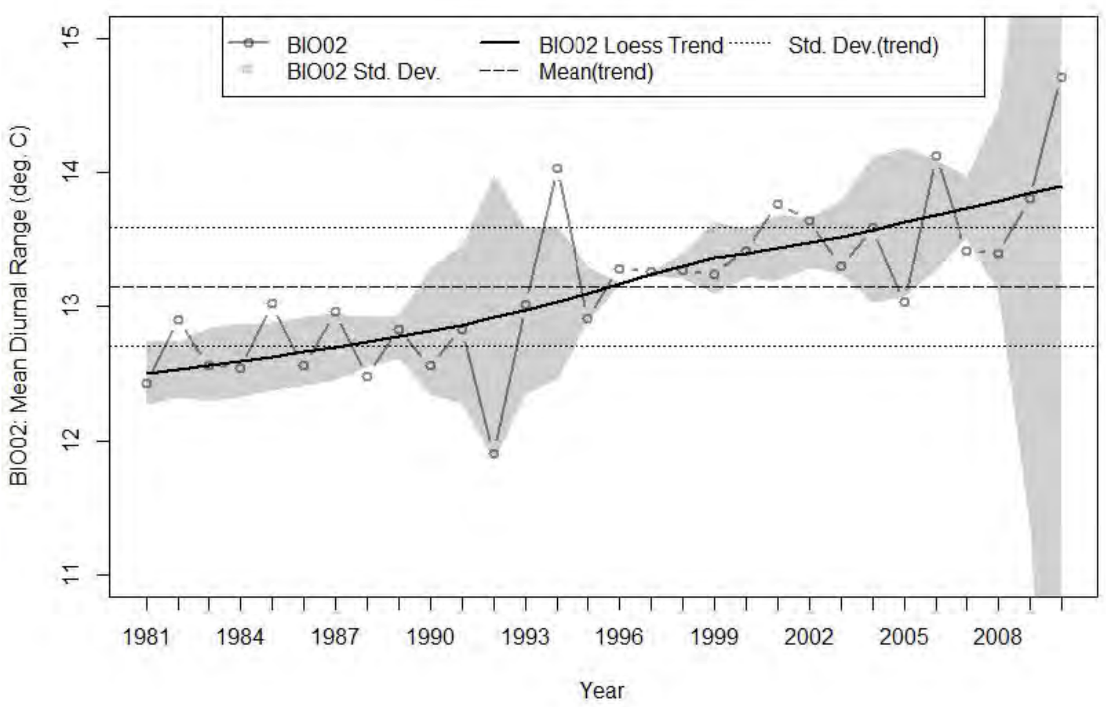

Figure 4.9. BIO02 is the 'Mean Diurnal Range', the mean of the difference of the monthly maximum and minimum temperature (Nix, 1986), for the period 1971-2010. Derived from the AWAP (Raupach et al., 2009) using Hijmans et al. (2012).

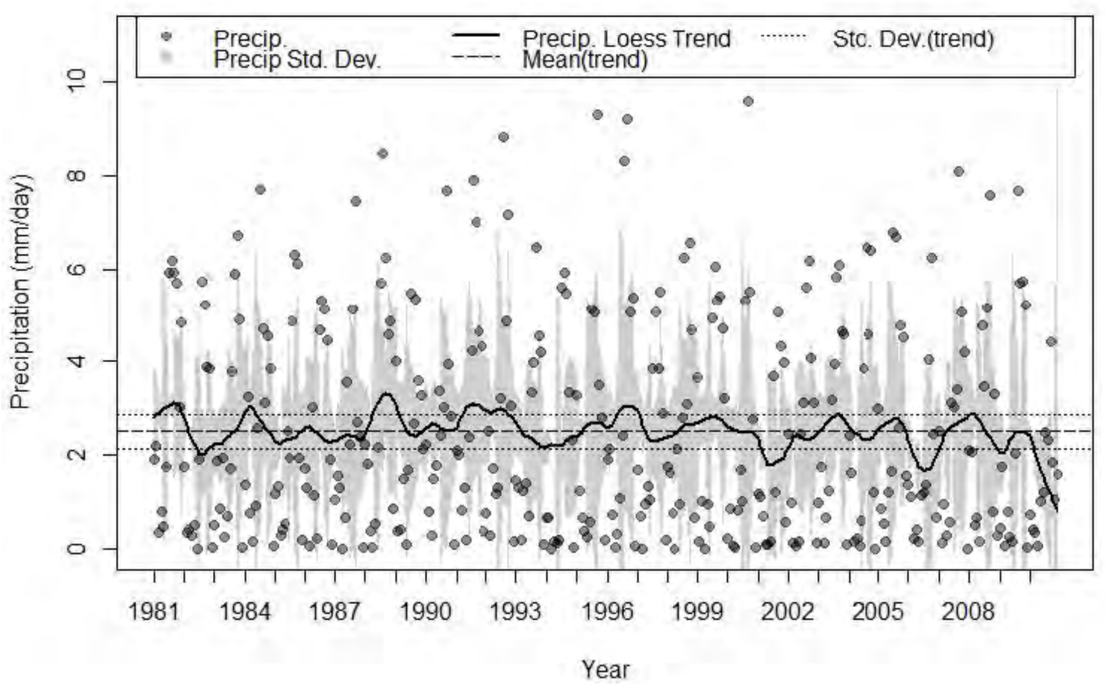

Figure 4.10. Spatial aggregated monthly time series of mean daily rainfall (mm) across the study area showing the loess trend, mean and standard deviations and the original monthly data, extracted from AWAP (Raupach et al., 2009) for the period 1981–2010.

The precipitation indices, BIO12-BIO19 (Figure 4.8) show the observed reduction in rainfall progressively increasing over the last decade which decreases to an extreme minimum over the last three years with the most extreme deficit occurring in 2010. The AWAP precipitation data (Figure 4.10) shows the significance of these drier years over recent decades and significant declines (i.e., less than the MSD) occurring in 2001, 2006 and 2009. Prior to 2000 there were significantly wet years (i.e., greater than the MSD) in 1981, 1984, 1988, 1992 and 1997 and none between 1998 and 2010. The annual precipitation (BIO12) clearly shows both a reduction in the magnitude of the wet years (1981–1990) and an increase in the magnitude of the dry years (1991–2010). The frequency of wet years shifts (BIO14 and BIO15) away from a cycle of a one-in-five marked wet years (1981–2000) to an eight year run of below-average precipitation (2001–2008) preceding the extremely dry period 2008–2010. This tendency is also captured in the seasonal precipitation indicators (BIO16-BIO19); whilst less strong, there are no extremely wet events since 1990.

4.6 Discussion

Over the last decade the study area has become drier, and the mean annual diurnal temperature range more extreme, increasing the risk of damage and mortality from a change in the frequency and intensity of heat waves and the potential for frost. As precipitation decreased the forest was exposed to greater mean annual diurnal temperature range which in turn contributed to an increase in evapotranspiration and gradually resulted in a bioclimatic shift towards aridity. These results suggest the bioclimatic factors preconditioning the POM across the study area were:

1. A succession of warm summers with summer maximum temperatures in 2010–2011 1.4 °C hotter than the 30 year average.
2. A sustained multi-decadal reduction in wet years over the last 30, with 1982 being the wettest.
3. A succession of extremely dry years, 2009 was 69% less than the 30 year average and 2010 was 47% less over the same period.
4. A sustained increase in BIO02 over the last decade, peaking in 2010 at 1.6 °C above the 30 year average.

Whilst it is well documented that climatic warming is expected for the southwest of Western Australia, we found that the increased diurnal temperature range (BIO02) was a stronger indicator than an independent change in the maximum temperature- which was expected (Neilson and Marks, 1994). Minimum temperatures also declined as the temperatures become more extreme (hot and cold) the mean annual diurnal temperature range is increasing, reaching a study period maximum of

14.7 °C ± 0.5 °C in 2010. This greater range increases the chance of frost in winter and heat waves in summer. In combination, the results suggests that in the presence of drought, exposure to both more intense cold and heat compounded vegetation water stress sufficiently to exhaust available energy reserves required for rooting and transpiration defense strategies- an effect found in plantation forests where soil depth and water storage capacity were found to be low (Harper et al., 2009).

This 2010–2011 event is also similar to the documented genesis of other forest mortality episodes (Allen et al., 2010) for which it is argued that they will ultimately accelerate species turnover and drive landscape evolution as climates shift under global climate change (Frelich and Reich, 2010; Wang et al., 2012). These results also concur with the pioneering bioclimatic analysis of Gentilli (1948) who predicted a similar precipitation threshold (+/− 300 mm) as that which sustains the forest in its present geographic location. The spatial analysis shows a reduction of 1038 mm accumulated precipitation (2009 + 2010), over 700 mm in excess of the Gentilli (1948) threshold. When compared to the 1981–2011 mean, this equates to 69% less in 2009 and 47% less in 2010. As the climate of SWWA continues to become dryer and warmer we need to improve our understanding of the relationships between key climatic indicators and the spatiotemporal responses of our native forests at the landscape scale.

More recently, numerous studies have identified the bioclimatic envelopes that drive trait based species distribution across landscapes. The underlying objective of these studies is to parameterise models that attempt to predict future climate change vulnerability and the adaptive capacity of specific forest types (e.g. Griesbauer et al., 2011; West et al., 2012). Many of these studies claim there is no clear link between strong-drought induced water stress and plant physiological responses (e.g. Griesbauer et al., 2011; West et al., 2012) on the basis that stomatal control limits carbon assimilation during drought (Chaves, 1991; Chaves et al., 2003). The precipitation data shown here suggests water limitation (i.e., drought and water stress) has been the primary driver of this mortality event.

Recent studies of Mediterranean climates indicate that severe droughts can result in non-stomatal limitation of photosynthesis relative to leaf water stress (Misson et al., 2010) when driven by low water availability and high evaporative demand over time (McDowell, 2011a, 2011b). Such responses confound the assimilatory capacity of vegetation and in severe drought conditions, can exceed physiological water-carbon deficiency thresholds that could in turn trigger reduced recovery hysteresis, cascading effects and mortality (Gutschick and BassiriRad, 2003; Galmés et al., 2007; Granier et al., 2007; Haldimann et al., 2008). Further confounding this debate is evidence that slightly warmer temperatures within a tree's optimum range could enhance forest growth under enhanced CO_2 (Luo, 2007).

Satellite imagery has become a well-accepted source of information, providing useful information on the spatio-temporal variation of vegetated landscapes. In this study we used 3 different types of remotely sensed data; (1) DMSI airborne imagery (0.5 m), (2) SPOT-5 high-resolution (10 m) and (3) MODIS moderate resolution (0.5 km) satellite imagery that were further aggregated to 5 km. We combined them to first detect and map a decline event at a single point in time, highlighting the significant spatial extent of the event. Then analyzed historical data to understand how the past impacted on the changes in photosynthetic cover (i.e., forest canopy) we observed and modelled following the summer of 2010–2011. We found both satellite sensors (SPOT-5 and MODIS) detected changes in photosynthetic and non-photosynthetic cover following the summer of 2010–2011. The MODFC data provided a long-term (2000–2012) baseline for fractional cover suggesting that in the years prior to the 2010–2011 event the POM modeled sites were persisting within their environmental niche- in a "healthy" state with no evidence of widespread stress. In addition to the independent validation, the MODFC analysis provides greater confidence in this multiple sensor methodology. The similar results following spatial down-aggregation of the MODFC data, i.e., to the same resolution as the climatologies, adds yet further confidence to the usefulness of MODFC for mapping such events at lower resolutions when no better data are available. Additionally, this approach demonstrates the potential use of programmable satellites such as SPOT-5 to acquire these data on demand and for broad-scale, near-real time post-mortem POM detection.

The threat of fire in the NJF remains significant as long as the residues of each POM remain scattered across the forest. Should the POM combust; it could potentially create a wildfire in the same way that the 1998 Yellowstone fires evolved from distributed patches into one large conflagration which persisted for months (Knight and Wallace, 1989). Such an event could have a significant impact on the biodiversity of the flora and fauna of the forest's and threaten the welfare of the local population.

4.7 Conclusion

Expansion of the thermal extremes of minimum and maximum temperature and prolonged drought were major drivers of forest mortality in the NJF following the summer of 2010-2011. This forest scale mortality event was successfully captured using SPOT 5 imagery using a three-rule feature extraction algorithm that produced a map of their distribution across the landscape. Used in this way, the combination of remote sensing and gridded climatologies provides a means of monitoring, mapping and analyzing the drivers of bioclimatic induced change of forested ecosystems for known events and a basis for a new generation of models on similar spatial and temporal scales. As such, this approach makes a significant contribution towards a robust methodology for monitoring the impact of climate induced drought and the underlying ecological consequences of extreme climate variability on forest dynamics.

CHAPTER 5
LINKING A DECADE OF FOREST AND WOODLAND DECLINE IN THE SOUTHWEST OF WESTERN AUSTRALIA TO BIOCLIMATIC CHANGE

5.1 Overview of author contributions

This chapter addresses the specific aim of applying the methodology developed in chapter 4 to include several forest and woodland areas across the southwest of Western Australia (SWWA). Rather than going back 30 years, as is the case in chapter 4, this chapter focuses on the last decade for which MODIS fractional cover data is available (2000-2012). The results define a set of thresholds for the key bioclimatic variables identified in chapter 4, including precipitation, diurnal temperature range and the aridity index based solely on the remote sensing and bioclimatic analysis. This chapter has been published by the Journal of Australian Forestry.

A number of decline events have been reported over the last decade. Whilst their reported causes vary, most consider or conclude that drought is an inciting factor. This chapter relies on these reported events, which do not necessarily present detailed temporally or spatially explicit observations of decline or mortality, yet provide an indication of time and place. By extending the spatial domain to include SWWA, it adds additional value as a guide for future monitoring and modeling the forested and woodland ecosystems generally. Additionally, this chapter demonstrates that this methodology is applicable to a diverse range of ecosystems, robust and consistent yet uses only freely available data and software.

Evans wrote all sections of this chapter, performed all of the data reformatting and analysis. Evans prepared the manuscript for publication. Stone and Barber contributed significantly to the publication and provided feedback on the chapter together with Lyons and Hardy.

5.2 Abstract

The south-west of Western Australia has experienced severe and prolonged drought over the last three decades. This has coincided with forest declines and more recently (following the summer of 2010–2011) sudden stand mortality in the Northern Jarrah Forest. Over the same period the Southern Jarrah and Southern Karri Forests remained unaffected. The bioclimatic linkage between these localised climatic events and forest responses is key to developing a predictive capability that permits timely interventionist management strategies. We looked at the temporal dynamics of three accessible bioclimatic parameters (monthly mean diurnal temperature range, monthly mean precipitation and an aridity index derived from evaporation data) that were spatially registered with forested areas known to have been affected by this shift towards dryer and hotter conditions. Changes in forest condition were determined by accessing the vegetation fractional-cover dataset, freely available from the high temporal resolution satellite MODIS. This dataset provided estimates of three vegetation-related indices, namely photosynthetic vegetation, non-photosynthetic vegetation and bare soil cover. Both the climatic variables and the vegetative response variables were spatially co-registered over each of the three selected forest areas and a time series analysis undertaken for each variable. From the observed trends, we identify a set of threshold values for each bioclimatic metric and the approximate time lag associated with observed notable deterioration in the vegetation cover metrics.

5.3 Introduction

The south-west of Western Australia (SWWA) has been getting dryer and warmer over the last three decades and this sustained and substantial shift in climate has been linked to forest decline and mortality throughout the region (Brouwers et al., 2012a, b; Evans and Lyons, 2013; Matusick et al., 2013). Wardell-Johnson et al. (2011) showed this sustained decadal change in climate threatens both biodiversity and carbon stocks in the region. This shift towards aridity has also been demonstrated as consistent amongst decline and mortality events observed in Mediterranean climate forests in eastern Australia and overseas (e.g. Allen et al., 2010). In fact, most past decline events in Australia have been attributed to a complex of causes but with drought as the inciting factor. For example, drought has been implicated as one of the single factors most likely causing the widespread decline and mortality of *Eucalyptus crebra* and *E. xanthoclada* in Queensland (Rice et al., 2004). Palzer (1983) similarly attributed the most likely cause of dieback of *E. regnans* and *E. obliqua* to be water-deficit (i.e. drought) and high leaf temperatures (i.e. heatwaves) although his work was confounded by the possibility of a virus or mycoplasma. The proposed causes of dieback affecting *E. obliqua* in Tasmania included a combination of drought followed by attack from leaf-consuming insects and a root-colonising fungus (Felton et al., 1981; Palzer et al., 1981). Similarly, dieback of *E. rossii* and *E. macrorhyncha* in the ACT and NSW was attributed to the susceptibility of these species to drought followed by secondary attack from stem borers (*Phoracantha* spp.) (Pook et al., 1981; Pook and Forrester, 1984).

A number of Western Australian eucalypt species have also suffered a severe decline in health associated with drought or diminished access to soil moisture, including *E. marginata* (Scott et al., 2012), *E. gomphocephala* (Archibald et al., 2004; Cai et al., 2010), and *C. calophylla* (Paap et al., 2008; Matusick et al., 2012). Matusick et al. (2012) reported the occurrence of a severe and sudden dieback event within an *E. gomphocephala* woodland coincided with extreme drought and heat conditions experienced in south-west WA during early 2011. They concluded that reduced precipitation resulted in a significant lowering of groundwater and lake levels in the entire study area and stand vulnerability was influenced by local precipitation drainage patterns. Recent observed outbreaks of insect infestations and fungal diseases in this region have also been attributed to altered climatic conditions presenting complex and damaging aetiologies (e.g. Hooper and Sivasithamparam, 2005).

The observed catastrophic collapse of forest stands throughout parts of SWWA following the summer of 2010–2011 (Evans et al., 2013; Matusick et al., 2013) highlights the sensitivity of these forest types to prolonged drought and elevated temperatures and, coupled with a predicted increase in the incidence and severity of extreme rainfall and temperature events, exposes the vulnerability of these forests to future climate-change scenarios. Forest managers in this region and elsewhere now require access to software tools that improve their capacity to forecast drought-induced stand mortality with sufficient time to implement adaptive management strategies.

Fortunately there has been an unprecedented release of global and national earth observation climatologies and remote sensing data in recent years. For example, the Terrestrial Ecosystem Research Network (TERN) established AusCover, which is coordinated by the CSIRO's Marine and Atmospheric Research Division (CSIRO CMAR), and provides a data distribution service by connecting remote-sensing science groups and providing the infrastructure to support data collection, in-situ calibration, validation and technical documentation. Remotely-sensed data, such as those used in this study, are freely downloadable from the AusCover Distributed Data Archive and Access Capability (DAAC) data portal (AusCover, 2013). In addition, the South Eastern Australian Climate Initiative (SEACI) funded the Australian Water Availability Project (AWAP), a collaboration between CSIRO CMAR, the Australian Government Bureau of Meteorology (BoM) and Bureau of Rural Sciences (BRS), to monitor the state and trend of the terrestrial water balance of the Australian Continent (Raupach et al., 2009). Combined, these data present a powerful capacity for monitoring changes in forest condition and degradation. These data are also needed for the parameterisation of models that attempt to predict the vulnerability of forests to climate change (Griesbauer et al., 2011; West et al., 2012).

Many consider satellite technology as the only cost-effective method for monitoring forest condition or disturbance across landscapes at high temporal frequencies, despite the spatial trade-off (i.e. reduction in spatial resolution) inherent in these data (e.g. Kerr and Ostrovsky, 2003; Coops et al., 2009; Verbesselt et al., 2009 and 2010; Caccamo et al., 2011). Recently, Evans and Lyons (2013) showed that when combining these datasets for quantifying bioclimatic shifts in forest mortality over large areas, a resolution of 0.05° was sufficient to characterise the time and intensity of the event. Evans and Lyons (2013) showed that a MODIS-based vegetation fractional (F_C) cover dataset developed by Guerschman et al., (2009) was able to quantify the natural variability experienced by the forest against observed mortality of the 2010–2011 event. F_C accurately represented changes in the photosynthetically active cover, non-photosynthetically active cover and bare soil (Evans and Lyons, 2013). Furthermore, Evans and Lyons (2013) analysed 20 bioclimatic variables over the Northern Jarrah Forest (NJF) and showed that although temperatures were hotter preceding the event, the diurnal temperature range (DTR) best captured the total contribution of temperature on the mortality of patches of the forest. Whilst Evans and Lyons (2013) covered the NJF 2010–2011 mortality event in detail, the method was not tested across other forested regions in SWWA. Accordingly, we apply a subset of the Evans and Lyons (2013) method in this study. We use monthly aggregated gridded climatologies of the DTR, precipitation, evapotranspiration and fractional cover at 0.05° resolution for the period 2002–2012 (Raupach et al., 2009).

In this study we identify and map canopy declines of three forests in the SWWA documented between 2002 and 2013 (Evans et al., 2012a, b; 2013; Brouwers et al., 2012a; Matusick et al., 2012, 2013) and extract temporal climatic data spatially co-incident with these forests. In doing so we demonstrate the potential of three bioclimatic parameters (i.e. monthly mean DTR, monthly mean precipitation and an aridity index derived from evaporation data) to forecast forest decline in terms of loss of canopy cover at the landscape scale.

5.4 Methods

5.4.1 Study areas and region selection

The study area, SWWA, lies between 30°0′S and 35°0′S and 115°0′E and 118°0′E (Figure 5.1). The region has a Mediterranean climate that is typified by dry and hot (temperatures in excess of 40°C) summers and mild-to-cool, wet winters (Gentilli, 1989). The dominant landform, the Darling Scarp, rises sharply east of the Swan Coastal Plain and is a substrate of archaen granite and metamorphic rocks with an average elevation of 300 m above sea level (Heddle et al., 1980; Williams and Mitchell, 2002). Rainfall varies from around 1000 mm on the western side of the scarp to 400 mm to the northern and eastern extremes (Williams and Mitchell, 2002). Petrone et al. (2010) showed that since the 1970s the south-west has received 15–20% less than average rainfall and this resulted in a step-change reduction in stream flow across the Northern Jarrah Forest (NJF) (Hughes et al., 2012). Bates et al. (2008) showed the south-west has had a 0.4°C increase in temperature over the same period.

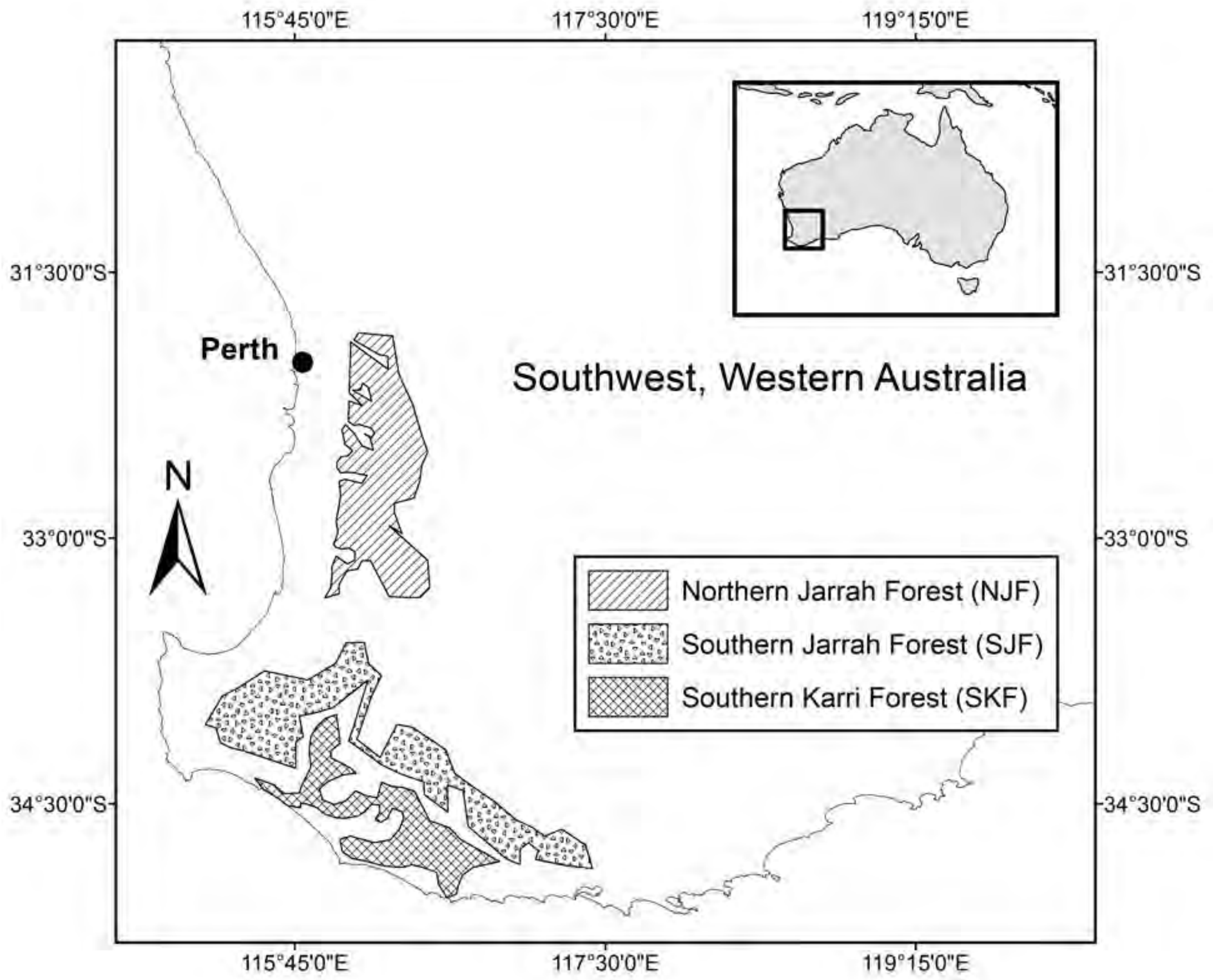

Figure 5.1. Map of the study area showing the three forested areas considered in this study, the Northern Jarrah Forest (NJF), the Southern Jarrah Forest (SJF) and the Southern Karri Forest (SKF).

Table 5.1. Forest and woodland zones across the SWWA

Zone	Description	Reference
NJF	Northern Jarrah Forest	Evans and Lyons (2013); Matusick et al. (2012); Brouwers et al. (2012a)
SJF	Southern Jarrah Forest	Shearer and Smith, 2000
SKF	Southern Karri Forest	Wardell-Johnson et al. (2004, 2007); Dean and Wardell-Johnson (2010)

We used two Geographical Information System (GIS) layers to determine and manually delineate three forest zones for comparison (Table 5.1). Firstly, we used Geoscience Australia's dynamic land cover dataset (DLCD) because it provided the most recent validated estimate of land cover over the region and is completely remote-sensing-based (i.e. NASA's Moderate Resolution Imaging Spectroradiometer-MODIS) at 250 m resolution (Lymburner et al., 2010; AusCover, 2013). Secondly, we overlaid this with the Interim Biogeographic Regionialisation of Australia (IBRA) zones because they provide a biologically and geographically justified distinction between the forested zones (Australian Government, 2012). The resulting map of the study area (Figure 5.1) shows the three forested areas listed in Table 1.1, the Northern Jarrah Forest, the Southern Jarrah Forest (SJF) and the Southern Karri Forest (SKF).

This approach was necessary because the DLCD revealed areas inside the IBRA zones that contained cover other than forest (e.g. water and crops), that were excluded, and provided a buffer between the zones, thus avoiding edge-effects between land-use classes. The spatial layers were used as a guide to ensure the selection of forest regions as classified by both the DLCD and IBRA datasets and either reported in the literature as declining (Table 5.1) or in the case of SKF, assumed to be stable in condition over the 2000–2012 period of available MODIS data.

5.4.2 Fractional cover dataset and statistical analysis of time series

We use a MODIS-based F_C that was developed by Guerschman et al., (2009) and more recently by Evans and Lyons (2013) for monitoring changes in evergreen forest cover. F_C provides an estimate of photosynthetic vegetation (f_{pv}), non-photosyntheic vegetation (f_{npv}) and bare soil (f_{bs}). The F_C model has been evaluated for use in Australia (Guerschman et al., 2012) and found to reproduce vegetation cover with root mean squared error between 13% and 16%. F_C uses information from both the Normalised Difference Vegetation Index (NDVI) and Cellulose Absorption Index (CAI) known to be sensitive to cellulose and lignin foliar content and the amount of vegetative cover (i.e. green biomass). Linear endmember unmixing links in-situ observations of classes of canopy cover to the reflectance properties of the satellite pixels. Through assessing combinations of NDVI and CAI, the model evaluates the pixels' location relative to the vertices of a triangle (empirically assigned as $f_{pv,}$ f_{npv} or f_{bs}) and assigns an appropriate cover fraction. Whilst the model is constrained by the information contained in the underlying vegetation indices (NDVI and CAI) and limited by observations, it remains informative of total canopy fractional cover. Evans and Lyons (2013) showed that it is useful for disentangling canopy mortality as it is observed transitioning from one mix of cover to another.

We extracted the F_C data for each of the three zones between 2002 and 2012. We then spatially and temporally aggregated the data to 0.05° and a monthly time step. To determine significant change or trends we used the Seasonal Decomposition of Time Series procedure within the Loess (STL) package in the R-Project framework after Cleveland et al., (1990). The STL is a filtering procedure for decomposing a time series into trend, seasonal and remainder (noise) composition. Parameterisation of the seasonal smoothing parameters is set to 'periodic', which assumes the seasonal component is constant throughout the time series and analogous to replacing the smoothing parameter with the mean (Cleveland et al., 1990). Accordingly, a significantly positive trend is said to occur when the loess trend is greater than the sum of the time series mean (M) and standard deviation (SD), for example, we define significant growth when f_{pv} is greater than the sum of the M and SD (MSD) and a decline in cover when f_{pv} is less than MSD.

5.4.3 Climatologies

We used The AWAP dataset (Raupach et al., 2009) because it has been recognised as an accurate resource of the terrestrial water balance of the Australian continent (van Dijk and Renzullo, 2011). For each of the zones (Table 5.1) we extracted monthly AWAP data of minimum and maximum temperature and derived a monthly mean diurnal temperature range (T_R in degrees Celsius), that is, the maximum minus the minimum, which is known to be a biologically significant factor affecting vegetation growth (Nix, 1986). We also extracted monthly mean precipitation (P_A in mm day^{-1}), actual (total) evaporation and potential evaporation over the period 2001–2012. Finally, using the potential and actual evaporation we calculated an aridity index, α (unitless), which was designed by Prentice et al., (1993) to capture the seasonal variability of soil moisture independently of vegetation interception and thus considered indicative of the growth-limiting drought stress as per Evans and Lyons (2013). We used the STL package in the R-Project framework (Cleveland et al., 1990) as per the F_C time series data analysis and calculated M, SD and an MSD for each variable.

5.5 Results

5.5.1 Changes in fractional cover

A visual comparison of changes in $f_{pv,}$ f_{npv} and f_{bs} reveal a common trend of declining f_{pv} (Figure 2.1) and increasing f_{npv} (Figure 3.1) across all study zones since 2007 and relative stability in f_{bs} throughout the period (data not shown). All three study zones show a significant increase in f_{npv} following the summer of 2010–2011 (Figure 3.1). This corresponded to a significant decrease in f_{pv} at all sites except SKF which suffered a significant decrease 12 months prior (i.e. 2009–2010) and was recovering following the summer of 2010–2011. The early 2000s had slightly significant increases in f_{pv} at SJF (2002, 2005) and SKF (2003–2005). Accordingly, these growth events corresponded to reductions in f_{npv} (i.e. low) and f_{bs} (i.e. low). The jarrah (NJF, SJF) and karri (SKF) forests show a similar and significant sinusoidal pattern between 2006 and 2008, with significant decreases in f_{npv} (starting after the summer of 2005–2006) followed by significant increases which peak in summer 2007–2008.

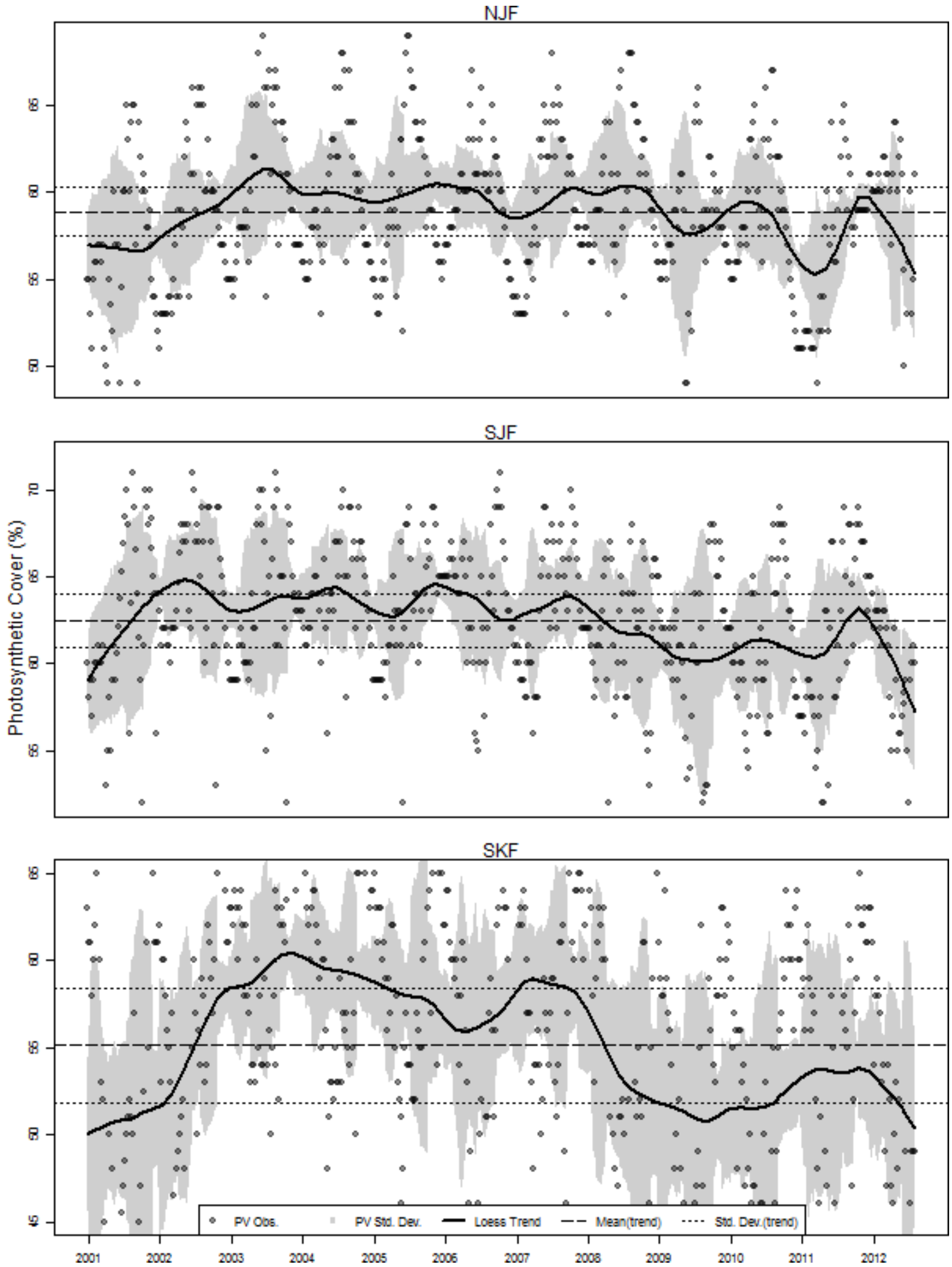

Figure 5.2. Loess trends of Photosynthetic Fractional Cover percent (%) for the period 2000–2012 at the Northern Jarrah Forest (NJF), Southern Jarrah Forest (SJF) and Southern Karri Forest (SKF) zones across the south-west of Western Australia (see Table 5.1 for zones details).

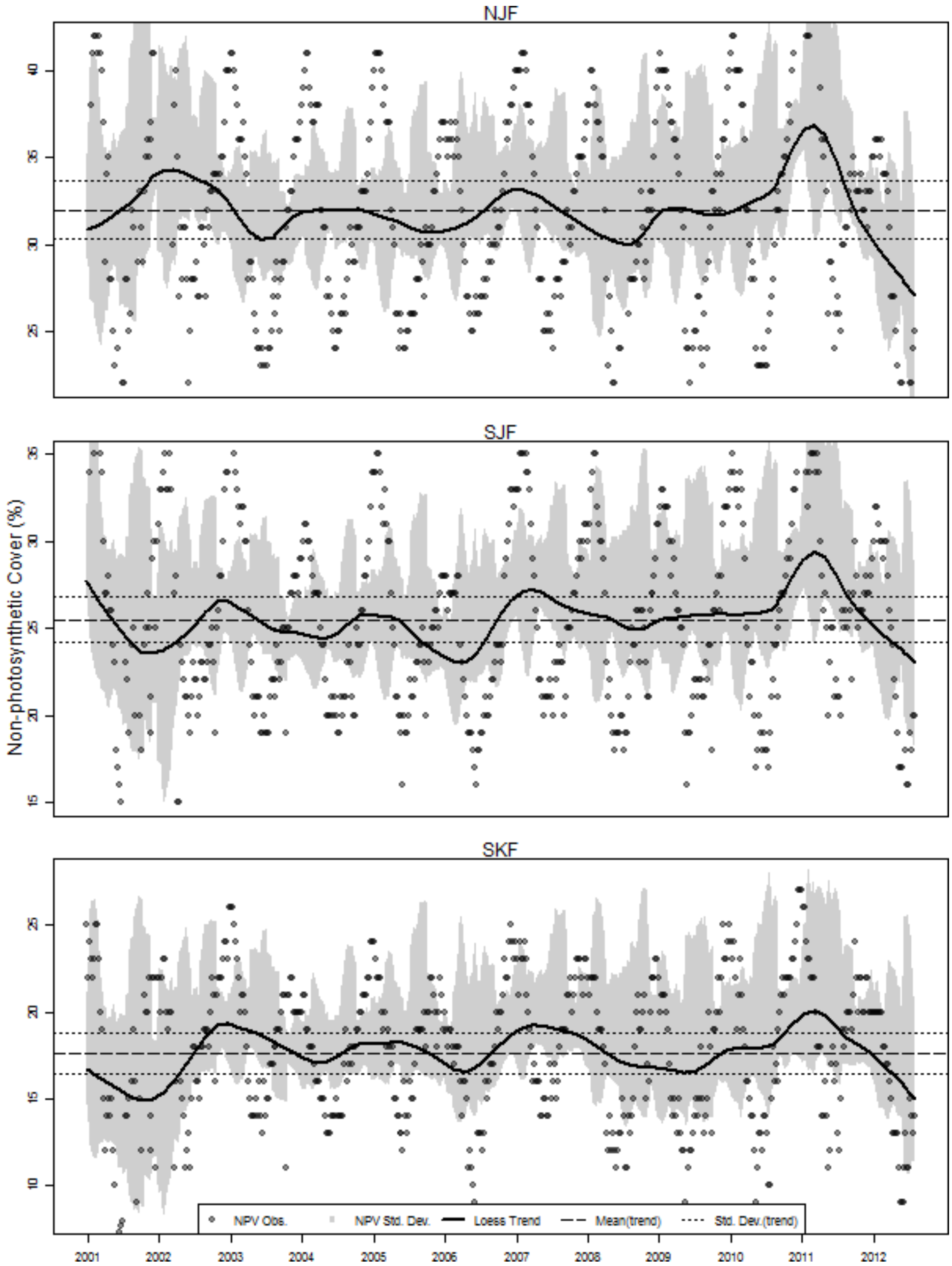

Figure 5.3. Loess trends of Non-Photosynthetic Fractional Cover percent (%) for the period 2000–2012 at the Northern Jarrah Forest (NJF), Southern Jarrah Forest (SJF) and Southern Karri Forest (SKF) zones across the south-west of Western Australia (see Table 5.1 for zones details).

5.5.2 Changes in the bioclimate

Significant departures from T_{MDR} and α between 2000 and 2011 precede the trends in the F_C, particularly around the decline events observed following the summer of 2007 and 2010–2011 (Figures 5.2 and 5.3). Specifically, both of these decline events were preceded by a peak in T_R. Accordingly, there is a similarly strong relationship between rainfall and F_C trends with a regular, approximate six-monthly gap between the trends (Figure 5.4). Starting in early 2009, all zones show a continued high-level T_R which exhibited a 'saddle back' bimodal peak feature occurring around the summer 2008–2009 and autumn 2010–2011; the latter was of greater intensity than the former.

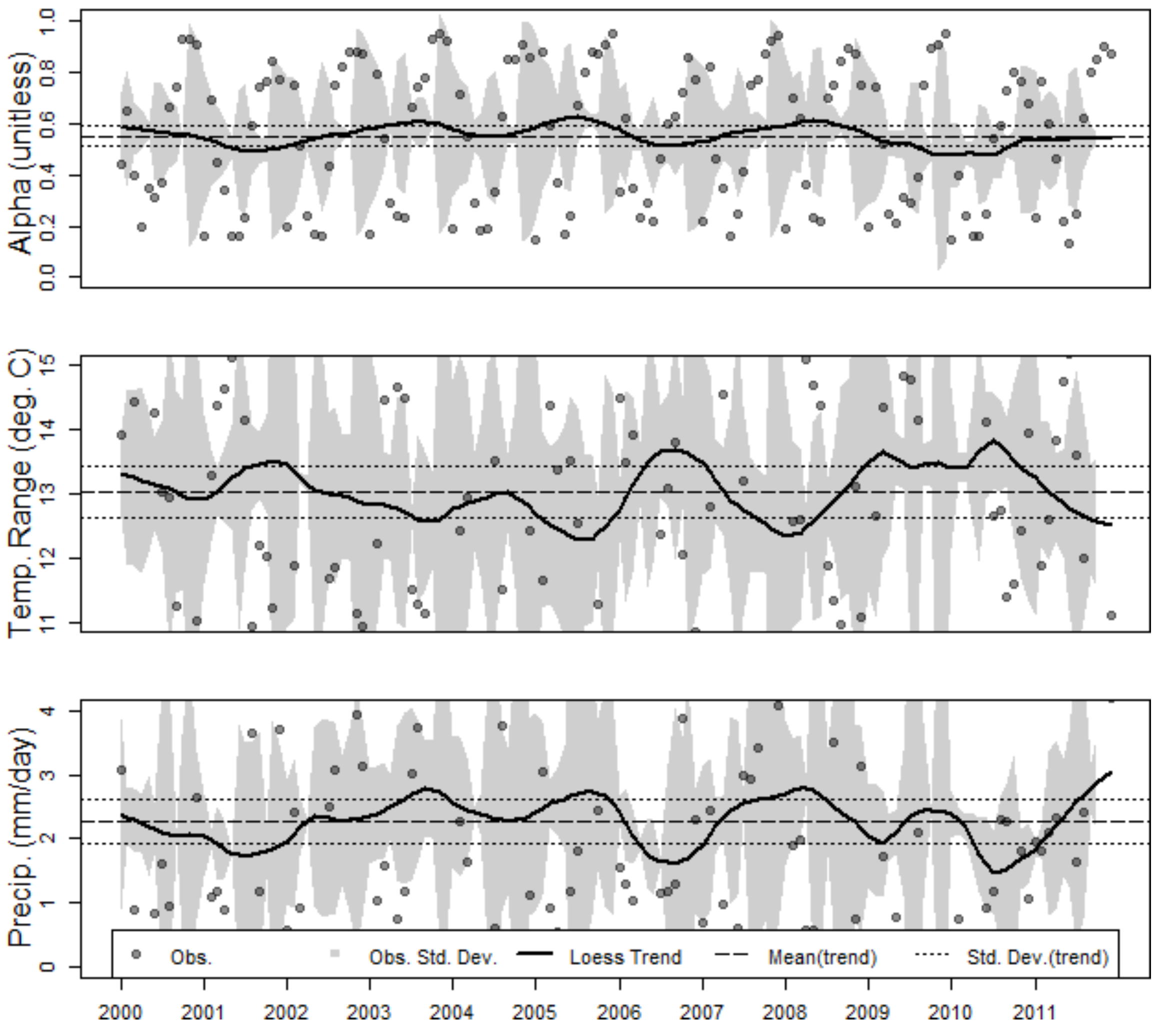

Figure 5.4. Loess trends for the Northern Jarrah Forest (NJF) of monthly alpha (α unitless), the unitless aridity index, monthly average diurnal temperature range (T_R in degrees Celsius) and monthly precipitation (P_A in mm day^{-1}) for the period 2000–2011 at each of the zones across the south-west of Western Australia (see Table 5.1 for zones details).

Considering only the T_R trends, the 2010–2011 event was significantly strong at NJF and mildly significant (data not shown) at the SJF and SKF. However, a peak of strongly high T_R occurred at all zones in the second half of 2007, following an almost equally intense dip in the T_R for the preceding 12 months (i.e. a sinusoidal trend). The period 2011–2012 is ignored since the remote-sensing time series begins a year later and ends a year earlier. Variances in the first year are considered to be biased by the truncation of the time series and ignored.

The aridity index, α, followed a similar (i.e. inverse or significantly below the mean) trend to the temperature data surrounding the 2010–2011 decline event. Additionally, the α trends follow the f_{pv} with high synchronicity at a number of mildly significant departures from the mean (both positive and negative) throughout the time series. The mild 2007 decline event, featuring significant preceding T_R (high) and P_A (low) across all sites, did not feature a significantly low α as expected across all zones; as was the case in 2010–2011. By comparison, the previous (wet) year (2008–2009) had significantly high f_{pv}, corresponding to a significantly low T_R and high P_A across the zones and a significantly high α, indicative of the high humidity (refer Figures 5.2–5.4).

5.5.3 Bioclimate thresholds for modeling

A summary of the key bioclimatic thresholds that were exceeded and identified as preceding the inter-zonal occurring decline events of 2007 and 2010–2011 (Table5.2). Mean T_R values range between 10.34°C ± 0.32°C across the SKF up to 13.06°C ± 0.42°C in the NJF and have a relatively low variance. P_A has a higher standard deviation, and the driest (NJF) zone has a monthly average of 2.24 mm/day ± 0.37 mm/day and the wettest; SKF has an average of 2.82 mm/day ± 0.36 mm/day. The aridity index, α, follows this basic trend, the driest region, NJF had a mean α of 0.55 ± 0.04 and the wettest, most thermally variable region was SKF 0.69 ± 0.03.

Table 5.2. Bioclimatic thresholds resulting in declines of vegetation fractional cover dataset (F_C) photosynthetic cover derived from 2000–2011 mean and standard deviations of the loess trend for three forests in the south-west of Western Australia

Forest	T_R (°C) Time (t) – 12 months	P_A (mm day^{-1}) t – 6 months	α (unitless) t – 12 months
NJF	⇧ > 13.48 mean: 13.06 sd: 0.42	⇩ > 1.87 mean: 2.24 sd: 0.37	⇩ > 0.51 mean: 0.55 sd: 0.04
SJF	⇧ > 12.21 mean: 11.85 sd: 0.36	⇩ > 1.93 mean: 2.21 sd: 0.28	⇩ > 0.57 mean: 0.6 sd: 0.03
SKF	⇧ > 10.66 mean: 10.34 sd: 0.32	⇩ > 2.46 mean: 2.82 sd: 0.36	⇩ > 0.66 mean: 0.69 sd: 0.03

We suggest that these three climatic variables could be used in a simple model for predicting drought-induced canopy decline by incorporating two or three of the local threshold values identified to occur over the preceding 6–12-month period for each forest (Table 5.2), initially using only T_R and P_A (time minus 6 and 12 months) and then, in the last 6 months, α for additional confidence. A practical implementation of this approach could be to monitor these metrics to achieve a 6–12 months advanced warning of broad-scale decline. In this example these three metrics could have been used 6–12 months in advance as a warning that the summer of 2010–2011 T_R was exceeding these thresholds. Similarly, P_A was significantly less than these thresholds for the wettest months (June, July and August) of the six months prior. Finally, α was significantly lower than these thresholds for most of the 12 months prior. A similar pattern can be observed preceding the 2007 declines and an inverse relationship prior to growth events (e.g. 2005–2006). Similarly, the FC data exhibits declining trends throughout this period and may provide additional predictive potential.

5.6 Discussion

By definition, drought refers to a sustained reduction in rainfall of some magnitude, yet this threshold is seldom defined for forests at the landscape level. The bioclimatic thresholds identified in this study (Table 5.2) provide the potential to predict forthcoming changes in canopy condition, namely the risk of drought-induced decline for specific forested landscapes, up to 12 months preceding the event. We stress that the development of such a model would require substantial field validation beyond the scope of this work. Yet, once developed it could offer a near real-time indicator of the potential of canopy decline and mortality. Our time series analysis demonstrates a strong temporal and spatial agreement with decline events recorded in the literature and the aggregated F_C trends. This relationship was significantly strong at zones with known decline episodes over recent years (2007–2011), for example in the NJF (Matusick et al., 2012, 2013; Evans and Lyons, 2013). Our results also suggest that this method is equally applicable to other areas where declines have not been recorded (e.g. SKF) or are weaker in intensity (SJF and some examples across the NJF).

The high temporal resolution of the datasets used in this study not only enables long-term trends to be identified, but also captures the variability inherent in rainfall and temperature records. The jarrah forests appear not only to be responding to long-term climatic trends (Bates et al., 2008) but also through acute fluctuations in f_{pv}, f_{npv} and $f_{bs,}$ presenting phases of decline and in some cases, canopy recovery. These finer-scale responses are known to be significantly influenced by local terrain and hydrological factors (e.g. Mitchell et al., 2012). For example, in the case of the NJF, the recent severe drought and subsequent decline event has been linked to marked depletion of stream flow (Petrone et al., 2010; Kinal and Stoneman, 2011). Potential evaporation was found to exceed precipitation in the NJF (Petrone et al., 2010) and only a small portion (3–20%) of runoff is generated directly from rainfall (Ruprecht and Stoneman, 1993; Hughes et al., 2012). This finding is of particular significance to our results and the use of T_R, P_A and α together because they suggest that relying on T_R or P_A independently might not account for the significant contribution from evaporation inherent in α—which is designed to quantify the seasonal variability of soil moisture independently (Prentice et al., 1993). In the context of these results, it suggests that the decline in forest condition and cover was a product of both a severe shortage of surface water (rainfall converted to soil moisture in-situ) and stream-flow-(sub-surface) derived water. This could be confirmed through access to low-resolution surface hydrology models.

Periods of reduced rainfall can also correspond to dry cloudless winter conditions, which contribute to surface cooling and increase the chance of frost damage to foliage, which in turn represents an additional stressor. This effect is captured in T_R because it contains the difference between the maximum and minimum temperatures. Whilst the minimum temperatures experienced in the SWWA (data not shown) are relatively mild and seldom result in retardation of growth, acute episodic frost can damage the cells of eucalypt foliage and result in defoliation (Brookhouse and Brack, 2006). Frost is well known to impact on eucalypt foliage and therefore contributes to vegetation stress (Barry et al., 2008). As such, the T_R results suggest variations in diurnal temporal variability have not only increased significantly since 2007, but sustained high values since then have preceded forest declines across the south-west.

The coldest zone considered in this study, the SKF, has no reported episodes of canopy decline in the literature. There was no significant change in the F_C and T_R trends despite a significant reduction in P_A and α. The SKF PA trend features the greatest variability of all zones 2007–2011. The SKF peak rainfall event (2008–2009) was the overall greatest in magnitude across all the zones monitored. This may suggest that a strongly significant positive T_R is an essential pre-cursor to a decline (as was the case at the other sites) or merely confirm that there was sufficient surface or sub-surface water available in the SKF at the time—enough to maintain normal F_C. Following the aridity-humidity index classification of Middleton (1997), the SKF is the only 'Humid and Wet' zone considered. We suggest that the climatic thresholds of canopy decline cannot be determined in this time series, yet the method remains useful for this and potentially other humid and wet zones.

Finally, this study also confirms the results of Evans and Lyons (2012), in that 0.05° provided an adequate estimate of the most appropriate pixels for comparison and the highest temporal resolution gain appropriate for strategic planning activities (Kerr and Ostrovsky, 2003; Gillanders et al., 2008). When higher-resolution climatology surfaces become available, this work could be repeated using the 500 m F_C surfaces and hence be more appropriate for operational-scale decisions. These data were all freely downloadable and publicly available through the TERN and other Australian Government funding initiatives, making this an affordable approach for high temporal resolution monitoring of forest canopy condition at the landscape scale (Raupach et al., 2009; AusCover, 2013). However, further work is required to confirm whether these three climatic variables T_R, P_A and α could provide a simple means for predicting regional drought-induced mortality events in other forest types and in other regions.

CHAPTER 6
GENERAL DISCUSSION, RECOMENDATIONS AND CONCLUSION

6.1 General discussion and conclusions

The methods and tools developed in this study have made several key contributions to our scientific understanding of monitoring and mapping forest declines using remote sensing and climatologies across a range of scales from the individual tree to the landscape scale. General discussion and conclusions on how these knowledge gaps are addressed are presenting in two parts. The first part discusses how the total crown health index and digital multispectral imagery can be applied to monitoring and modeling the condition of individual crowns across landscapes and thereby addresses the first and second specific aims of the thesis and their associated knowledge gaps. The second part discusses monitoring, modeling and quantification of forest and woodland declines through space and time at the landscape scale using remote sensing and climatologies and thereby addresses the remaining thesis aims and knowledge gaps.

6.1.1 Development and application of the total crown health index and digital multispectral imagery for monitoring and modeling individual tree crowns across landscapes

Whilst *in-situ* crown assessments have been applied to a number of eucalypt species (Stone and Haywood, 2006), including *E.gomphocephala* (tuart) (Horton et al., 2011) across SWWA, no previous study has attempted to (a) combine these measures into a single metric, nor (b) related them to digital multispectral imagery (DMSI). In this study, high resolution digital multi-spectral imagery (DMSI) was combined with *in-situ* observations of individual crown health. A novel Total Crown

Health Index (TCHI) was developed from repeatable and operationally (USDAFS, 2005; Schomaker et al., 2007) and scientifically (Stone et al., 2003; Souter et al., 2010) proven crown condition metrics and applied to tuart, a species in decline in the southwest of Western Australia. In doing so, a strong biophysically relevant relationship between crown condition and the TCHI and the DMSI was established.

Applying the new model, the crown condition of 80 tuart, spatially distributed across a forest, was assessed using inter-annual DMSI images, therefore demonstrating the effectiveness of the technique on individual trees across landscapes. The model was used to indicate changes in crown condition through space and time and a declining trend was identified in the healthiest class of tuart. Whilst the precision of this modeled TCHI was investigated in Chapter 3, it is suggested that future research using either approach (i.e. Chapters 2 or 3) should carefully consider the appropriate condition or health classification resolution (i.e. number of classes). For example, for research questions addressing the presence or absence case of 'health' or 'decline' (or 'mortality'), it may not be necessary to estimate a five or ten class TCHI, such as presented in Chapters 2 and 3. It may be more appropriate to use a simple binary classification, because it is reasonable to expect this would yield improved results. Similarly, it would be reasonable to expect that increasing the sample number of *in-situ* observations, in terms of the overall total, would increase the reliability of the models estimate.

The temporal resolution of the imagery is also an important consideration. For example, in Chapter 2 and 3 single annual images were used to detect inter-annual change in condition. Moderate resolution satellite imagery, such as MODIS, provide 8 daily, 16 daily and monthly and annual composite images. Depending on the scientific question or management objective, an appropriate spatial and temporal scale may provide additional insight into the timing of broadscale changes in forest condition. Whilst it is costly and technologically prohibitive to have 0.5m DMSI resolution imagery at the temporal frequency of MODIS for large forested areas, this study adds support to a case for continued scientific research into the combination of limited temporal, high spatial resolution data (such as DMSI) with moderate spatial and high temporal resolution data (such as MODIS and Landsat).

The TCHI-DMSI method presented in Chapters 2 and 3 has the potential to be used on other forest ecosystems, both evergreen and deciduous, in any location. In considering such use, it is recommended that the variable influence of understory, soil and atmospheric moisture (Huete et al., 2002) is considered. In Chapter 2 this was demonstrated by comparing a range of vegetation indices (VI), each selected in an attempt to deal with the noise associated with over-story and understory dynamics. In Chapter 3, this was extended using a range of textural, spectral and geometric indices. It is important to note these chapters considered 100's of pixels across a tuart crown using 0.5m DMSI and found that the effects of soil and atmospheric noise were not an issue. For similar reasons, choosing the most appropriate resolution for the target objective itself is critical. For example, in Chapters 2 and 3, 0.5m DMSI was satisfactory for individual tuart crowns, yet in Chapter 4 it was found that SPOT-5 10m satellite imagery was not satisfactory for similarly sized crowns in the NJF.

The methods presented in Chapters 2 and 3 demonstrate the usefulness of DMSI for forest and woodland condition monitoring and therefore provide land managers with additional tools for quantifying changes in individual tree crown condition over large areas. However, careful consideration of the appropriate degree of change to be detected remains critical to scientific and operational applications of the methodology. Accordingly, this issue raises the question; Should one take a simple or complex approach? If limited computing resources are available and precision is not an issue, the simple linear regression based approach might be more appropriate (i.e. Chapter 2). Alternatively, if this is not an issue, Chapter 3 may be considered. In this study, this question was addressed by the extension of the regression based model developed in Chapter 2 to make use of more complex textural, spectral and geometric variance indices calculated from the DMSI (Chapter 3). This improved estimate of the biophysical relationship was achieved by using the machine learning algorithm Random Forest (Breiman, 2001) to identify, from a large number of predictor variables, which combinations better explained the variance.

In summary, Chapters 2 and 3 demonstrate the use of state-of-the-art, high resolution remote sensing imagery and a number of statistical modeling and validation techniques for combining ground based and remotely sensed data to quantifying the health of individual trees across a forested landscape. We suggest these methods are best combined as part of an integrated low-to-moderate resolution monitoring system and therefore dispatched to identify individual condition changes when landscape scale decline and mortality events occur.

6.1.2 Combining remote sensing and climatologies for monitoring, mapping and quantifying forest declines and mortality events and defining bioclimatic envelopes

The methodologies developed in Chapters 4 and 5 were a response to questions arising from an unexpected forest mortality event which took place across NJF following the summer of 2010-2011. Namely; Can we effectively map the decline event using high resolution satellite imagery and feature extraction? and Can be determine the bioclimatic drivers which preceded the event? This second question motivated further questions to be addressed, including; Are the impacts of the event evident in moderate resolution satellite sensors (i.e. MODIS)? and What resolution is necessary to compare the remote sensing with climatologies in order to determine the bioclimate drivers of the mortality event?

Accordingly, Chapter 4 addresses the related knowledge gaps presented in Chapter 1 and in doing so demonstrates the ability to progress in scale from Chapters 2 and 3 to study changes in forest condition (and health) at the patch and landscape scales. This was achieved using SPOT 5 imagery (10m) by extracting these features as patches or mortality (POM) across the NJF. Once the POM were established, a nationally validated MODIS based fractional cover dataset (500m) was used to demonstrate that POM represented a significant change in long term forest condition and these data were further aggregated to a resolution comparable to the available climatologies (around 5000m). Once this spatial resolution gap was bridged, the data were used to quantify the bioclimatic drivers, and relevant thresholds, that surrounded both the NJF mortality event (Chapter 4) and declines across SWWA over the last decade (Chapter 5).

As such, the step from one region (NJF) too many (i.e. across SWWA) demonstrates the potential to apply this methodology to any region in Australia and perhaps beyond. Additionally, these data were used to establish a relevant spatial scale for combining and comparing the MODIS data and the available Australian Water Availability Project (AWAP) climatologies and around 5000m was determined satisfactory in this case. Furthermore, the bioclimatic analysis quantified the climatic drivers preceding the event and establish a set of thresholds; changes in the environmental envelopes proceeding the declines. This led to the discovery that the NJF had not only experienced an increase in temperature (well documented) but significant increase in the mean diurnal temperature range (T_R), which has not been previously reported in the literature. Combination of T_R with monthly mean precipitation (P_A) and an aridity index, alpha (α or Mean Annual Aridity Index (MAAI)) were shown to explain changes in the forest condition up to 12 months in advance. This significant result provided a foundation for Chapter 5.

Addressing a knowledge gap in the understanding of the bioclimatic envelopes of the forests and woodlands of SWWA, Chapter 5 defines this set of comparable bioclimatic thresholds, based on T_R, P_A and α. Analysis showed, when considering their decadal variability (mean plus or minus standard deviation), some forest and woodland areas, known to have experience declines, exhibited a similar response to the findings of Chapter 4 and others did not. Analysis of the predictive ability of the T_R, P_A and α together suggested that combining them enabled a prediction of the 2010-2011 decline at between 6 and 12 months prior to the event after these variables showed significant changes in magnitude. As such, the thresholds offer the potential to assist in the modeling of the ecosystems and therefore provide guidance in the development of adaptive management strategies for the forest.

It is reasonable to expect that in the application of this methodology to other regions, one should consider all of the bioclimatic variables analysed in Chapter 4 rather than just T_R, P_A and α. This is because, whilst T_R, P_A and α were found to be statistically significant in explaining the forest declines in NJF and SWWA, these effects may not easily transfer to other wetter or drier climates around Australia or beyond. Although, the limited evidence provided by the mildly significant changes in the southern karri forest (SKF in Chapter 5) suggest they may transfer to slightly more humid and wet bioclimates. Nonetheless, it stands that with an appropriate consideration of the limitations of the methodology that these strong results on the forest and woodlands of SWWA justify further exploration of the applicability of this methodology to other regions. For example, in the transfer of the methodology from Chapter 4 to Chapter 5 the temporal resolution was enhanced (from annual to monthly) and the spatial resolution was kept at 5000m to make use of a new version of the AWAP data that became available in the interim (i.e. run 26h). It is reasonable to expect that future improvements in the spatial and temporal resolution of climatologies and remotely sensed datasets may provide further improvements. In the case of the continental United States of America and Europe such datasets already exist.

One of these adaptive strategies could be the inclusion of the use of DMSI and *in-situ* assessments of crown condition to employ the TCHI-DMSI approach presented in Chapters 2 and 3. To achieve this at the MODIS scale (250-500m) considerable effort would be required to validate an aggregate canopy condition at a scale relevant to these pixels. Therefore, a sub-pixel or hybrid approach is suggested because it is expected this would be more economically viable, and therefore more likely of being adopted. The approach would involve use of the moderate scale remote sensing data to detect change, then the deployment of the high resolution and on-ground resources as necessary. For example, it would be critical to set the temporal frequency of the TCHI *in-situ* assessments to be relevant to the desired temporal frequency of any research question and perhaps repeat these measurements through time.

In summary, the methodologies presented in Chapters 4 and 5 have been shown to be useful in monitoring, mapping and potentially predicting forest declines in SWWA. Combined, these tools and methodologies represent an opportunity for scientific and operational (i.e. land managers) re-use of these methods and if conditions are similar to those found in SWWA, potentially predicting the most critical areas that are likely to become drought stressed by up to 12 months in advance. Combined with Chapters 2 and 3, Chapters 4 and 5 constitute a framework for monitoring, mapping and modelling forest condition and declines across a range of temporal and spatial resolutions.

6.2 Recommendations for land managers and policy makers

The following recommendations are suggested for consideration by land managers and policy makers in the development of operational land management procedures and adaptive management strategies of forests and woodlands facing declines which are likely to be associated with climatic change;

1. Mandate the research, definition and publication of bioclimatic envelopes using the methodology developed in Chapters 4 and 5. These bioclimatic metrics should be based the best available gridded climatologies at spatially and temporally relevant scales to the land management units of interest. The technical limitation of this recommendation is access to satellite remote sensing and climatology data such as that used in this study.

2. Implement or extend existing continuous monitoring of the condition of forested and woodland areas using the best available remote sensing (a balance of spatial and temporal considerations) in a spatially explicit manner, such as that proposed in Chapters 4 and 5, yet remain relevant to management units or at the highest possible temporal resolution available at the time. It is expected that this recommendation will require scientific validation of target specific spatial metrics (i.e. size and composition of forest or woodland region or target species) in order to achieve an effective monitoring program design. With this limitation in mind, it is important to note that it is likely the highest publicly available (and therefore free) remotely sensed data will be at 25m resolution from the Landsat sensor.

3. Combine the data suggested in points (1) and (2) to identify key bioclimatic indices, such as those identified in this research (i.e. T_R, P_A and α) yet extend this to consider all of the bioclimatic indices analyzed in Chapter 4. Once identified, implement them as an advanced warning of the potential for forest and woodland declines. The objectives of such an advanced warning system should include the potential for intervention or at least, preparation for adaptation. For example, preventative burning or thinning of forested areas likely to experience extreme heat or drought stress could reduce the risk of

mortality or gradual decline.

4. Integrate the use of high spatial resolution DMSI and *in-situ* assessments of individual crowns for critical areas identified using the landscape scale methods suggested in points (1) and (2). This provides the "ground truth" necessary to improve confidence in the biophysical changes expected from lower resolution monitoring. It is expected that, similar to the spatial and temporal limitations inherent in the monitoring proposed in point (2) any scientific or operational implementation of the TCHI-DMSI approach should consider the appropriate spatial and temporal resolution necessary to achieve the scientific and operational objectives at the time. Similarly, these objectives should be relevant to both the spatial and temporal resolution needed to effectively measure the target objective, for example, a number of individual tree crowns scattered across woodland. In the case of the TCHI this would likely involve the identification and selection of a suitably large sample of trees for the *in-situ* monitoring campaign. The total number of trees to be assessed, the range of conditions sampled and their spatial distribution should all be included as considerations dependent on the objectives of the research.

5. Combine the use of these tools to provide a means of quantifying, from the landscape right down to an individual tree, the impacts of adaptive land management practices, such as thinning and hydrological intervention (diversion of water by physical or political means) of critical forest and woodland regions. Then apply this knowledge to ensure the succession of our forest and woodlands under changing climatic conditions.

6. Consider the application of this methodology to other events which lead to defoliation and mortality, such as wildfires, land clearing and storm damage.

REFERENCES

Abbott, I., and Le Maitre, D. (2009). "Monitoring the impact of climate change on biodiversity: The challenge of megadiverse Mediterranean climate ecosystems." *Aust. Ecol.*, 35(4): 406–422.

Allen, C. D., Macalady, A. K., Chenchouni, H., Bachelet, D., McDowell, N., Vennetier, M., Kitzberger, T., Rigling, A., Breshears, D. D., Hogg, E. H. (Ted), Gonzalez, P., Fensham, R., Zhang, Z., Castro, J., Demidova, N., Limp, J.-H., Allard, G., Running, S. W., Semerci, A., and Cobb, N. (2010). "A global overview of drought and heat-induced tree mortality reveals emerging climate change risks for forests." *For. Ecol. Manag.*, 259(4): 660–684.

Archibald, R. D. (2006). "Fire and the persistence of tuart woodlands." PhD Thesis, Murdoch University, Perth.

Archibald, R., Bowen, B., Hardy, G. E. S. J., Fox, J. and Ward, D. (2004). "Changes to tuart woodland in Yalgorup over four decades." In A forest conscienceness, Proceedings 6th National Conference of the Australian Forest History Society Inc, Millpress Science Publishers, Rotterdam, 740 pp.

Archibald, R. D., Bradshaw, J., Bowen, B. J., Close, D. C., McCaw, L., Drake, P. L., and Hardy, G. E. St. J. (2010). "Understorey thinning and burning trials are needed in conservation reserves: The case of Tuart (*Eucalyptus gomphocephala DC*)." *Ecol.Manag. Rest.*, 11(2): 108-112.

Australian Government (2012). "Australia's Bioregions. Department of Sustainability Environment Water, Populations and Communities, Canberra ACT, Australia." Available from http://www.environment.gov.au/parks/nrs/science/ibra.html

AusCover (2013). "Terrestrial Ecosystem Research Network: AusCover facility." Available from http://data.auscover.org.au/

Barry, K. M., Stone, C., and Mohammed, C. L. (2008). "Crown-scale evaluation of spectral indices for defoliated and discoloured eucalypts." *Int. J. Remote Sens.*, 29(1):47–69.

Bastin, G.N., Ludwig, J. A., Eager, R. W., Chewings, V. H., and Liedloff, A. C. (2002). "Indicators of landscape function : comparing patchiness metrics using remotely-sensed data from rangelands." *Ecol. Indi.*, 1: 247-260.

Bates, B. C., Hope, P., Ryan, B., Smith, I., and Charles, S. (2008). "Key findings from the Indian Ocean Climate Initiative and their impact on policy development in Australia." *Clim. Chang.*, 89(3-4): 339–354.

Beaumont, L. J., Hughes, L., and Poulsen, M. (2005). "Predicting species distributions: use of climatic parameters in BIOCLIM and its impact on predictions of species' current and future distributions." *Ecol. Model.*, 186(2): 251–270.

Boland, D. J., Brooker, M. I. H., Chippendale, G. M., McDonald, M. W., Hall, N. and Hyland, B. P. M. (2006). "Forest Trees of Australia", 5th ed. Collingwood, VIC: CSIRO Publishing.

Bosch, A., Zisserman, A., and Muoz, X. (2007). "Image Classification using Random Forests and Ferns." In Computer Vision, 2007. ICCV 2007. IEEE 11th International Conference. 1-8 pp.

Breiman, L. (1996). "Bagging predictors." *Machine learning*, 24(2): 123-140.

Breiman, L. (2001). "Random forests." *Machine learning*, 45(1): 5-32.

Brookhouse, M. and Brack, C. (2008). 'The effect of age and sample position on eucalypt tree-ring width series. " *Can. J. Forest Res.,* 38: 1144–1158.

Brouwers, N., Matusick, G., Ruthrof, K., Lyons, T., and Hardy, G. (2012a). "Landscape-scale assessment of tree crown dieback following extreme drought and heat in a Mediterranean eucalypt forest ecosystem." *Landscape Ecol.*, 28(1): 69-80.

Brouwers, N., Mercer, J., Lyons, T., Poot, P., Veneklaas, E., and Hardy, G. (2012b). "Climate and landscape drivers of tree decline in a Mediterranean ecoregion." *Ecol. Evol.*, 3: 67-79.

Caccamo, G., Chisholm, L.A., Bradstock, R.A. and Puotinen, M.L. (2011). "Assessing the sensity of MODIS to monitor drought in high biomass ecosystems." *Remote Sens. Environ.,* 115: 2626–2639.

Caccetta, P., Allen, A. and Watson, I., (2000). "The land monitor project." In Proceedings of the 10th Australasian Remote Sensing Photogrammetry Conference, 21–25 August 2000, Adelaide, 97–107 pp.

Caccetta, P., Furby, S., Wallace, J., and Wu, X. (2007). "Continental monitoring: 34 years of land cover change using Landsat imagery." In 32nd International Symposium on Remote Sensing of Environment, 25-29 pp.

Cai, Y. F., Barber, P. A., Dell, B., O'Brien, P. A., Williams, N., Bowen, B. and Hardy, G. (2010). "Soil bacterial functional diversity is associated with the decline of Eucalyptus gomphocephala." *For.Ecol. Manag*., 260: 1047-1057.

Campbell, B. (2011). "Seasonal climate summary southern hemisphere (autumn 2010): rapid decay of El Niño, wetter than average in central, northern and eastern Australia and warmer than usual in the west and south." *Aust. Meteorol. Oceanogr. J*., 61(May 2009): 65–76.

Chaves, M. M. (1991). "Effects of Water Deficits on Carbon Assimilation." *J. Exp. Bot*., 42(1): 1-16.

Chaves, M. M., Maroco, J. P., and Pereira, J. S. (2003). "Understanding plant responses to drought — from genes to the whole plant." *Funct. Plant Biol*., 30(3): 239.

Cleveland, R. B., Cleveland, W. S., McRae, J. E., and Terpenning, I. (1990). "STL: A Seasonal-Trend Decomposition Procedure Based on Loess. " *J. Official Stat.,* 6: 3 –73.

Close, D., Davidson, N., Johnson, D., Abrams, M., Hart, S., Lunt, I., Archibald, R.,

Horton, B. and Adams, M. (2009). "Premature decline of eucalyptus and altered ecosystem processes in the absence of fire in some Australian forests." *Bot. Rev*., 75: 191–202.

Close, D. C., Davidson, N. J., Swanborough, P. W., and Corkrey, R. (2011). "Does low-intensity surface fire increase water- and nutrient-availability to overstorey Eucalyptus gomphocephala?" *Plant and Soil*., 349: 203-214.

Cohen, J. (1960). "A Coefficient of Agreement for Nominal Scales." *Edu. Psychol. Measurement*, 20(1): 37-46.

Cohen, J. (1968). "Weighted Kappa: Nominal Scale Agreement with Provision for scaled disagreement or partial credit." *Psychol. Bull*., 70(4): 213-220.

Coops, N., Dury, S., Smith, M.-L., Martin, M., and Ollinger, S. (2002). "Comparison of green leaf eucalypt spectra using spectral decomposition." *Aust. J. Bot*., 50(5): 567.

Coops, N. C., Stone, C., Culvenor, D. S., Chisholm, L. A., and Merton, R. N. (2003). "Chlorophyll content in eucalypt vegetation at the leaf and canopy scales as derived from high resolution spectral data." *Tree Physiol.*, 23(1): 23-31.

Coops, N. C., Stone, C., Culvenor, D. S., and Chisholm, L. (2004). "Assessment of crown condition in eucalypt vegetation by remotely sensed optical indices." *J. Environ. Qual*., 33: 956–964.

Coops, N., Wulder, M. A., Duro, D. C., Han, T., and Berry, S. (2008). "The development of a Canadian dynamic habitat index using multi-temporal satellite estimates of canopy light absorbance." *Ecol.Ind*., 8(5): 754-766.

Coops, N.C., Wulder, M.A. and Iwanicka, D. (2009). "Large area monitoring with a MODIS-based disturbance index (DI) sensitive to annual and seasonal variations." *Remote Sens. Environ.,* 113: 1250–1261.

Cowling, R. M., Rundel, P. W., Lamont, B. B., Arroyo, M. K., and Arianoutsou, M. (1996). "Plant diversity in mediterranean-climate regions." *TREE*, 11. PII: SOlSS-5347(96)10044-6.

Curran, P. J., Dungan, J. L., and Gholz, H. L. (1990). "Exploring the relationship between reflectance red edge and chlorophyll content in slash pine." *Tree Physiol.*, 7: 33–48.

Cutler, D. R., Edwards, T. C. Jr., Beard, K. H., Cutler, A., Hess, K. T., Gibson, J., and Lawler, J. J. (2007). "Random forests for classification in ecology." *Ecol.*, 88(11): 2783-92.

Datt, B. (1998). "Remote Sensing of Chlorophyll a, Chlorophyll b, Chlorophyll a+b, and Total Carotenoid Content in Eucalyptus Leaves." *Remote Sens. Environ.*, 66(2): 111-121.

Dawson, T. P., and Curran, P. J. (1998). "Technical note a new technique for interpolating the reflectance red edge position." *Int. J. Remote Sens.,* 19: 2133–2139.

Dean, C. and Wardell-Johnson, G. (2010). "Old-growth forests, carbon and climate change: functions and management for tall open-forests in two hotspots of temperate Australia." *Plant Biosyst.*, 144: 180–193.

de Beurs, K. M., and Henebry, G. M. (2005). "A statistical framework for the analysis of long image time series." *Int. J. Remote Sens.*, 26: 1551 - 1573.

Deering, D. W., and Rouse, J. W. (1975). "Measuring 'forage production' of grazing units from Landsat MSS data." In Proceedings of the 10th International Symposium on Remote Sensing of Environment, 6–10 October 1975, Ann Arbor, MI (Ann Arbor, MI: ERIM), 1169–1178 pp.

Demetriades-Shah, T. H., Steven, M. D., and Clark, J. A. (1990). "High resolution derivative spectra in remote sensing." *Remote Sens. Environ.*, 33: 55–64.

Díaz-Uriarte, R., and de Andrés, S. A. (2006). "Gene selection and classification of microarray data using random forest." *BMC bioinformatics*, 7: 3.

Dunlop, M., and Brown, P. R. (2008). "Implications of climate change for Australia's National Reserve System: A preliminary assessment." Report to the Department of Climate Change, February 2008, Canberra.

Edwards, T.A. (2002). "Environmental Correlates and Associations of Tuart decline." Edith Cowan University, Perth, Western Australia.

Edwards, T. (2004). "Environmental correlates and associations of tuart (*Eucalyptus gomphocephala* DC.) decline." Master's Thesis, Edith Cowan University*,* 291 pp.

Eklundh, L., Johansson, T., and Solberg, S. (2009). "Mapping insect defoliation in Scots pine with MODIS time-series data." *Remote Sens. Environ*., 113: 1566-1573.

Elith, J., Graham, C. H., Anderson, R. P., Dudík, M., Ferrier, S., Guisan, A., Hijmans, R. J., Huettmann, F., Leathwick, J. R., Lehmann, A., Li, J., Lohmann, L. G., Loiselle, B. A., Manion, G., Moritz, C., Nakamura, M., Nakazawa, Y., Overton, J. McC. M., Townsend Peterson, A., Phillips, S. J., Richardson, K., Scachetti-Pereira, R., Schapire, R. E., Soberón, J., Williams, S., Wisz, M. S., and Zimmermann, N. E. (2006). "Novel methods improve prediction of species' distributions from occurrence data." *Ecogr.,* 29: 129-151.

Evans, J.S., and Cushman, S. A. (2009). "Gradient modeling of conifer species using random forests." *Land. Ecol*., 24(5): 673-683.

Evans, B. J., Lyons, T. J., Barber, P. A., Stone, C., and Hardy, G. (2012a). "Dieback Classification Modelling using High Resolution Digital Multi Spectral Imagery and *in-situ* Assessments of Crown Condition." *Remote Sens. Lett*., 3: 541-550.

Evans, B., Lyons, T., Barber, P., Stone, C., and Hardy, G. (2012b). "Enhancing a eucalypt crown condition indicator driven by high spatial and spectral resolution remote sensing imagery." *J. Appl. Remote Sens*., 6, doi:10.1117/1.JRS.6.063605.

Evans, B.J., and Lyons, T. (2013). "Bioclimatic Extremes Drive Forest Mortality in Southwest, Western Australia." *Clim.,* 1, 28-52.

FAO (2000) “Forest Resources Assessment WP 33: FRA 2000 ON DEFINITIONS OF FOREST AND FOREST CHANGE, Food and Agricultural Organisation of the United Nations, Rome

Felton, K., Old, K., Kile, G., and Ohmart, C. (ed.) (1981). “Eucalypt diebacks in Tasmania.” In Eucalypt dieback of forests and woodlands, CSIRO, Canberra, 51-54 pp.

Fischer, J., Lindenmayer, D., and Manning, A. (2006). “Biodiversity, ecosystem function, and resilience: ten guiding principles for commodity production landscapes.” *Front. Ecol. and Environ*., 4: 80-86.

Florence, R., Keane, P., Kile, G., Podger, F., and Brown, B. (ed.) (2000). “Growth habits and silviculture of eucalypts.” Diseases and Pathogens of Eucalypts, CSIRO Publishing, 35-46 pp.

Fraser, R. H., Abuelgasim, A., and Latifovic, R. (2005). “A method for detecting large-scale forest cover change using coarse spatial resolution imagery.” *Remote Sens. Environ*., 95(4): 414-427, doi:10.1016/j.rse.2004.12.014.

Frelich, L. E., and Reich, P. B. (2010). “Will environmental changes reinforce the impact of global warming on the prairie–forest border of central North America?” *Front Ecol. Environ*., 8(7): 371-378.

Furby, S., and Campbell, N. (2001). “Calibrating images from different dates to “like-value” digital counts.” *Remote Sens. Environ*., 77(2): 186-196.

Galmés, J., Medrano, H., and Flexas, J. (2007). “Photosynthetic limitations in response to water stress and recovery in Mediterranean plants with different growth forms.” *N. Phytol*., 175(1): 81-93.

Gentilli, J. (1948). “Bioclimatic Controls in Western Australia EVAPORANSPIRATION.” The West. Aust. Natur., Perth, 1(5): 104-107.

Gentilli, J. (1989). “Climate of the jarrah forest.” In Dell B, Havel JJ, Malajczuk N (eds) The jarrah forest: a complex Mediter- ranean ecosystem. Kluwer Academic, Dordrecht, 23–40 pp.

Gillanders, S.N., Coops, N.C., Wulder, M.A., Gergel, S.E., and T. Nelson, (2008). "Multitemporal remote sensing of landscape dynamics and pattern change: 161 describing natural and anthropogenic trends." *Progress in Phys. Geogr.*, 32(2): 503-528.

Gislason, P., Benediktsson, J., and Sveinsson, J. (2006). "Random Forests for land cover classification." *Pattern Recog. Lett.*, 27(4): 294-300.

Gitelson, A. A., and Merzlyak, M. N. (1996). "Signature analysis of leaf reflectance spectra: algorithm development for remote sensing of chlorophyll." *J. Plant Physiol.*, 148: 494–500.

Goodwin, N. R., Coops, N. C.,Wulder, M. A., Gillanders, S., Schroeder, T. A., and Nelson, T. (2008). "Estimation of insect infestation dynamics using a temporal sequence of Landsat data." *Remote Sens. Environ.*, 112: 3680−3689.

Government of Western Australia (2002). Available from http://www.dec.wa.gov.au/pdf/national_parks/management/tuart_forest_strategy_draft_06.pdf

Granier, A., Reichstein, M., Bréda, N., Janssens, I. A., Falge, E., Ciais, P., Grünwald, T., Aubinet, M., Berbigier, P., Bernhofer, C., Buchmann, N., Facini, O., Grassi, G., Heinesch, B., Ilvesniemi, H., Keronen, P., Knohl, A., Köstner, B., Lagergren, F., Lindroth, A., Longdoz, B., Loustau, D., Mateus, J., Montagnani, L., Nys, C., Moors, E., Papale, D., Peiffer, M., Pilegaard, K., Pita, G., Pumpanen, J., Rambal, S., Rebmann, C., Rodrigues, A., Seufert, G., Tenhunen, J., Vesala, T., and Wang, Q. (2007). "Evidence for soil water control on carbon and water dynamics in European forests during the extremely dry year: 2003." *Agri. For. Meteorol.*, 143(1-2): 123-145

Grassi, G., and Magnani, F. (2005). "Stomatal, mesophyll conductance and biochemical limitations to photosynthesis as affected by drought and leaf ontogeny in ash and oak trees." *Plant, Cell and Environ.*, 28(7): 834-849.

Griesbauer, H., Green, D. S., and O'Neill, G. A. (2011). "Using a spatial temporal climate model to assess population-level Douglas-fir growth sensitivity to climate change across large climatic gradients in British Columbia, Canada.” *For. Ecol. Manag.*, 261: 589-600.

Guerschman, J. P., Hill, M. J., Renzullo, L. J., Barrett, D. J., Marks, A. S., and Botha, E. J. (2009). “Estimating fractional cover of photosynthetic vegetation, non-photosynthetic vegetation and bare soil in the Australian tropical savanna region upscaling the EO-1 Hyperion and MODIS sensors.” *Remote Sens. Environ.*, 113: 928-945.

Guerschman, J.P., Oyarzábal1, M., Malthus, T.J., McVicar, T.R., Byrne, G., Randall, L.A. and Stewart, J.B. (2012). “Evaluation of the Modis-Based Vegetation Fractional Cover Product.” CSIRO Publishing, Canberra, 40 pp.

Gutschick, V. P., and BassiriRad, H. (2003). “Extreme events as shaping physiology, ecology, and evolution of plants: toward a unified definition and evaluation of their consequences.” *N. Phytol.*, 160(1): 21–42.

Haldimann, P., Gallé, A., and Feller, U. (2008). “Impact of an exceptionally hot dry summer on photosynthetic traits in oak (Quercus pubescens) leaves.” *Tree Physiol.*, 28(5): 785-795.

Hansen, A.J., and Dale, V. (*2001*). “*Biodiversity* in U.S. Forests Under Global Climate Change.” *Ecosys.*, 4: 161-163.

Haralick, R. M. (1979). “Statistical and structural approaches to texture.” *Proceedings of the IEEE*, 67(5): 786-804.

Haralick, R. M., Shanmugam, K., and Dinstein, I. H. (1973). “Textural features for image classification.” *IEEE Transactions on Systems, Man Cyber.,* 3(6): 610-621.

Harper, R. J, Smettem, K. R. J., Carter, J. O., and McGrath, J. F. (2009). “Drought deaths in Eucalyptus globulus (Labill.) plantations in relation to soils, geomorphology and climate.” *Plant and Soil.*, 324(1-2): 199–207.

Harper, R. J., Smettem, K. R. J., and Tomlinson, R. J. (2005). “Using soil and climatic data to estimate the performance of trees, carbon sequestration and recharge potential at the catchment scale.” *Aust. J. Exp. Agri.*, 45(11): 1389.

Haywood, A., and Stone, C. (2011a). “Mapping eucalypt forest susceptible to dieback associated with bell miners (Manorina melanophys) using laser scanning, SPOT 5 and ancillary topographical data.” *Ecol. Model.*, 222(5): 1174-1184.

Haywood, A., and Stone, C. (2011b). “Semi-automating the stand delineation process in mapping natural eucalypt forests.” *Most*, 74(1): 13-22.

Heddle, E. M., Loneragan, O. W., and Havel, J. J. (1980). “Vegetation complexes of the Darling system, Western Australia.” In Atlas of Natural Resources, Darling System, Western Australian Government Department of Conservation and Environment, Perth, 37-72 pp.

Hijmans, R. J., Phillips, S., Leathwick, J., and Elith, J. (2012). “An {R} Package for species distribution modeling.” Available from http://cran.r-project.org/web/packages/dismo/index.html.

Hooper, R. J., and Sivasithamparam, K. (2005). “Characterization of damage and biotic factors associated with the decline of *Eucalyptus wandoo* in southwest Western Australia.” *Can. J. For. Res.*, 35(11): 2589-2602.

Horton, B. M., Close, D. C., Wardlaw, T. J. and Davidson, N. J. (2011). “Crown condition assessment: an accurate, precise and efficient method with broad applicability to Eucalyptus.” *Aust. Ecol.*, 36: 709–721.

Huete, A. (2002). “Overview of the radiometric and biophysical performance of the MODIS vegetation indices.” *Remote Sens. Environ.*, 83: 195–213.

Huete, A., Justice, C., and Liu, H. (1994). “Development of vegetation and soil indices for MODIS-EOS.” *Remote Sens. Environ.*, 49: 224–234.

Hughes, L. (2010). “Climate change and Australia: key vulnerable regions.” *Reg Environ. Chang.*, 11(S1): 189–195.

Hughes, J.D., Petrone, K.C., and Silberstein, R.P. (2012). “Drought, groundwater storage and stream flow decline in southwestern Australia.” *Geophys. Res. Lett.,* 39: L03408.

Imielska, A. (2012). "Seasonal climate summary southern wettest Australian summer on record and one of the strongest La Niña events on record." *Aust. Meteorol. Oceanogr*. J., 61(2011): 241–251.

Jackson, M., and Jensen, J. R. (2005). "Evaluation of Remote Sensing-derived Landscape Ecology Metrics for Reservoir Shoreline Environmental Monitoring," *Photogram. Eng. Remote Sens*., 71(12): 1387-1397.

Jago, R. A., Cutler, M. E. J., and Curran, P. J. (1999). "Estimating canopy chlorophyll concentration from field and airborne spectra." *Remote Sens. Environ*., 68(3): 217 -224.

Johansen, K., Arroyo, L. A., Armston, J., Phinn, S., and Witte, C. (2010). "Mapping riparian condition indicators in a sub-tropical savanna environment from discrete return LiDAR data using object-based image analysis." *Ecol. Ind*., 10: 796-807.

Jumbe, C., and Angelsen, A. (2007). "Forest dependence and participation in CPR management: Empirical evidence for forest co-management in Malawi." *Ecol. Econ*., 62: 661-672.

Jurskis, V. (2005). "Eucalypt decline in Australia, and a general concept of tree decline and dieback." *For. Ecol. Manag*., 215(1-3): 1-20.

Kala, J., Lyons, T. J., and Nair, U. S. (2011). "Numeral simulations of the impact of land-cover change on cold fronts in south-west Western Australia." *Boundary Layer Meteorol*., 138: 121–138.

Ke, Y., Quackenbush, L. J., and Im, J. (2010). "Synergistic use of QuickBird multispectral imagery and LIDAR data for object-based forest species classification." *Remote Sens. Environ*., 114(6): 1141-1154.

Keith, D., and Gorrod, E. (2006). "The meanings of vegetation condition." *Ecol. Manag. Rest*., 7(s1): S7-S9.

Kerr, J. T., and Ostrovsky, M. (2003). "From space to species: ecological applications for remote sensing." *Trends in Ecol, Evol*., 18: 299-305.

Kile, G. A., Turnbull, C. R. A., and Podger, F. D. (1981). "Effect of regrowth dieback on some properties of Eucalyptus obliqua trees." *Aust. For. Res*., 1: 55-62.

Kimber, P., Old, K., Kile, G., and Ohmart, C. (ed.) (1981). "Eucalypt diebacks in the southwest of Western Australia." Eucalypt Dieback in Forests and Woodlands Proceedings of a conference held at the CSIRO Division of Forest Research, Canberra, 37-43 pp.

Kinal, J. and Stoneman, G. L. (2011). "Hydrological impact of two intensities of timber harvest and associated silviculture in the jarrah forest in south-western Australia." *J. Hydrol*., 399: 108–120.

Klausmeyer, K. R., and Shaw, M. R. (2009). "Climate change, habitat loss, protected areas and the climate adaptation potential of species in mediterranean ecosystems worldwide." *PLos Once*., 4, doi: 10.1371/journal.pone.0006392.

Knight, D. H., and Wallace, L. L. (1989). "The Yellowstone Fires: Issues in Landscape Ecology." *BioSci*., 39(10): 700–706.

Koch, J. M., and Samsa, G. P. (2007). "Restoring Jarrah Forest Trees after Bauxite Mining in Western Australia." *Rest. Ecol*., 15(4): 17–25.

Landis, J. R., and Koch, G. G. (1977). "An Application of Hierarchical Kappa-type Statistics in the assessment of Majority Agreement among Multiple Observers." *Biometrics*, 33(2): 363-374.

Lane, P. N. J., Feikema, P. M., Sherwin, C. B., Peel, M. C., and Freebairn, A. C. (2010). "Modelling the long term water yield impact of wildfire and other forest disturbance in Eucalypt forests." *Environ. Model Soft*., 25(4): 467–478.

Lawrence, R., Wood, S., and Sheley, R. (2006). "Mapping invasive plants using hyperspectral imagery and Breiman Cutler classifications (randomForest)." *Remote Sens. Environ*., 100(3):356-362.

Lawton, J. (1983). "Plant architecture and the diversity of phytophagous insects." *Ann. Rev. Entomol*., 28: 23-29.

Liaw, A., and Wiener, M. (2002). "Classification and Regression by randomForest." *R. News*, 2(3): 1822.

Lichtenthaler, H. K. (2001). "Chlorophylls and Carotenoids : Measurement and Characterization by UV-VIS." *Anal. Chem.*, 1-8.

Lichtenthaler, H. K. (1996). "Vegetation stress: an introduction to the stress concept in plants." *J. Plant Physiol.*, 148(1): 4-14.

Lichtenthaler, H. K. (1987). "Applications of Chlorophyll Flourescence," Dordrecht, The Netherlands: Klewer Academic Publishers. Available from http://books.google.com.au/books?id=Z8K2CN924OMC&pg=PA144&lpg=PA144&dq=Lichtenthaler,+1987&source=bl&ots=qiRa_XtLLy&sig=0O6Bdsa6S21oZaBD7t06rGLbkmE&hl=en&ei=lvqoTvDxPI6jiQfOryVDg&sa=X&oi=book_result&ct=result&resnum=6&ved=0CEAQ6AEwBQ#v=onepage&q=Lichtenthaler,1987&f=false.

Limousin, J. M., Misson, L., Lavoir, A. V., Martin, N. K., and Rambal, S. (2010). "Do photosynthetic limitations of evergreen Quercus ilex leaves change with long-term increased drought severity?" *Plant, Cell and Environ.*, 33(5): 863-875.

Llorens, L., Penuelas, J., and Estiarte, M. (2003). "Ecophysiological responses of two Mediterranean shrubs, Erica multiflora and Globularia alypum, to experimentally drier and warmer conditions." *Physiol. Plant.*, 119(2): 231–243.

Luo, H. (2007). "Mature semiarid chaparral ecosystems can be a significant sink for atmospheric carbon dioxide." *Glob. Chang. Biol.*, 13(2): 386-396.

Lymburner, L., Tan, P., Mueller, N., Thackway, R., Lewis, A., Thankappan, M., Randall, L., Islam, A., and Senarath, U. (2010). "250 metre Dynamic Land Cover Dataset of Australia (1st Edition)", Geoscience Australia, Canberra.

Lyons, T. J. (2002). "Clouds prefer native vegetation." *Meteorol. Atmos. Phys.*, 80: 131–140.

Manion, P. (1981). "Decline diseases of complex biotic and abiotic origin." Tree Disease Concepts, Prentice Hall., 324-339 pp.

Manning, A., Fischer, J., and Lindenmayer, D. (2006). "Scattered trees are keystone structures - implications for conservation." *Biol. Cons*., 132: 311-321.

Matusick, G., Ruthrof, and Hardy, G. (2012). "Drought and Heat Triggers Sudden and Severe Dieback in a Dominant Mediterranean-Type Woodland Species", *Open J. Forest.*, 2 (4): 183-186.

Matusick, G., Ruthrof, K., Brouwers, N. C., Dell, B., and Hardy, G. (2013). "Sudden forest canopy collapse corresponding with extreme drought and heat in a 1 mediterranean-type forest in south-western Australia." *Eur. J. For. Res.,* doi:10.1007/s10342-013-0690-5.

McDougal, K. L., Hargy, G., and Hobbs, R. J. (2007). "Comparison of colonisation of Phytophthora cinnamomi in detached stem tissue of Eucalyptus marginata in relation to site disease status." *Aust.Plant Pathol*., 36(2): 498–500.

McDowell, N., Pockman, W. T., Allen, C. D., Breshears, D. D., Cobb, N., Kolb, T., Plaut, J., Sperry, J., West, A., Williams, D. G., and Yepez, E. A. (2008). "Mechanisms of plant survival and mortality during drought: why do some plants survive while others succumb to drought?" *N. Phytol*. 178: 719-739.

McDowell, N., Beerling, D. J., Breshears, D. D., Fisher, R. A., Raffa, K. F., and Stitt, M. (2011). "The interdependence of mechanisms underlying climate-driven vegetation mortality." *Trends in Ecol. Evol*., 26(10): 523-532.

Middleton, N. (1997). "World Atlas of Desertification 2nd ed.", N. Middleton, Nick Middleton, & D. S. G. Thomas, eds., Arnold.

Misson, L., Degueldre, D., Collin, C., Rodriguez, R., Rocheteau, A., and Ourcival, J.-M., Rambal, S. (2011). "Phenological responses to extreme droughts in a Mediterranean forest." *Glob. Chang. Biol*., 17(2): 1036–1048.

Misson, L., Limousin, J. M., Rodriquez, R., and Letts, M. G. (2010). "Leaf physiological responses to extreme droughts in Mediterranean Quercus ilex forest." *Plant, Cell and Environ*., 33(11): 1898-1910.

Mitchell, P. J., Benyon, R. G., and Lane, P. N. J. (2012). "Responses of evapotranspiration at different topographic positions and catchment water balance following a pronounced drought in a mixed species Eucalypt forest, Australia." *J. Hydrol*., 440-441: 62–74.

Moss, R. A., and Loomis, W. E. (1951). "Absorption spectra of leaves I. the Visible Spectrum." *Plant Physiol*., 27(2): 370-391.

Neilson, R. P., and Marks, D. (1994). "A global perspective of regional vegetation and hydrologic sensitivities from climatic change." *J. Veg. Sci*., 5(5): 715–730.

Nix, H. (1986). "A Biogeographic Analysis of Australian Elapid Snakes in Atlas of Elapid Snakes of Australia", Australian Government Publishing Service, Canberra, 4-15 pp.

Oliver, C. D., and Larson, B. C. (1990). "Forest and dynamics". 1st edition, 1990, By: Chadwick Dearing Oliver, Bruce C. Larson., McGraw-Hill, Inc.

Paap, T., Burgess, T., McComb, J., Shearer, B. and Hardy, G. (2008). "Quambalaria species, including Q. coyrecup sp. nov., implicated in canker and shoot blight diseases causing decline of Corymbia species in the southwest of Western Australia." *Mycol. Res*., 112: 57-69.

Pal, M., and Mather, P. M. (2003). "An assessment of the effectiveness of decision tree methods for land cover classification." *Remote Sens. Environ*., 86(4): 554-565.

Palzer, C. (1983). "Crown symptoms of Regrowth Dieback." *Pacific Sci.*, 37: 465-470.

Palzer, C., Old, K., Kile, G., and Ohmart, C. (ed.) (1981). "Aetiology of gully dieback." Eucalypt Dieback in Forests and Woodlands, Proceedings of a conference held at the CSIRO Division of Forest Research, Canberra, 174-178 pp.

Parkes, D., Newell, G., and Cheal, D. (2003). Available from http://www.environment.gov.au/archive/biodiversity/toolbox/templates/pubs/habitat-hectares.pdf

Peel, D., Pitman, A. J., Hughes, L. A., Narisma, G. T., and Pielke, Sr. R. A. (2005). "The impact of realistic biophysical parameters for Eucalypts on the simulation of the January climate of Australia." *Environ. Model Softw*., 20(5): 595–612.

Pepper, L. R., Cho, Y. K., Boder, E. T., and Shusta, E.V. (2008). "A decade of yeast surface display technology: Where are we now?" *Comb. Chem. High Throughput. Screen*., 11: 127-134.

Petrone, K. C., Hughes, J. D., Van Niel, T. G., and Silberstein, R. P. (2010). "Streamflow decline in south-western Australia, 1950–2008." *Geophys. Res. Lett*., 37: 1–7.

Pietrzykowski, E., Stone, C., Pinkard, E., and Mohammed, C. (2006). "Effects of Mycosphaerella leaf disease on the spectral reflectance properties of juvenile Eucalyptus globulus foliage." *For. Pathol*., 36(5): 334-348.

Pinar, A., and Curran, P. J. (1996). "Technical Note Grass chlorophyll and the reflectance red edge." *Int. J. Remote Sens*., 17(2): 351-357.

Podger, F., Kile, G., Bird, T., Turnbull, C., and McLoed, D. (1980). "An unexplained decline in some forests of Eucalyptus obliqua and E. regnans in southern Tasmania." *Aust. For. Res*. 10: 53-70.

Pook, E., Old, K., Kile, G., and Ohmart, C. (ed.) (1981). "Drought and dieback of eucalypts in dry sclerophyll forests and woodlands of the southern tablelands, New South Wales.", Proceedings of a conference held at the CSIRO Division of Forest Research, Canberra, 179-189 pp.

Pook, E. W., and Forrester, R. I. (1984). "Factors influencing dieback of drought-affected dry sclerophyll forest tree species." *Aust. For. Res*., 14: 201-217.

Portlock, C., Koch, A., Wood, S., Hanly, P., and Dutton, S. (1993). "Yalgorup National Park Management Plan 1995–2005", Western Australian Government Department of Environment and Conservation, Perth.

Prasad, A. M., Iverson, L. R., and Liaw, A. (2006). "Newer classification and regression tree techniques: bagging and random forests for ecological prediction." *Ecosyst.*, 9(2): 181-199.

Prentice, C. I., Sykes, M. T., and Cramer, W. (1993). "A simulation model for the transient effects of climate change on forest landscapes." *Ecol. Model.*, 65(1-2): 51–70.

Priestley, C. H. B., and Taylor, R. J. (1972). "On the Assessment of Surface Heat Flux and Evaporation Using Large-Scale Parameters." *Mon. Weather Rev.*, 100(2): 81–92.

Prober, S. M., Thiele, K. R., Rundel, P. W., Yates, C. J., Berry, S. L., Byrne, M., Christidis, L., Gosper, C. R., Grierson, P. F., Lemson, K., Lyons, T., Macfarlane, C., O'Connor, M. H., Scott, J. K., Standish, R. J., Stock, W. D., Etten, E. J. B., Wardell-Johnson, G. W., and Watson, A. (2011). "Facilitating adaptation of biodiversity to climate change: a conceptual framework applied to the world's largest Mediterranean-climate woodland." *Clim. Chang.*, 110(1-2): 227-248.

Rabideau, G. S., French, C. S., and Holt, A. S. (1946). "The Absorption and Reflection Spectra of Leaves, Chloroplast Suspensions, and Chloroplast Fragments as Measured in an Ulbricht Sphere." *Am. J. Bot.*, 33(10): 769-777.

Raupach, M. R., Briggs, P. R., Haverd, V., King, E. A., Paget, M., and Trudinger, C. M. (2009). "Australian Water Availability Project (AWAP): CSIRO Marine and Atmospheric Research Component: Final Report for Phase 3, Bureau of Meteorology and CSIRO". Available from http://www.cawcr.gov.au/publications/technicalreports/CTR_013.pdf Accessed May 12, 2011

Renton, M., Childs, S., Standish, R., and Shackelford N. (2012). "Plant migration and persistence under climate change in fragmented landscapes: Does it depend on the key point of vulnerability within the lifecycle?" *Ecol. Mod*., 249: 50-58.

Rice, K., Matzner, S., Byer, W., and Brown, J. (2004). "Patterns of tree dieback in Queensland, Australia: the importance of drought stress and the role of resistance to cavitation." *Oecol*., 139: 190-198.

Rouse, J. W., Haas, R. H., Schell, J. A., and Deering, D. W. (1974). "Monitoring vegetation systems in the Great Plains with ERTS." In Proceedings of the Third ERTS Symposium, 10–14 December 1973, Washington, DC (Greenbelt, MD: NASA), vol. SP–351, 309–317 pp.

Ruprecht, J. K., and Stoneman, G. L. (1993). "Water yield issues in the jarrah forest of south-western Australia." *J. Hydrol*., 150: 369–391.

Schomaker, M. E., Zarnoch, S. J., Bechtold, W. A., Latelle, D. J., Burkman, W. G., and Cox, S. M. (2007). "Crown-Condition Classification : A Guide to Data Collection and Analysis", Gen. Tech. Rep. SRS-102, Asheville, NC. Available from http://www.treesearch.fs.fed.us/pubs/27730.

Scott, P. M., Jung, T., Shearer, B. L., Barber, P. A., Calver, M., and Hardy, G. E. St. J. (2011). "Patheogenicuty of Phytopthora multivora to Eucalyptus gomphocephala and E. marginata." *For. Pathol*., 42 (4): 289-298.

Shea, S., Shearer, B., Tippett, J. and Deegan, P. (1984). "A new perspective on jarrah dieback." Forest Focus, Forests Department Western Australia, 31: 3-11.

Shearer, B. and Smith, I. (2000). "Diseases of eucalypts caused by soilborne species of Phytophthora and Pythium." Diseases and Pathogens of Eucalypts, CSIRO, 259-291 pp.

Sims, D. A., and Gamon, J. A. (2002). "Relationships between leaf pigment content and spectral reflectance across a wide range of species, leaf structures and developmental stages." *Remote Sens. Environ*., 81: 337–354.

Souter, N. J., Cunningham, S., Little, S., Wallace, T., McCarthy, B., and Henderson, M. (2010). "Evaluation of a visual assessment method for tree condition of eucalypt floodplain forests." *Ecol. Manag. Rest.*, 11(3): 210-214.

Southwood, T. R. E. (1961). "The number of species of insect associated with various trees." *J. Animal Ecol.*, 30: 1-8.

Spot Image (2010). "Preprocessing levels and location accuracy." Available from http://www.astrium-geo.com/files/pmedia/public/r454_9_preprocessing_levels_sept2010.pdf

Stewart, J. B., Rickards, J. E., Bordas, V. M., Randall, L. A., and Thackway, R. M. (2011). "Ground cover monitoring for Australia – establishing a coordinated approach to ground cover mapping: Workshop proceedings." Canberra 23–24 November 2009, ABARES, Canberra, March 2009.

Stone, C., Chisholm, L., and Coops, N. (2001). "Spectral reflectance characteristics of Eucalypt foliage damaged by insects." *Aust. J. Bot.*, 49(6): 687–698.

Stone, C., and Haywood, A. (2006). "Assessing canopy health of native eucalypt forests." *Ecol. Manag. Rest.*, 7: S24–S30.

Stone, C., Wardlaw, T., Floyd, R., Carnegie, A., Wylie, R., and de Little, D. (2003). "Harmonisation of methods for the assessment and reporting of forest health in Australia — a starting point. A discussion paper prepared by a sub-committee of the Forest Research Working Group on Forest Health." *Aust. For.*, 66(4): 233-246.

Strobl, C., Boulesteix, A.-L., Kneib, T., Augustin, T., and Zeileis, A. (2008). "Conditional variable importance for random forests." *BMC Bioinformatics*, 9: 307.

Svetnik, V., Liaw, A., Tong, C., Culberson, J. C., Sheridan, R. P., and Feuston, B. P. (2003.) "Random forest: a classification and regression tool for compound classification and QSAR modeling." *J. Chem. Inf. Comput. Sci.*, 43(6): 1947-1958.

Tobin, S. (2010). “Seasonal climate summary southern hemisphere (summer 2009 – 2010): an El Niño summer?; wetter than average for east, north and central areas, dry in Western Australia and Tasmania.” *Aust. Meteorol. Oceanogr. J.* 60: 289–299.

USDAFS, U.S.D. of A.F.S. (2002). “Forest Inventory and Analysis: National Core Field Guide, 1: Field Data Collection Procedures for Phase 2 Plots, Version 1.6.” Available from http://www.fia.fs.fed.us.

USDAFS (2005). “Forest Inventory and Analysis: National Core Field Guide: Field Data Collection Procedures for Phase 2 Plots, Version 3.0, Section 12: Crowns: Measurements and Sampling (Washington, DC: U.S. Department of Agriculture, Forest Service, Southern Research Station).” Available from http://www.fia.fs.fed.us/library/fieldguides-methods-proc/docs/2006/p3_3-0_sec12_10_2005.pdf

van Dijk, A. I. J. M., and Renzullo, L. J. (2011). “Water resource monitoring systems and the role of satellite observations.” *Hydrol. Earth Syst. Sci*., 15(1): 39–55.

Verbesselt, J., Robinson, A., Stone, C. and Culvenor, D. (2009). “Forecasting tree mortality change metrics derived from MODIS satellite data.” *Forest Ecol. Manag.,* 258: 1166–1173.

Verbesselt, J., Hyndman, R., Newnham, G., and Culvenor, D. (2010a). “Detecting trend and seasonal changes in satellite image time series.” *Remote Sens. Environ*., 114: 106–115.

Verbesselt J, Hyndman R, Zeileis, A., and Culvenor, D. (2010b). “Phenological change detection while accounting for abrupt and gradual trends in satellite image time series.” *Remote Sens. Environ*., 114: 2970–2980.

Wallace, J. F., Caccetta, P. A., and Kiiveri, H.T. (2004). “Recent developments in analysis of spatial and temporal data for landscape qualities and monitoring.” *Aust. Ecol*., 29(1): 100-107.

Wang, W., Peng, C., Kneeshaw, D. D., Larocque, G. R., and Luo, Z. (2012). "Drought-induced tree mortality: ecological consequences, causes, and modelling." *Environ. Rev*., doi: 10.1139/A2012-004.

Wardell-Johnson, G.W., Williams, M., Mellican, A., and Annells, A. (2007). "Floristic patterns and disturbance history in karri forest, south-western Australia: 2. Origin, growth form and fire response." *Acta Oecol.,* 31: 137–150.

Wardell-Johnson, G. W., Keppel, G., and Sander, J. (2011). "Climate change impacts on the terrestrial biodiversity and carbon stocks of Oceania." *Pacific Conservation Biol.,* 17: 220-240.

Wardlaw, T. J. (1989). "Management of Tasmanian forests affected by regrowth dieback." *N. Z. J. For. Sci*., 19: 265-276.

Weiss, M., Baret, F., Smith, G. J., Jonckheere, I., and Coppin, **P. (2004). "**Review of methods for in situ leaf area index (LAI) determination: Part II. Estimation of LAI, errors and sampling**."** *Agri. For. Meteorol.,* 121(1-2): 37-53.

West, A. G., Dawson, T. E., February, E. C., Midgley, G. F., Bond, W. J., and Aston, T.L. (2012). "Diverse functional responses to drought in a Mediterranean-type shrubland in South Africa." *N. Phytol*., 195(2): 396-407.

Williams, K., and Mitchell, D. (2002). "Jarrah Forest 1 (JF1- Northern Jarrah Forest subregion): A Biodiversity Audit of Western Australia's 53 Biogeographical Subregions in 2002, Perth." Western Australian Government Department of Environment and Conservation, Perth.

Wilson, B. (2002) "Influence of scattered paddock trees on surface soil properties: A study of the Northern Tablelands of NSW." *Ecol. Manag. Rest*., 3: 211-219.

Wilson, K. B., Baldocchi, D., and Hanson, P. (2000). "Quantifying stomatal and non-stomatal limitations to carbon assimilation resulting from leaf aging and drought in mature deciduous tree species." *Tree Physiol*., 20(12): 787-797.

Woodcock, C. E., and Strahler, A. H. (1987). "The factor of scale in remote sensing." *Remote Sens. Environ*., 21(3): 311-332.

Wulder, M. A., White, J. C., Goward, S. N., Masek, J. G., Irons, J. R., Herold, M., Cohen, W. B., Loveland, T. R., and Woodcock, C. E. (2008). "Landsat continuity: Issues and opportunities for land cover monitoring." *Remote Sens. Environ*., 112: 955−969.

WWF (2013). Available from http://worldwildlife.org/pages/conservation-science-data-and-tools

Yu, Q., Gong, P., Clinton, N., Biging, G., Kelly, M., and Schirokauer, D. (2006). "Object-based Detailed Vegetation Classification with Airborne High Spatial Resolution Remote Sensing Imagery." *Photogram. Eng. Remote Sens*., 72(7): 799-811.

Zarnoch, S. J., Bechtold, W. A., and Stolte, K. W. (2004). "Using crown condition variables as indicators of forest health." *Can. J. For. Res*., 34(5): 1057-1070.